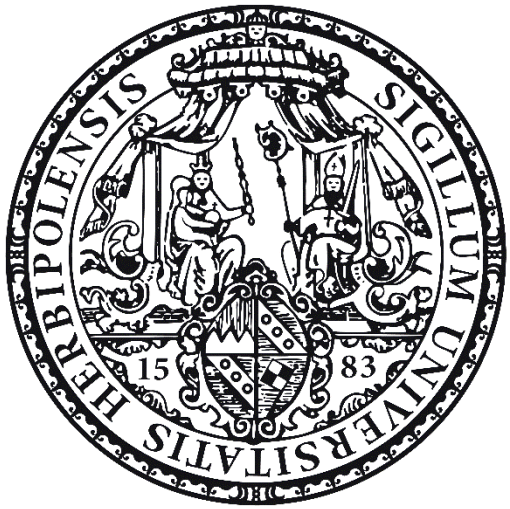

Mode of Action of Adjuvants for Foliar Application

Wirkmechanismen von Adjuvantien für die Blattflächenapplikation

Doctoral thesis for a doctoral degree
at the Graduate School of Life Sciences,
Julius-Maximilians-Universität Würzburg,
Section Integrative Biology

submitted by

Elisabeth Asmus
from
Bad Salzungen

Würzburg 2016

Submitted on:……..……..

Office stamp

Members of the *Promotionskomitee*:

Chairperson: Prof. Dr. Thomas Müller

Primary Supervisor: Prof. Dr. Markus Riederer

Supervisor (Second): Prof. Dr. Wolfgang Dröge-Laser

Supervisor (Third): Dr. Christian Popp

Supervisor (Fourth): Dr. Katja Arand

Date of Public Defence: ……

Date of Receipt of Certificates……..……...

TABLE OF CONTENTS

SUMMARY

Adjuvants are compounds added to an agrochemical spray formulation to improve or modify the action of an active ingredient (AI) or the physico-chemical characteristics of the spray liquid. Adjuvants can have more than only one distinct mode of action (MoA) during the foliar spray application process and they are generally known to be the best tools to improve agrochemical formulations. The main objective for this work was to elucidate the basic MoA of adjuvants by uncoupling different aspects of the spray application. Laboratory experiments, beginning from retention and spreading characteristics, followed by humectant effects concerning the spray deposit on the leaf surface and ultimately the cuticular penetration of an AI, were figured out to evaluate overall *in vivo* effects of adjuvants which were also obtained in a greenhouse spray test. For this comprehensive study, the surfactant classes of non-ionic sorbitan esters (Span), polysorbates (Tween) and oleyl alcohol polyglycol ether (Genapol O) were generally considered because of their common promoting potential in agrochemical formulations and their structural diversity.

The reduction of interfacial tension is one of the most crucial physico-chemical properties of surfactants. The dynamic surface tension (DST) was monitored to characterise the surface tension lowering behaviour which is known to influence the droplet formation and retention characteristics. The DST is a function of time and the critical time frame of droplet impact might be at about 100 ms. None of the selected surfactants were found to lower the surface tension sufficiently during this short timeframe (chapter I). At ca. 100 ms, Tween 20 resulted in the lowest DST value. When surfactant monomers are fully saturated at the droplet-air-interface, an equilibrium surface tension (STeq) value can be determined which may be used to predict spreading or run-off effects. The majority of selected surfactants resulted in a narrow distribution of STeq values, ranging between 30 and 45 mN m^{-1}. Nevertheless, all surfactants were able to decrease the surface tension considerably compared to pure water (72 mN m^{-1}). The influence of different surfactants on the wetting process was evaluated by studying time-dependent static contact angles on different surfaces and the droplet spread area on *Triticum*

aestivum leaves after water evaporation. The spreading potential was observed to be better for Spans than for Tweens. Especially Span 20 showed maximum spreading results. To transfer laboratory findings to spray application, related to field conditions, retention and leaf coverage was measured quantitatively on wheat leaves by using a variable track sprayer. Since the retention process involves short time dynamics, it is well-known that the spray retention on a plant surface is not correlated to STeq but to DST values. The relationship between DST at ca. 100 ms and results from the track sprayer showed increasing retention results with decreasing DST, whereas at DST values below ca. 60 mN m^{-1} no further retention improvement could be observed.

Under field conditions, water evaporates from the droplet within a few seconds to minutes after droplet deposition on the leaf surface. Since precipitation of the AI must essentially being avoided by holding the AI in solution, so-called humectants are used as tank-mix adjuvants. The ability of pure surfactants to absorb water from the surrounding atmosphere was investigated comprehensively by analysing water sorption isotherms (chapter II). These isotherms showed an exponential shape with a steep water sorption increase starting at 60% to 70% RH. Water sorption was low for Spans and much more distinct for the polyethoxylated surfactants (Tweens and Genapol O series). The relationship between the water sorption behaviour and the molecular structure of surfactants was considered as the so-called humectant activity. With an increasing ethylene oxide (EO) content, the humectant activity increased concerning the particular class of Genapol O. However, it could be shown that the moisture absorption across all classes of selected surfactants correlates rather better with their hydrophilic-lipophilic balance values with the EO content.

All aboveground organs of plants are covered by the cuticular membrane which is therefore the first rate limiting barrier for AI uptake. *In vitro* penetration experiments through an astomatous model cuticle were performed to study the effects of adjuvants on the penetration of the lipophilic herbicide Pinoxaden (PXD) (chapter III). In order to understand the influence of different adjuvant MoA like humectancy, experiments were performed under three different humidity levels. No explicit relationship could be found between humidity levels and the PXD penetration which might be explained by the fact that humidity effects would rather affect

hydrophilic AIs than lipophilic ones. Especially for Tween 20, it became obvious that a complex balance between multiple MoA like spreading, humectancy and plasticising effects have to be considered.
Greenhouse trials, focussing the adjuvant impact on *in vivo* action of PXD, were evaluated on five different grass-weed species (chapter III). Since agrochemical spray application and its following action on living plants also includes translocation processes *in planta* and species dependent physiological effects, this investigation may help to simulate the situation on the field. Even though the absolute weed damage was different, depending both on plant species and also on PXD rates, adjuvant effects in greenhouse experiments displayed the same ranking as in cuticular penetration studies: Tween 20 > Tween 80 > Span 20 ≥ Span 80.

Thus, the present work shows for the first time that findings obtained in laboratory experiments can be successfully transferred to spray application studies on living plants concerning adjuvant MoA. A comparative analysis, using radar charts, could demonstrate systematic derivations from structural similarities of adjuvants to their MoA (summarising discussion and outlook). Exemplarily, Tween 20 and Tween 80 cover a wide range of selected variables by having no outstanding MoA improving one distinct process during foliar application, compared to non-ethoxylated Span 20 and Span 80 which primarily revealed a surface active action. Most adjuvants used in this study represent polydisperse mixtures bearing a complex distribution of EO and aliphatic chains. From this study it seems alike that adjuvants having a wide EO distribution offer broader potential than adjuvants with a small EO distribution. It might be a speculation that due to this broad distribution of single molecules, all bearing their individual specific physico-chemical nature, a wide range of properties concerning their MoA is covered.

ZUSAMMENFASSUNG

Adjuvantien sind chemische Verbindungen, die einer Pflanzenschutzformulierung hinzugefügt werden, um die Wirkung der Aktivsubstanz oder die physikalisch-chemischen Eigenschaften der Spritzbrühe zu verbessern oder zu modifizieren. Sie können mehr als nur einen einzigen bestimmten Wirkmechanismus während der Blattflächenapplikation aufweisen, sodass sie gemeinhin als wirksamste Hilfsmittel in Pflanzenschutzformulierungen benutzt werden. Der Schwerpunkt dieser Arbeit lag darauf, ihre wesentlichen Wirkmechanismen aufzuklären, indem verschiedene Aspekte der Applikation entkoppelt und unabhängig voneinander untersucht wurden. Hierzu wurden Laborversuche durchgeführt, beginnend mit dem Retentions- und Spreitungsverhalten, über die *„humectant“*- Eigenschaft, den Tropfenrückstand betreffend und schließlich die kutikuläre Penetration einer Aktivsubstanz. Um schlussendlich die ineinander übergreifenden *in vivo* Mechanismen von Adjuvantien zusammenfassend bewerten zu können, wurde zusätzlich ein Gewächshausprayversuch ausgeführt. Für diese mechanismenübergreifende Studie wurden aufgrund ihrer allgemein begünstigenden Eigenschaften in Formulierungen und ihrer strukturellen Vielfalt die Tensidklassen der Sorbitanester (Span), Polysorbate (Tween) und Oleylalkoholpolyglykolether (Genapol O) verwendet.

Die Absenkung der Grenzflächenspannung ist eine der wesentlichen physikalisch-chemischen Eigenschaften von Tensiden. Die dynamische Oberflächenspannung (DST) wurde untersucht, um das Verhalten beim Absenken der Oberflächenspannung einzuschätzen, welches die Tropfenbildung und die Retentionseigenschaften beeinflusst. Die DST ist zeitabhängig und das kritische Zeitfenster, in dem ein Tropfen auf die Pflanzenoberfläche auftrifft, beläuft sich auf ca. 100 ms. Innerhalb dieses Zeitrahmens konnte keines von den ausgewählten Tensiden die Oberflächenspannung hinreichend herabsetzen (vgl. Kapitel I). Bei ca. 100 ms wies Tween 20 die niedrigsten DST-Werte auf. Bei vollständiger Absättigung der Tropfen-Luft-Grenzfläche durch Tensidmonomere kann eine statische Oberflächenspannung (STeq) bestimmt werden. Diese physikalische Größe kann benutzt werden, um Spreitungs- und *„run-off“*- Effekte abzuschätzen. Der Großteil der betrachteten Tenside zeigte ähnliche STeq-Ergebnisse zwischen

30 und 45 mN m^{-1}. Somit waren alle Tenside in der Lage, die Oberflächenspannung von Wasser (72 mN m^{-1}) beträchtlich abzusenken. Der Einfluss von Tensiden auf den Benetzungsprozess wurde sowohl mit Hilfe von zeitabhängigen, statischen Kontaktwinkelmessungen auf verschiedenen Oberflächen, als auch nach der Wasserverdunstung auf Basis der Spreitungsfläche der Tropfen auf *Triticum aestivum* Blättern analysiert. Dabei zeigte die Klasse der Spans, besonders Span 20, ein besseres Benetzungsverhalten als die Klasse der Tweens. Um die Erkenntnisse aus dem Labor auf die Sprayapplikation auf dem Feld zu übertragen, wurden Retention und Blattbedeckung quantitativ auf Weizenoberflächen mit Hilfe eines *„tracksprayers“* bestimmt. Da der Retention ein sehr schnell ablaufender, dynamischer Prozess zugrunde liegt, korreliert sie nicht mit der statischen, sondern mit der dynamischen Oberflächenspannung. Die Beziehung zwischen DST, bei ca. 100 ms und den *„tracksprayer“*- Ergebnissen zeigte eine Retentionszunahme bei abnehmender DST. Dabei konnte keine weitere Retentionsverbesserung bei DST-Werten unterhalb von ca. 60 mN m^{-1} erzielt werden.

Nachdem der Tropfen auf der Blattoberfläche gelandet ist, verdunstet Wasser unter Feldbedingungen aus dem Sprühtropfen innerhalb weniger Sekunden bis Minuten. Da das Auskristallisieren der Aktivsubstanz zwingend vermieden werden muss, werden sog. *„humectants“* (dt. Feuchthaltemittel) als Tankmix-Adjuvantien eingesetzt, um die Aktivsubstanz in Lösung zu halten. Die Fähigkeit von Tensiden, Wasser aus der umgebenden Atmosphäre zu binden, wurde mit Hilfe von Wassersorptionsisothermen umfassend analysiert (vgl. Kapitel II). Diese Isothermen zeigten einen exponentiellen Verlauf mit einem steilen Anstieg der Wassersorption, beginnend ab ca. 60 bis 70% RH (relative Luftfeuchte). Dabei zeigten Spans eine geringere Wassersorption als die polyethoxylierten Tenside (Tweens und Genapol O). Die Beziehung zwischen dem Wassersorptionsverhalten und der molekularen Struktur der Tenside wurde als sog. *„humectant Aktivität“* betrachtet. Speziell für die Klasse der Genapol O Tenside, wurde mit zunehmenden Ethylenoxidgehalt (EO) eine Zunahme der *„humectant Aktivität“* nachgewiesen. Es konnte jedoch auch gezeigt werden, dass die Wassersorption über alle Klassen der hier ausgewählten Tenside eher mit dem *„hydrophilic-lipophilic-balance“*- Wert (HLB) als mit dem EO-Gehalt korreliert.

Die Kutikula ist eine Membran, die alle oberirdischen Pflanzenorgane bedeckt. Damit stellt sie die wichtigste transportlimitierende Barriere für die Aufnahme von Pflanzenschutzmittelwirkstoffen dar. Um die Wirkung von Adjuvantien auf die Penetration des lipophilen Herbizids Pinoxaden (PXD) zu bestimmen, wurden *in vitro* Penetrationsexperimente durch eine astomatäre Modellkutikula durchgeführt (vgl. Kapitel III). Um den Einfluss verschiedener Wirkmechanismen, wie z.B. die der *„humectant"*- Eigenschaft zu verstehen, wurden diese Versuche unter drei verschiedenen Luftfeuchtebedingungen durchgeführt. Hierbei konnte kein klarer Zusammenhang zwischen der relativen Luftfeuchte und der PXD-Penetration nachgewiesen werden. Eine Ursache dafür könnte sein, dass sich Luftfeuchteeffekte eher auf hydrophile als auf lipophile Stoffe auswirken. Vielmehr wurde deutlich, dass hier eine komplexe Kombination aus verschiedenen Wirkmechanismen, wie z.B. Spreitungs-, „*humectant"*- und Weichmachereffekte, zum Tragen kommt.
Um den Einfluss von Adjuvantien auf die *in vivo* Wirkung von PXD zu analysieren, wurden Gewächshausstudien mit fünf verschiedenen Ungräsern durchgeführt (vgl. Kapitel III). Da die Applikation von Pflanzenschutzwirkstoffen auch deren nachfolgende Wirkung auf lebende Pflanzen, wie z.B. Translokationsprozesse *in planta* und speziesspezifische physiologische Effekte beinhaltet, kann diese Untersuchung helfen, die Situation auf dem Feld besser zu simulieren. Durch die sowohl verschiedenen Pflanzenspezies als auch PXD-Konzentrationen variierte die absolute Schädigung der Ungräser stark. Dennoch kam es zur gleichen Reihenfolge der Auswirkung der Adjuvantien wie in den *in vitro* Kutikula-Penetrationsversuchen: Tween 20 > Tween 80 > Span 20 ≥ Span 80.

Somit konnte in der vorliegenden Arbeit zum ersten Mal gezeigt werden, dass Erkenntnisse aus Laborversuchen, die die Wirkmechanismen von Adjuvantien betreffen, erfolgreich auf die Sprayapplikation auf Pflanzen übertragen werden können. Um eine systematische Herleitung der Wirkmechanismen von Adjuvantien abschließend zusammenzufassen, vergleichen und bewerten zu können, wurde dies mit Hilfe von Netzdiagrammen grafisch dargestellt (vgl. Zusammenfassende Diskussion und Ausblick). Dabei konnten Zusammenhänge zwischen strukturellen Ähnlichkeiten von Adjuvantien und deren Wirkmechanismen gefunden werden.

Tween 20 und Tween 80 beispielsweise deckten ein sehr breites Spektrum an Mechanismen ab, zeigten dabei aber keinen herausragenden Wirkmechanismus einen bestimmten Prozess betreffend. Im Gegensatz dazu wiesen die nicht-ethoxylierten Span 20 und Span 80 hauptsächlich nur den oberflächenaktiven Mechanismus auf. Fast alle Adjuvantien, die in dieser Arbeit analysiert wurden, stellen komplexe polydisperse Mischungen dar, denen eine komplizierte Verteilung von EO-Gruppen und aliphatischen Ketten zugrunde liegt. Aus den Ergebnissen der vorliegenden Arbeit kann gemutmaßt werden, dass Adjuvantien mit einer eher breiten EO-Verteilung ein breiteres Anwendungsspektrum bieten können als Adjuvantien mit einer kleineren Verteilung. Es lässt sich vermuten, dass durch das Vorhandensein einer enormen Vielzahl einzelner Moleküle, die jeweils einen individuellen spezifischen physikalisch-chemischen Charakter aufweisen, ein großes Spektrum von Eigenschaften bezüglich der Sprayapplikation abgedeckt wird.

ABBREVIATIONS

Δc	Concentration gradient
A	Area
ACCase	Acetyl-CoA carboxylase
AI	Active ingredient
ALOMY	*Alopecurus myosuroides*
ASTM	American society for testing and materials
AVEFA	*Avena fatua*
BBCH	„Biol. Bundesanstalt, Bundessortenamt und chemische Industrie“
c	Concentration
CA	Contact angle (°)
CM	Cuticular membrane
cmc	Critical micelle concentration
D	Diffusion coefficient
DAA	Days after application
dm	Difference in mass
DST	Dynamic surface tension (mN m^{-1})
EC	Emulsion concentrate
EO	Ethylene oxide
EW	Emulsion in water
F	Flow (µg s^{-1})
GC	Gas chromatography
HLB	Hydrophilic-lipophilic balance
HRAC	Herbicide resistance action committee
J	Flux or flow density (mol m^{-2} s^{-1})
k	Rate constant
$K_{C/W}$	Cuticle/water partition coefficient
$K_{O/W}$	1-octanol/water partition coefficient
LC	Liquid chromatography
LOLMU	*Lolium multiflorum*
MD	Median
MoA	Mode of action
M_0	Mass at time 0
MS	Mass spectrometer
M_t	Mass at time t
MV	Molar volume (m^3 mol^{-1})
MW	Molecular weight (g mol^{-1})
MX	Matrix membrane
n_{ws}	humectant activity, number of mols of water sorbed per mol surfactant
n_{ws}/n_O	humectant activity per oxygen content of surfactant
P	Permeance (m s^{-1})
POE	Polyoxyethylene
PXD	Pinoxaden
RH	Relative humidity (%)
SC	Suspension concentrate
SD	Standard deviation
SEM	Scanning electron microscopy
SIR	Selected ion recording

SETVI	*Setaria viridis*
SOFP	Simulation of foliar penetration
STeq	Surface tension at equilibrium (mN m^{-1})
T	Temperature (°C)
t	Time
TEHP	Tris(2-ethylhexyl)phosphate
TIC	Total ion count
TRZAW	*Triticum aestivum*
UDOS	Unilateral desorption from the outer surface
UPLC	Ultra high pressure liquid chromatography
σ	Surface tension and/or surface free energy (mN m^{-1})
σ_D	Dispersive fraction of surface tension
σ_L	Surface tension of a liquid phase
σ_{LS}	Interfacial tension between solid and liquid phase
σ_P	Polar fraction of surface tension
σ_S	Surface tension of a solid phase

1 INTRODUCTION

1.1 Challenges of crop protection application

The global population will continue to grow by 70 million per year to 9 billion by the middle of this century (Godfray *et al.,* 2010). Despite the fact that food production is rapidly growing for more than 50 years, one in seven people is still suffering from micronutrient malnourishment today (Godfray *et al.,* 2010). In the near future, enormous challenges of making agricultural production sustainable while controlling greenhouse gas emissions need to be overcome. There is a great demand for scientific and technological innovations in the agricultural production systems, because of factors like land and water competition, limited energy resources, environmental factors and pests (Popp *et al.,* 2012). Since the loss potential for crops, caused by pests worldwide, varied from less than 50% (on barley) to more than 80% (on sugar beet and cotton) (Oerke & Dehne, 2004), chemical plant protection plays a crucial role in modern conventional agricultural systems (Castro *et al.,* 2014; Foy, 1993). Although, the general public has a critical opinion in determining the role of pesticides in agriculture, the annual global agrochemical market is about 3 million tons associated with expenditures around USD 40 billion (Popp, 2011).

A crop protection product includes the active ingredient (AI) which is the chemical substance that is biologically active, also known as biocide (Krämer *et al.,* 2012). Depending on the target organisms being in general either weeds, pests or plant pathogens, AIs are classified as herbicides, insecticides or fungicides (Börner, 2009). This definition includes that the AI has to come into contact with the organism targeted to control. By this it is obvious that these biocidal compounds have different modes of action (MoA) when applied to the field (Krämer *et al.,* 2012). The MoA of a chemical determines the location and the basic mechanism of action. For example, herbicides have different MoA affecting the light process, the cell metabolism or the growth and cell division of weeds (Krämer *et al.,* 2012). Depending on the cellular compartments and the location of the key enzymes which need to be inhibited, AIs need to be transported and bind to this target where they can develop their full potential.

Therefore, mechanisms of translocation of AIs inside the plant also must be considered. The so-called acropetal translocation signifies the transport towards the new growing leaf tips and the apical meristems (Börner, 2009). The transport of chemicals to the leaf basis and branches is named basipetal translocation. AIs can also have translaminar properties acting mainly on the opposing, untreated side of the leaf. Moreover, the transport routes of molecules in plants can be distinguished between the apoplastic, the symplastic and the root systemic transport (Steudle & Frensch, 1996). While the apoplastic pathway transports the AIs via the xylem sap, they can also be transported together with assimilates with the phloem stream (symplastic transport) (Castro *et al.,* 2014). So-called root systemic AIs are taken up by the root system being further translocated (Fernández *et al.,* 2013, chapter 4). This action premises the chemical application via the soil. In this work, the foliar application will be in focus, considering the spray process on plant leaves and subsequently the uptake by the plant. Most agrochemicals have the purpose to operate systemically in all parts of the plant (Buchholz & Trapp, 2016), as described by the different routes of transport (Börner, 2009). In contrast to that, so-called contact insecticides are examples for AIs which must not be taken up by the plant necessarily because of their direct action on target insects (Börner, 2009; Buchholz & Trapp, 2016). In conclusion, it is important to notice that an AI must not be taken up by the plant in any case, but there are also substances that have to stay outside the plant or effect another target organism.

1.2 The plant cuticular membrane

All aerial organs of higher land-living plants are covered by a thin morphological layer called the *'plant cuticle'* (Martin & Juniper, 1970). The development of the cuticle as a hydrophobic protective coverage was one of the key innovations enabling plants to overcome their physiological complications connected to the new environment, when plants moved from their aqueous habitat to the drier atmosphere on land, approximately 460 million years ago (Riederer & Müller, 2006).

The primary function of the cuticle is to protect the plant from uncontrolled water loss to the atmosphere and so it is the first barrier between the interior of the plant and the surrounding atmosphere (Burghardt & Riederer, 2006; Riederer & Schreiber, 2001) Generally, the plant cuticle consists of a cross-linked biopolymer matrix (cutin) in which long-chain aliphatic and cyclic plant waxes are embedded and overlaid (Heredia, 2003). Cuticular waxes are diverse mixtures consisting mainly of alkanes, alkanols, alkanoic acids, alkylesters and cyclic compounds like triterpenoids (Jetter *et al.,* 2006; Yeats & Rose, 2013). The complex wax composition and amount varies not only across species, but also across plant organs and during plant development. The cuticle structure as presented by (Bird, 2008) (Figure 1) distinguishes a number of different main zones.

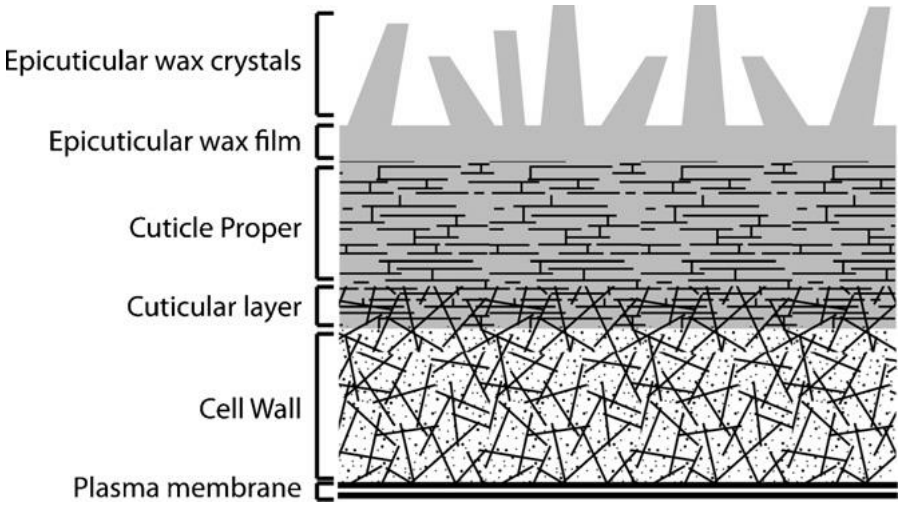

Figure 1: Schematic cross-section of the plant cuticle (Bird, 2008).

The cuticular layer, containing mainly cutin, embedded waxes and polysaccharides is bonded to periclinal walls of the epidermal cells by a pectin-rich layer. This pectinaceous layer is equivalent to the middle lamella. The hydrolysis of this layer by pectinolytic enzymes enables the isolation of the cuticular membranes of many plant species (Orgell, 1955). The cuticle proper is located on the cuticular layer and contains no more cellulose or cell wall components. Many species lack the cuticle proper, but in most cases the layer is described as a lamellate structure (Jeffree, 1996). The outermost layer of the plant cuticle is made of epicuticular waxes which are of different morphology. Most plants have thin films, but there are also diverse three-dimensional structures with highly morphological varieties (Buchholz, 2006). Depending on their chemical composition, epicuticular waxes may form amorphous films, granules, or crystalline structures of various shapes (Barthlott *et al.,* 1998) (see chapter I).

Depending on the plant species and the ontogeny, leaf cuticles vary tremendously in their thickness, ranging from 0.1 µm to about 10 µm (Holloway, 1994; Jeffree, 1996). It was shown that the cuticle thickness does not correlate with permeability for water and other solutes (Schönherr, 1982; Kerstiens, 1996; Riederer & Schreiber, 2001; Jetter & Riederer, 2016). Furthermore, a lot of effort was put into the elucidation of the relationship between the cuticular permeability and environmental conditions like temperature and humidity (Martin & Juniper, 1970; Schreiber 2001; Baur *et al.,* 1997c). Many studies report inconsistent results and those fundamental questions have been discussed controversially until today (Martin & Juniper, 1970).

Being the first barrier between the interior of the plant and the surrounding atmosphere, the cuticle has other important functions like to protect the plant against abiotic and biotic stresses (Yeats & Rose, 2013; Zabka *et al.,* 2008). Plants are exposed to abiotic and biotic environmental factors, for example mechanical abrasion by wind and rain, UV radiation, xenobiotics, pests and plant pathogens (Kerstiens, 1996; Serrano *et al.,* 2015). Therefore, the cuticle is also the first contact layer and obstacle for plant protection agents to penetrate and then to be further translocated to the target cell.

Transport mechanisms across the cuticular membrane considering the hydrophilic and the lipophilic pathway

Although the main function of the cuticle is to protect the plant against uncontrolled water loss, it is not a complete barrier. Water molecules, minerals and nutrients, like carbohydrates, are able to cross the cuticle as leachates (Tukey, 1970; van der Wal & Leveau, 2011) or by transpiration (Burghardt & Riederer, 2006). Whereas water transpiration across the cuticle is generally believed to be of minor relevance compared to water loss through stomatal pores, (Martin & Juniper, 1970) transpiration via the cuticle occurs in a considerable extent. Compounds like polar electrolytes and non-electrolytes and apolar organics like most agrochemicals can enter the plant after foliar application via cuticular pathways, when stomatal pores are closed (Riederer & Schreiber, 1995).

In the literature, two basic routes of solute penetration across the plant cuticle are extensively discussed: the *'lipophilic pathway'* (Niederl *et al.,* 1998; Baur, 1998; Schönherr *et al.,* 2001; Coret & Chamel, 1994), and the *'hydrophilic route'* (Schönherr, 2002; Schönherr & Luber, 2001; Schreiber, 2005). Since foliar application plays a pivotal role in plant protection, cuticular permeability of agrochemicals has been studied intensively. Most agrochemicals and other xenobiotics have a non-ionic and lipophilic nature, thus the lipophilic pathway was extensively studied (Schreiber, 2005). The mobility of AIs is discussed to be tremendously accelerated via the lipophilic pathway by substances that are add to the agrochemical solution acting as plasticising compounds, mainly in the cuticle, especially in the waxes (Figure 2) (Schreiber *et al.,* 1996; Riederer & Friedmann, 2006; Schreiber, 2006). On the other hand, the hydrophilic pathway was considered to enable penetration of smaller ionic and also non-ionic water-soluble molecules (Schreiber, 2005; Popp *et al.,* 2005; Arand *et al.,* 2010; Remus-Emsermann *et al.,* 2011; Schlegel *et al.,* 2005). It was suggested that hydrated polar functional groups constitute the hydrophilic route (Stock *et al.,* 1992) across polysaccharide strands (Figure 2). Hygroscopic substances or so-called *'humectants'* (Tu & Randall, 2003) are added to the spray solution in order to re-hydrate a droplet deposit by the attraction of water from the atmosphere (Ramsey *et al.,* 2005). They are discussed to improve the AI uptake via the hydrophilic route by this mechanisms (Stock & Briggs, 2000; Ramsey *et al.,* 2015).

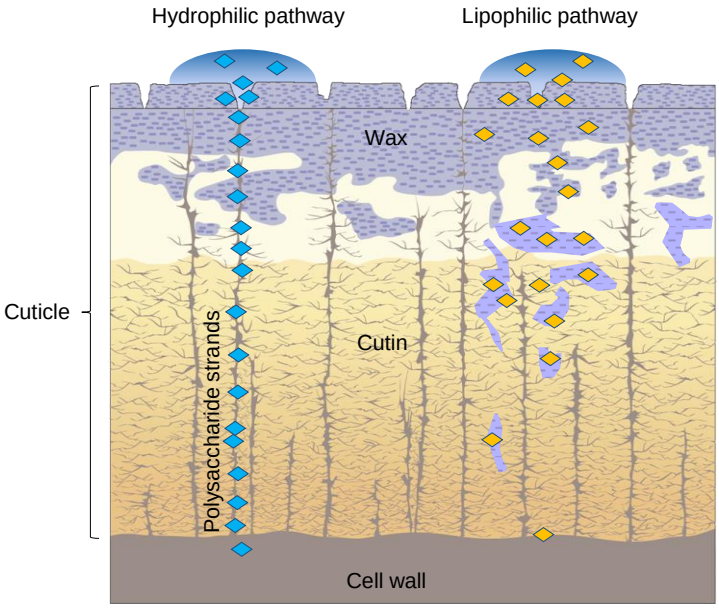

Figure 2: Schematic model of a cross-section of a plant cuticle, which tries to illustrate the lipophilic and the hydrophilic pathway (the figure is not to scale) (modified after a design by Markus Riederer). Blue symbols identify polar compounds, which might penetrate the cuticle along polysaccharide strands bearing hydrated polar functional groups. Orange symbols indicate lipophilic molecules, which may diffuse mainly across the rather apolar wax fraction in the cuticle.

Transport properties of molecules through cuticular waxes

The fundamental knowledge about physical and chemical mechanisms of the cuticular penetration process is a prerequisite for understanding the mode of action (MoA) of agrochemicals and their formulation ingredients. The general mechanism of transport through the plant cuticle can be described as a simple diffusion process along a gradient of chemical potential. The main transport limiting barriers for the diffusion process of water and solutes are cuticular waxes (Riederer & Schreiber, 1995).

A schematic, structural model of the arrangement of plant waxes, given by Riederer & Schreiber (1995), can be used to explain the transport limiting functions of plant waxes (Figure 3). Two basic regions or phases considering diffusion pathways can be distinguished: crystalline flakes are impermeable for water and solutes are embedded in an amorphous matrix.

Crystalline platelets consist of long chain aliphatic wax constituents are aligned highly regularly. These dense aggregates might be arranged in parallel across the cuticle. Moreover, the factor temperature also plays an important role considering the crystalline wax phases. At lower temperatures, hydrocarbon chains assemble

in an orthorhombic crystal lattice whereas at high temperatures, just below the melting point, they may structure in a hexagonal matrix (Riederer & Schreiber, 1995). Because of reducing the volume of the barrier, which is available for diffusion pathways, crystalline impermeable platelets are mainly responsible for the effective barrier function of the plant cuticle. Therefore, the diffusion pathway of a solute is more tortuous and thus much longer (Figure 3). Consequently, the diffusion coefficient might be very low. This would also affirm the finding that cuticle thickness does not correlate with the permeability of water (Schönherr, 1982; Jetter & Riederer, 2016) and other solutes. Crystalline flakes are embedded into a solid but amorphous matrix which allows a higher mobility of diffusing molecules. According to this structural model, diffusion pathways through plant waxes can be explained.

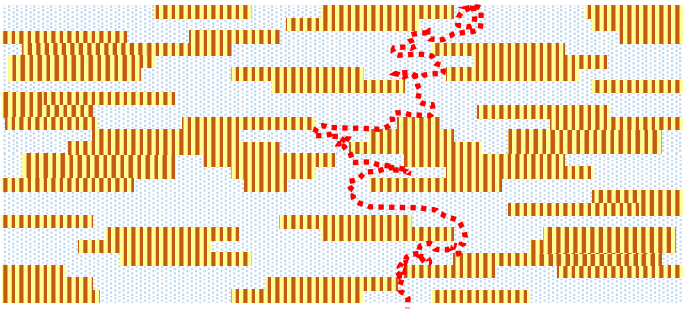

Figure 3: Structural model of the wax barrier (modified from Riederer & Schreiber, 1995). Illustration of path of diffusion of solutes (red) across amorphous wax regions (blue) and crystalline wax regions (orange).

Effects of accelerating compounds

So-called '*accelerators'* or '*plasticisers'* are compounds known to enhance the uptake of AIs into the plant by reversibly changing the structural properties of the plant cuticle (Schreiber *et al.,*1996). They might be absorbed in cuticular waxes as a result to increase fluidity of amorphous regions (Riederer & Schreiber, 1995). This results in a higher mobility of compounds diffusing through the cuticle, especially for molecules having a high lipophilic potential (Stock & Holloway, 1993; Burghardt *et al.,* 1998; Baur *et al.,* 1997a). It is hypothesised that these substances decrease the size of crystalline platelets and therefore enhance the fluidity of the amorphous phase (Figure 4) (Schreiber *et al.,*1996). The diffusion pathway through the wax would be shorter because of the decreased amount of impermeable

crystalline obstacles. Consequently, the diffusion coefficient would be enhanced. Thus, the overall resistance of the wax barrier of the plant cuticle would be reduced.

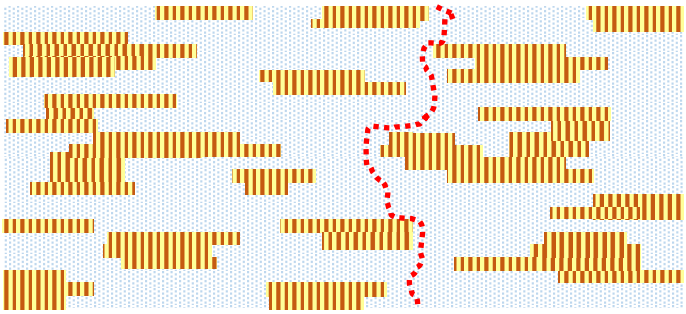

Figure 4: Plasticising effect of penetration aids: size of crystalline platelets (orange) decreases and fluidity of amorphous regions (blue) increases. The resistance of the wax barrier might be reduced.

As an example for a plasticising molecule, the organophosphate tris(2-ethylhexyl)phosphate (short: TEHP, see Figure 5) is used as an accelerating compound in formulations of plant protection agents. TEHP is also used for softening or deteriorating plastics and elastomers. In this work, TEHP was used to confirm the accelerating effect on the penetration of the plant cuticle.

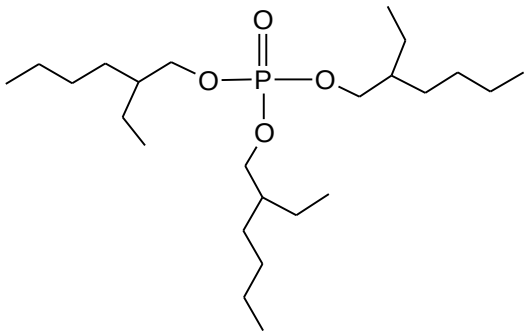

Figure 5: Chemical structure of tris(2-ethylhexyl)phosphate (TEHP; log K_{OW} = 9.49 (Bergman *et al.,* 2012) which is known to have strong accelerating effects on the uptake of the herbicide Pinoxaden.

1.3 Mode of action of adjuvants

With these essential reflections about translocation and transport properties of the chemical across the cuticle and target organisms in plant protection, the challenges of biodelivery of agrochemicals become clearly evident. Being aware of these biodelivery issues at any time is central for the farmer who is the final consumer of the agrochemical product. In conclusion, the requirement of precise targeting is the crucial issue for researchers and consumers. An effective biodelivery can be reached exclusively when the application parameters are optimised by choosing the right compound with the exact concentration at the right time of application (environmental conditions). If these aspects are not optimised, chemical wastage and environmental pollution can occur which are restricted by stringent toxicological and ecotoxicological regulations, because the target organism is not the only organism which comes in contact with the chemical (Rodham, 2000). All these aspects of biodelivery and product performance put greater demand to the formulation of the AI which can be understood as a kind of vehicle for the biocide. The formulation can be designed as a complex mixture of numerous substances and can have a significant impact on the stability, solubility and enhancing effects. Besides, handling, storage, technical application and safety issues can be controlled and improved by the formulation. Moreover, several AIs are innately biologically inactive and need other substances added to activate or they have physico-chemical properties making them difficult to apply because of insolubility. Therefore, a crop protection product is only effective if the diverse mixture of auxiliary substances is right. So-called '*adjuvants'* are known to be the best tools to improve agrochemical application (Green, 2000; Green & Beestman, 2007).

According to the American Society for Testing and Materials (ASTM), an adjuvant can be described as '*a material added to a tank mix to aid or modify the action of an agrichemical, or the physical characteristics of the mixture*' (ASTM - American Society for Testing and Materials (1999) Designation E 1519-95). This definition is only one of many different descriptions trying to convey a functional understanding of adjuvants. Basically, the term *'adjuvant'* is derived from the Latin word *'adjuvare'* which means 'to help' or 'to aid'. Therefore, it is commonly known that adjuvants enhance the efficacy and the foliar uptake of AIs (Foy, 1993; Kirkwood 1993; Holloway, 1998; Zabkiewicz, 2000). But on the other hand, there are different

perspectives of defining the beneficial usage of how adjuvants can improve the application process. To discuss the properties of adjuvants in a structured manner, a consistent form of classification is of high importance. Hazen (2000) discussed in detail different aspects as terminology, classification and chemistry of adjuvants. Unfortunately, there is no standard system of taxonomy used by all agrochemical manufacturers until now.

Kirkwood (1993) tried to define adjuvants based on their MoA. '*The mechanisms by which adjuvants convey beneficial effects to the action of herbicides may involve effects on (1) surface phenomena, (2) penetration via the cuticle or stomatal pores, and (3) tissue absorption and systemicity'*(Kirkwood; 1993). A likewise view, based on the potential sites of action of the adjuvants, was written by Stock & Holloway (1993) who suggested four main locations where the uptake of an agrochemical could possibly be enhanced: (1) on the surface of the cuticle, (2) within the cuticle itself, (3) in the outer epidermal wall underneath the cuticle or (4) at the cell membrane of internal tissues.

However, the most common opinion about the classification of adjuvants is the division into two basic types according to their function and usage based on suggestions by Kirkwood (1994). Later, the American Society for Testing and Materials (1999) considered the separation of adjuvants into utility and activator adjuvants, as several others like Hess (1999), Penner (2000) and McMullen (2000) did. While utility adjuvants modify the physical properties of the spray liquid (therefore also known as spray modifiers) (Penner, 2000), activators should enhance the biological efficacy of the AI (McMullen, 2000). Utility adjuvants are mainly used to stabilise the tank mix by changing its properties but not directly enhancing the AI activity. They are used, for example for pH adjustment and buffering, as compatibility agents, foaming and antifoaming agents, dyes, hygroscopic substances, wetting agents (spreaders), solubility agents, water conditioners, drift controllers and retention aids (stickers) (Tu & Randall, 2003).

The potential of activator adjuvants is more difficult to examine because of many interacting variables that can change the bioefficacy considerably. The most common types of activator adjuvants are surfactants (Penner, 2000). The term *'surfactant'* is derived from *'surface active agent'* and should not mixed-up with the term *'adjuvant'*, since adjuvants are not limited to surfactants (Penner, 2000).

Surfactants and oil adjuvants can influence the absorption of the herbicide by a direct interaction with the plant cuticle (McMullen, 2000). Additionally, surfactants having the ability to change surface tension properties of a fluid (Janku *et al.,* 2012), can also be defined as spray additives that facilitate or enhance the emulsifying, dispersing, spreading, sticking or wetting properties of liquids (Hess, 1999). Conversely, these properties were just described by the spray modifying utility agents.

Obviously, this classification involves many overlapping functions, as surfactants are also spray modifiers and some of them can have biocidal effects on their own (Tu & Randall, 2003). Because of this diverse and broad usage, surfactants can have more than only one distinct function during the application process (Hazen, 2000). As a result, surfactants are the most widely used products of the chemical industry and probably the most important group of all adjuvants (Tu & Randall, 2003) for foliar application.

1.4 Surfactants and their physicochemical properties

Surface active agents (short: surfactants) are defined by their amphiphilic character, combining a nonpolar lipophilic and a polar hydrophilic portion in one molecule, which is the most important requirement on physiochemical actions (Castro *et al.,* 2014). The lipophilic portion usually consists of an elongated alkyl chain and is often just called the *'tail'*. The polar hydrophilic part is called the *'head'* (Semenov *et al.,* 2015). They can have a different charge: nonionic, anionic, cationic or amphoteric (Moroi, 1992, chapter 2). The ratio between the polar and unpolar fraction of a surfactant molecule is described by the so-called '*HLB-value' ('hydrophilic-lipophilic balance'*) (Griffin, 1954) and can be used to predict the surfactant properties of a molecule.

The most important and fundamental physiochemical property of surfactants is the ability to lower interfacial tension between two phases (Rosen, 1989, chapter 1). Because of this behaviour they are used as emulsifiers, dispersing agents, detergents, foaming agents and wetting agents, for example. The broad utilization in cosmetics, pharmaceutics as well as in food and plant protection products makes surfactants play such an important role in life sciences (Rosen, 1989, chapter 1).

The ability to adsorb at surfaces or more general at interfaces is based on their chemical structure. The consequence of this adsorption is that surfactants trigger a reduction of the surface tension or interfacial tension which is physically measurable with the help of tensiometers. In the case of foliar applied plant protection products, the interface between an aqueous phase, like a spray droplet and the surrounding air has to be considered.

From an energetic point of view, surfactant molecules are preferred to stay in the interior of the volume phase or bulk phase rather than at the surface, because a molecule meets less molecules with which it can build interactions at the surface, than at the bulk phase. In contrast, due to the special amphiphilic structure of surfactants, their presence at the surface is more beneficial, and therefore the surface tension can be efficiently reduced already when only a small amount of surfactants is present (Rosen, 1989, chapter 1).

If the surface is fully saturated with surfactant molecules (Fig. 6.1), so-called *'micelles'* are produced in the bulk phase (Moroi, 1992, chapter 1). Micelles are diverse clusters of single surfactant molecules that structure in a spherical,

cylindrical, lamellar or vesical shape (Preston, 1948). They have the ability to incorporate substances which are not soluble in the bulk liquid (Preston, 1948). There is a characteristic concentration, depending on the nature of the surfactant, at which micelles start to build. This typical transition concentration is described as the *'critical micelle concentration'* (CMC), which is an important individual value for each surfactant. This action of surfactants as micelle forming substances is of special importance for the application as detergency and solubilisation aids (Preston, 1948).

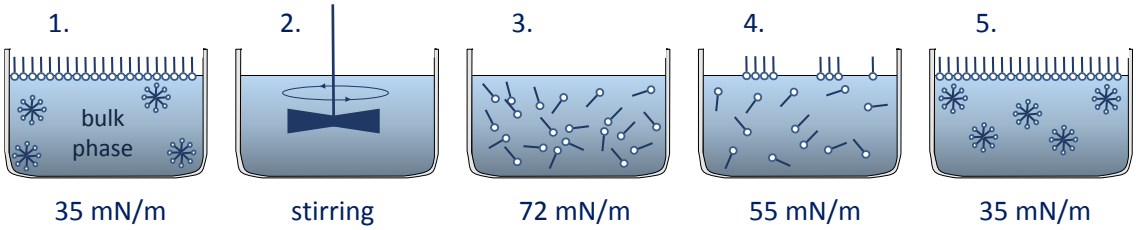

Figure 6: Schematic progress of the molecular mobility of surfactants in an aqueous phase (modified from Krüss GmbH, dynamic surface tension, 04.01.2016).

The interface between the aqueous phase and the surrounding gaseous phase is produced extremely quickly.

The surface tension of pure water has a typical value of 72.75 mN m^{-1} at 20 °C (Vargaftik *et al.,* 1983). If the surface is completely saturated with surfactant molecules (Fig. 6.1), the surface tension is reduced to a significant degree. When stirring these surfactant dilution, molecules become mobile (Fig. 6.2). Immediately after stopping stirring, no more molecules are located at the surface and the surface tension has the same value as the pure water (Fig. 6.3). Then, the value reduces until the surfactant specific equilibrium value is recovered (Fig. 6.4 -5). The time required for recovering the surface saturation after stirring depends on the specific diffusion and adsorption rate of a surfactant. In conclusion, also the kinetics of the interface formation have to be kept in mind considering high speed processes such as spraying of foliar applied liquids.

This work focusses on the diverse properties of polydisperse non-ionic surfactants concerning the spray application process. The following descriptions will give a general introduction to the main functions of surfactants used in this study. A

detailed list of substances including their chemical and physical properties can be found at the end of this chapter (Table 1).

1.4.1 Sorbitan fatty acid esters

The non-ionic surface active sorbitan fatty acid esters, or short sorbitan esters, are a mixture of esters formed from different fatty acids. The hydrophilic part of the molecules consist of a sorbitan ring derived from sorbitol. As sorbitan esters were achieved from Croda (Nettetal, Germany), the corresponding tradename *'Span'* will be adopted. Spans are widely used in pharmaceutical, cosmetical, healthcare and food products as emulsifiers and detergents.

The nomenclature was evolved by Imperial Chemical Industries (ICI Inc.) using two numbers after the tradename. The first number represents the esterified acid:

2 = lauric acid (12:0)
4 = palmitic acid (16:0)
6 = stearic acid (18:0)
8 = oleic acid (18:1)

The second number describes the type of esterification:

0 = monoester
5 = triester

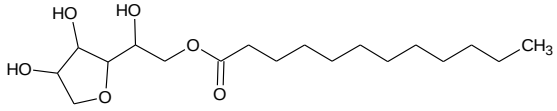

Figure 7: Chemical structure of sorbitan fatty acid ester with a lauric acid as alkyl chain (Span 20).

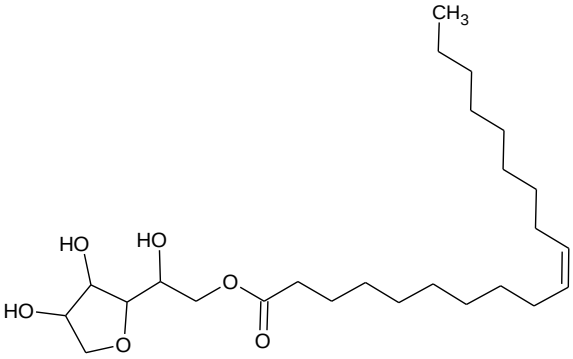

Figure 8: Chemical structure of sorbitan fatty acid ester with an oleic acid as alkyl chain (Span 80).

For example, the structure of Span 20 (Figure 7), carries one saturated lauric acid as lipophilic tail while Span 80 (Figure 8) is esterified with an unsaturated oleic acid which results in the branching of the alkyl chain (Croda, Product Range Home Care: 'Span and Tween').

Despite of this clear classification, Spans are diverse polydisperse mixtures differing in their fatty acid distribution. As an example, Span 20 carries a lauric acid as lipophilic group, but this is only the mean fatty acid for this product. A batch of Span 20 inhibits homologues bearing different fatty acids as shown before. This specific distribution is variable and depends on the manufacturing process of the supplier (Croda, Product Range Home Care: 'Span and Tween').

1.4.2 Polyoxyethylene sorbitan fatty acid esters

The polyethoxylation of Spans results in an extremely wide range of physico-chemical potential of this surfactant class (Rosen, 1989, chapter 1; Rothman, 1982; Brandner, 1998; Borisov *et al.,* 2011). Polyoxyethylene (POE) sorbitan fatty acid esters or short polysorbates, have many common trade names including *'Scattics', 'Alkest', 'Canarcel'*, and *'Tween'*. According to the supplying company Croda (Nettetal, Germany), the trade name *'Tween'* will be adopted for further descriptions of polysorbates in this work. Tweens are broadly used in agrochemical, food, cosmetical and pharmaceutical industries due to their formulation flexibility, low toxicity, cost effectiveness, biocompatibility and good stabilizing properties (Borisov *et al.,* 2011).

Tweens are highly heterogenic mixtures of fatty acid esters with sorbitol, polymerised with approximately 20 mols of ethylene oxide (EO) (Borisov *et al.,* 2011). The nomenclature for Tweens is basically similar to the as Spans shown before. The difference is that the second number is known to describe the type of esterification and also the mean number of EO units (Croda, Product Range Home Care: 'Span and Tween'):

0 = monoester with 20 EO units
5 = triester with 20 EO units
1 = monoester with 5 EO units

The chemical structure of Tweens consists either of a saturated fatty acid (Figure 9), e.g. for Tween 20 (Figure 11) or of branched-chain, unsaturated fatty acids (Figure 10) e.g. for Tween 80 (Figure 12). The molecular structure also includes four different locations/arms where ethoxylation can take place (marked with the letters w – z).

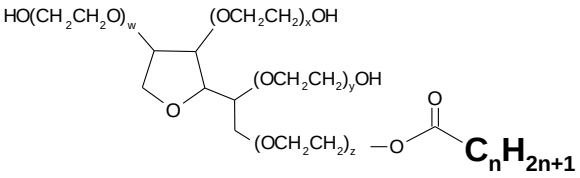

Figure 9: General chemical structure of a polyoxyetylene sorbitan mono fatty acid, where the fatty acid is saturated (e.g. Tween 20, Tween 40, Tween 60).

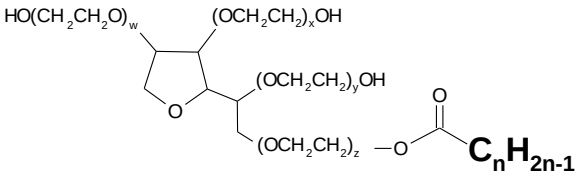

Figure 10: General chemical structure of a polyoxyetylene sorbitan mono fatty acid, where the fatty acid is unsaturated (e.g. Tween 80, Tween 81).

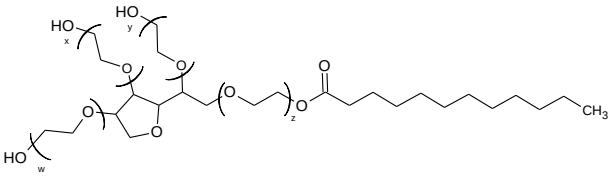

Figure 11: Chemical structure of Tween 20.

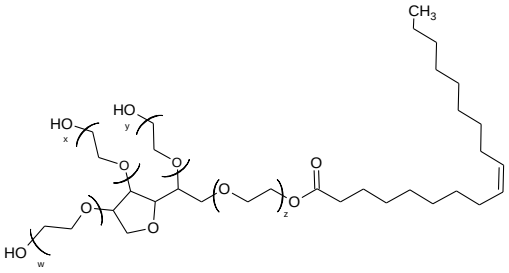

Figure 12: Chemical structure of Tween 80 or Tween 81.

Distribution of ethylene oxide (EO)

The molecular size distribution of the polar head depends on the number of EO units added during polymerisation (Moroi, 1992, chapter 2). The number *n* of a macromolecular chain of a basic molecule is the degree of polymerisation (n = w+x+y+z). This degree of polymerisation is always an average value. The general expression for the mole fraction of the polar portion of a surfactant sample typically follows a *'Poisson distribution'* (Borisov *et al.,* 2011; Rothman, 1982) (Figure 13). It was suggested that the number of EO units, which are added, remains constant throughout polymerisation (Borisov *et al.,* 2011).

Borisov *et al.* (2011) and Brandner (1998) stated that Tweens with the structural formula POE 20 sorbitan fatty acid ester contained on average more than only 20 EO units. Accordingly, this single term does not represent the real major EO content as it is commonly stated for the formal chemical definition. For example, Borisov *et al.* (2011) found an average content of 26 EO units (6.7 EO units per arm) for Tween 20 and Tween 80 (Figure 13).

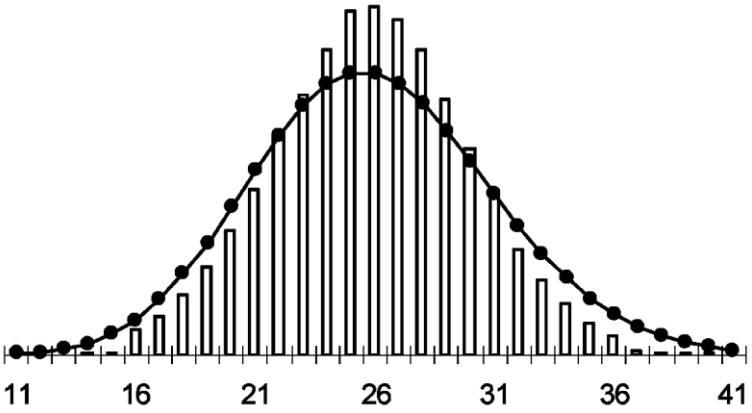

Figure 13: EO distribution of Tween 20 (based on the major component POE sorbitan monolaurate) follows approximately a Poisson distribution with an average EO number of 26 (diagram derived from Borisov *et al.,* 2011).

They ascertained that this average number is independent from the ester nature and the degree of esterification. Nevertheless, for calculations carried out in this work based on the EO distribution of Tweens, the average number of 20 EO units was adopted, due to general standardisation.

Distribution of fatty acids

The heterogeneity of Tweens is not only based on the differing number of EO units per molecule, but also on the nature of fatty acids and their degree of esterification. Borisov *et al.* (2011) identified POE sorbitan monolaurate as a major component of Tween 20. However, they evaluated their finding as '*only showing the tip of the iceberg, as these monoesters account for only about 30% of the total content'* of Tween 20 (Borisov *et al.,* 2011). A large amount of other fatty acid species depending on different batches was found (Figure 14). Interestingly, the relative amounts of unsaturated oleic acid ($C_{18:1}$) in Tween 20 batches ranged statistically significant from 0% to 15%.

In Tween 80, oleates as major components were found as expected having relative amounts of around 75% to 85% (Figure 14). Small amounts of myristic, palmitic, stearic and linoleic acids were found additionally (Figure 14).

Moreover, Borisov *et al.* (2011) revealed the degree of esterification by analytically specifying only the lauric acid component of Tween 20, containing significant amounts of other species, although POE sorbitan *mono*laurate was with 43% the

major component (POE sorbitan *di*laurate = 36.5% and POE sorbitan *tri*laurate = 20.5%).

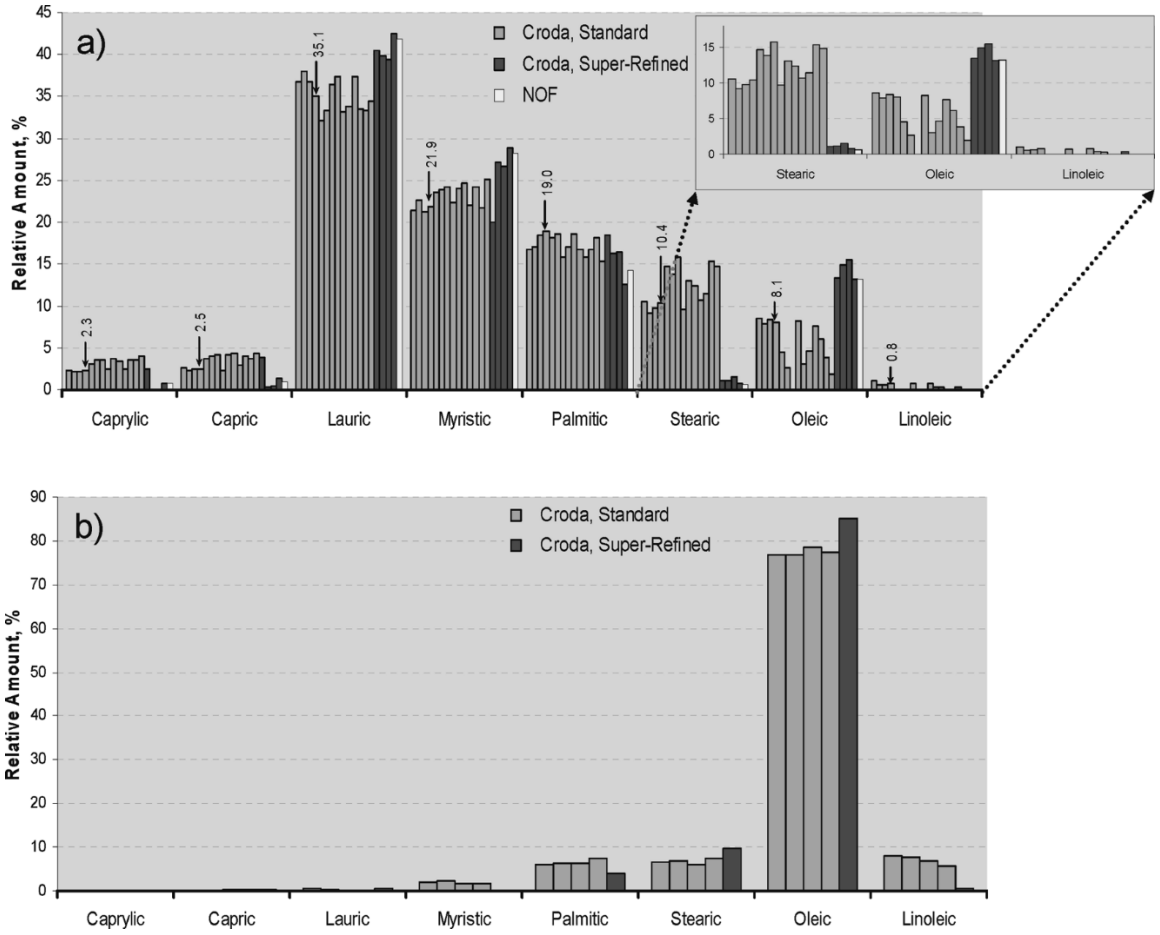

Figure 14: Fatty acid distribution of Tween 20 (a) and Tween 80 (b) based on POE sorbitan monoesters of different batches (diagram derived from Borisov *et al.,* 2011).

In summary, Tweens are highly complex mixtures of different molecules, inherited from their manufacturing process (Brandner, 1998). One batch of Tween consists of a vast amount of single homologues differing not only in the EO content, but also in the location of various polyethoxylations. Furthermore, the fact of variable fatty acid chains increases the amount of combinable structures and thus the complexity in total.

On the one hand, the high structural complexity, due to a broad EO and alkyl chain distribution, makes the class of Tweens so interesting and important for many fields of application of the chemical industry, as they are commonly used e.g. as oil-in-water emulsifiers, stabilisers, wetting agents, solubilisers and dispersants (Borisov *et al.,* 2011). The wide distribution of molecular structures of one product might be

the basis for its broad usage. On the other hand, the disadvantage of this complexity is to determine exactly the chemical background resulting in distinct beneficial physico-chemical properties. Empiric knowledge about the usage of these surfactants often cannot be confirmed by a specific chemical structure, because of the broad spectrum of single homologues.

In the present work, the detailed elucidation of MoA of Tweens was considered because of their general promoting functions in agrochemical formulations. There exist other adjuvants on the agrochemical market that would offer better effects on distinct formulation requirements than Tweens, but the reason for the general intermediate function of some representatives is still unclear. Another important advantage of Tweens is their simple and flexible integration into complex formulations compared to other adjuvants (personal communication Christian Popp). Despite the fact that polysorbates have only a relatively moderate function, it is an interesting, complex surfactant class which provides a structured analysis because of the wide variety of products.

1.4.3 Oleyl alcohol polyglycol ether

Another non-ionic polydisperse surfactant class selected for this work are the oleyl alcohol polyglycol ethers. The tradename *'Genapol O'* was introduced by the company Clariant (Muttenz, Switzerland) and will be adopted for further designations. Genapol O surfactants contain a hydrophilic head with 5, 8, 10 or 20 mean EO units. The lipophilic part consists of an unsaturated oleyl alcohol as the mean alkyl chain. The introduction of a cis double bond leads to the branching of the lipophilic tail (Figure 15). The general chemical formula for Genapol O is $HO(CH_2CH_2O)_n – C_{18}H_{35}$.

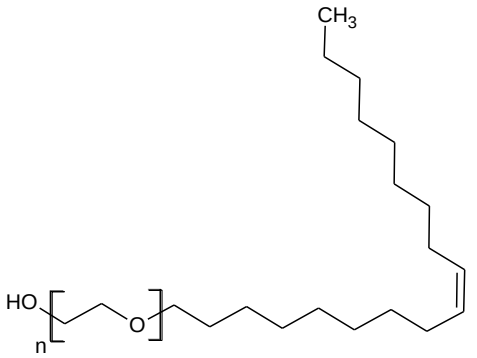

Figure 15: General chemical structure of oleyl alcohol polyglycol ether with a differing degree of ethoxylation.

Genapol O are mainly used as emulsifiers for waxes and organic solvents to produce stable emulsions. Moreover, they are applied as wetting and dispersing agents in industrial cleaning formulations. Beside the Genapol O group, the product range of Clariant includes a variety of other additives e.g. Genapol C (coconut fatty alcohol ethoxylates), Genapol LA (lauryl fatty alcohol ethoxylates) or Genapol X (Iso-tridecy alcohol ethoxylates). The Genapol O group was selected for this study because of the major branched alkyl chain (oleyl alcohol), which can be compared to the Tween 80 series inhibiting an oleic acid as major alkyl chain ($C_{18:1}$).

1.4.4 List of chemicals

Table 1: Selected chemical and physical properties of all substances used for this work

Tradename	Chemical name	CAS number	Mean MW g*mol^{-1}	HLB*	Mean EO content	Appearance	Major Chain length
Span 20[a]	Sorbitan monolaurate	1338-39-2	346.46	8.4	0	liquid	(12:0)
Span 40[b]	Sorbitan monopalmitate	26266-57-9	402.57	7.3	0	pellet-crystals	(16:0)
Span 60[b]	Sorbitan monostearate	1338-41-6	430.61	6.8	0	dry powder	(18:0)
Span 65[b]	Sorbitan tristearate	26658-19-5	963.54	2.3	0	dry powder	(18:0)
Span 80[a]	Sorbitan monooleate	1338-43-8	428.60	6.8	0	liquid	(18:1)
Span 85[a]	Sorbitan trioleate	26266-58-0	957.49	2.3	0	liquid	(18:1)
Tween 20[a]	Polyoxyethylene sorbitan monolaurate	9005-64-5	1227.72	16.7	20	liquid	(12:0)
Tween 40[b]	Polyoxyethylene sorbitan monopalmitate	9005-66-7	1283.57	16.0	20	liquid	(16:0)
Tween 60[b]	Polyoxyethylene sorbitan monostearate	9005-67-8	1311.62	15.7	20	pasty, wax-like	(18:0)
Tween 65[b]	Polyoxyethylene sorbitan tristearate	9005-71-4	1844.54	10.7	20	wax-like	(18:0)
Tween 80[a]	Polyoxyethylene sorbitan monooleate	9005-65-6	1309.66	15.7	20	liquid	(18:1)
Tween 81[a]	Polyoxyethylene sorbitan monooleate	9005-65-6	648.87	11.3	5	liquid	(18:1)
Tween 85[a]	Polyoxyethylene sorbitan trioleate	9005-70-3	1838.50	10.8	20	liquid	(18:1)
Genapol O050[c]	Oleyl alcohol polyglycol ether	9009-91-0	488.74	8.4	5	liquid	(18:1)
Genapol O080[c]	Oleyl alcohol polyglycol ether	9004-98-2	620.90	10.9	8	liquid-pasty	(18:1)
Genapol O100[c]	Oleyl alcohol polyglycol ether	68920-66-1	709.00	12.0	10	pasty, wax-like	(18:1)
Genapol O200[c]	Oleyl alcohol polyglycol ether	68920-66-1	1149.53	15.1	20	wax-like	(18:1)
Atlas G1096[a]	Polyoxyethylene sorbitol hexaoleate	57171-56-9	3887.59	11.3	50	liquid	(18:1)
TEHP EW400[d]	Tris(2-ethylhexyl)phosphate (400 g l^{-1})	78-42-2	434.63	/	/	liquid	
Trend 90[e]	Isodecyl alcohol ethoxylate (900 g l^{-1})	61827-42-7		/	/	liquid	
Glycerol[f]	Propane-1,2,3-triol	56-81-5	92.09	/	/	liquid	

Sources: [a] Croda (Nettetal, Germany), [b] Sigma-Aldrich Chemie GmbH (Steinheim, Germany), [c] Clariant (Muttenz, Switzerland), [d] Syngenta CropProtection Münchwilen AG (Münchwilen, Switzerland), [e] DuPont de Nemours (La Défense Cedex, France), [f] AppliChem GmbH (Darmstadt, Germany), * HLB values were taken from or recalculated according to (Pasquali *et al.,* 2008)

1.5 Motivations and objectives of this work

In the past, a lot of commercial research on adjuvants mainly based on empirical and heuristically studies with the central goal to maximise the effectiveness of products was conducted. Reflections about the basic principle of mode of action (MoA) were often disregarded. The modern point of view about the design of formulations and the choice of adjuvants is more rational and reasonable. Current research on optimization of agrochemicals is based on fundamental physico-chemical principles and the elementary knowledge of key properties of surfactants (Holloway, 1998).

Considering the application of foliar agrochemical sprays, a sequence of several primary stages can be distinguished (Stock & Briggs, 2000; Nairn *et al.,* 2015). To figure out how adjuvants can have an influence on these different stages or processes, the logical structure would be the chronological order.

1) The droplet formation during the flight from the nozzle to the target surface.
2) The contact (imping) of the droplet on the leaf which results either in the droplet retention, in bouncing off or in the drop shattering.
3) The wetting or spreading process on the leaf surface.
4) What happens on the leaf surface - properties of the spray deposit?
5) The penetration through the plant cuticular membrane which is the first barrier for organic molecules to pass.

By the structuring into distinct application processes, it is obvious that adjuvants can have a strong influence on these single stages, but it is important to know that one adjuvant can have more than only one distinct function during the application. Various publications discussed different aspects of MoA of adjuvants which were used to improve the performance of foliar applied active ingredients (Stock & Holloway, 1993; Kirkwood, 1993; Stock & Briggs, 2000; Fagerström *et al.,* 2013; Forster & Kimberley, 2015; Holloway & Edgerton, 1992). Most of such investigations focusing on adjuvant potential consider only one distinct phase during the complex spray application process and do not reflect the process in a holistic manner (Green & Hazen, 1998; Kirkwood, 1999).

The main objective of this work was to uncouple different aspects of the spray application, beginning from the droplet formation via retention and spreading

aspects on the leaf surface and the cuticular penetration of an AI. Ending up with a greenhouse spray test by including *in vivo* effects of adjuvants would bring all these factors together. The summarising conclusion should provide a better understanding of the MoA of adjuvants.

For this detailed elucidation, the class of polysorbates was generally considered because of their common promoting potential in foliar applied agrochemical formulations. Despite the fact, that polysorbates have only a relatively moderate function, it is an interesting, complex surfactant class which provides a structured analysis, because of the wide variety of products. The groups of Spans and Genapol O were selected because of aspects of their chemical structures which might be helpful to understand the effect of polysorbates. From this point of view, this study will systematically contribute to a basic understanding of the MoA of adjuvants in a foliar applied formulation mixture.

2 CHAPTER I: FROM THE NOZZLE TO THE LEAF SURFACE– SPRAY DROPLET RETENTION AND WETTING

2.1 Introduction

General aspects of foliar application

The application of plant protection agents is a time-dependent process (Stock & Briggs, 2000) which contains single steps to be considered, starting with the preparation of the aqueous spray solution in the tank of a boom sprayer. Then a spray nozzle atomises the liquid into small droplets (typical mean volume of 200 µm) (Taylor, 2011), which are formed during the first milliseconds of the flight. Since the ultimately impact on the leaf surface occurs typically after 50 to 400 ms (Wirth *et al.,* 1991; Butler Ellis *et al.,* 2004), the time frame during the droplet trajectory is a sensitive high speed process. Either the droplet successfully reaches the target plant and then spreads on the surface or bounces off and will be lost to the ground. The third possibility is that the droplet shatters or splashes on the solid plant surface. A droplet is said to shatter whenever it disintegrates into two or more secondary droplets, including the separation into tiny droplets after colliding (Rein, 1993). Often only less than 50% of the initial spray volume is retained to the plant (Bergeron *et al.,* 2000). Not only cost aspects, but also regulatory risks might result in adverse consequences to the farmer when the retention during the application is decreasing. For example, tiny splashed droplets can easily drift and pollute neighbouring fields, waters and preserved areas.

Accordingly, the adhesion of a droplet on the target surface is a key prerequisite for a successful application of plant protection agents, especially for superhydrophilic plant surfaces which are difficult to wet because of diverse surface structures like hairs, epicuticular wax crystals or others. Plants with smooth wax surfaces are easy to wet, so spray retention is less of a concern since a water droplet alone will adhere (Taylor, 2011).

Certainly, the first milliseconds of the application process are sensitively effected by a lot of factors. On the one hand, the retention is highly influenced by the surface characteristics. The plant species, the plant density in the field and their stage of development at the application time frame are from importance (de Ruiter *et al.,* 1990; Gaskin *et al.,* 2005; Taylor, 2011). Furthermore, the physical conditions of

the plants like turgor pressure of leaves and the leaf stability, meaning the angle of vertical direction, are factors that influence the spray adherence (Neinhuis & Barthlott, 1997; Koch *et al.,* 2008).

On the other hand, the spray solution itself can be designed to control different aspects. First, the adjuvant type and the concentration of the aqueous spray solution influence the physico-chemical properties of the spray solution like the dynamic surface tension. Moreover, droplet velocity and droplet size are issues affecting the trajectory by drift or droplet evaporation. These aspects can be adjusted by different technical issues like the spray nozzle or the speed and height of the boom (Butler Ellis *et al.,* 1997; Taylor, 2011). All these highly diverse variables have to be considered carefully when trying to optimise spray application.

Plant surfaces

The plant cuticular membrane is the first barrier between the interior of the plant and the surrounding atmosphere. It is a fundamental structural layer of ecological relevance for interaction between biotic and abiotic environmental factors (Riederer & Müller, 2006). The plant cuticle consists of a cross-linked cutin matrix in which long-chain aliphatic and cyclic plant waxes are embedded and overlaid (Jetter *et al.,* 2006; Jetter *et al.,* 2000). Cuticular waxes can be divided in intracuticular und epicuticular waxes, which are from high ultrastructural and chemical diversity (Barthlott *et al.,* 1998). Especially the epicuticular waxes are of particular interest for droplet retention, because they first come in contact with a droplet or other biotic factors (Zabka *et al.,* 2008). A lot of work is published about the structural and chemical composition of epicuticular waxes also in connection to their intracuticular waxes (Avato *et al.,* 1987; Barthlott *et al.,* 1998; Holloway, 1969; Ensikat *et al.,* 2006; Zeisler & Schreiber, 2016). So-called '*superhydrophobic surfaces'* and the self-cleaning phenomenon of plant surfaces (Koch & Barthlott, 2009; Neinhuis & Barthlott, 1997; Guo & Liu, 2007) or the wetting of hairy leaves (Nairn *et al.,* 2013; Xu *et al.,* 2011) are of outstanding relevance for the field of plant protection and material science. Most important key-functions of plant surface structures of a hydrophobic plant surface have been summarised by Koch *et al.* (2008) (Figure 16).

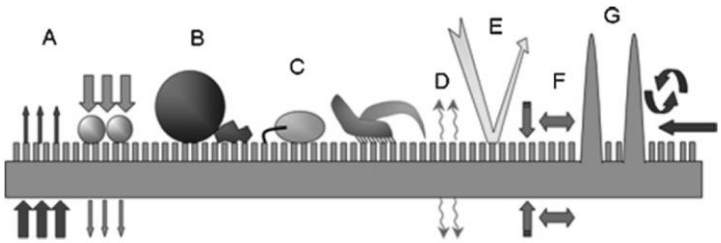

Figure 16: Schematic summary about the most important functions of a hydrophobic plant surface (illustration derived from Koch *et al.,* 2008).
A) Transport of molecules by diffusion through the plant cuticle (e.g. water transpiration, leaching of solutes, penetration of xenobiotics); B) Surface wettability (e.g. considering agrochemical spray application); C) Anti-adhesive and self-cleaning properties (e.g. a function of reduction of attachment of dirt particles, insects or pathogens); D) Signalling actions for plant-pathogen-interactions; E) Protection against harmful radiation; F) Barrier properties against mechanical abrasion; G) Regulation of plant surface micro-climate by controlling the turbulent air flow by surface structures as trichomes (Koch *et al.,* 2008).

Superhydrophobic plants, like the popular example of the Lotus plant (*Nelumbo nucifera*), are characterised by their multi-structured hierarchical surface. Therefore, structures can be organised in the micro- and nanoscale dimension, beginning from the plant epidermis having more or less convex cell shapes. The overlaying cuticle can have an irregular and complex folding. On top of the cuticle, most species are building a thin epicuticular wax layer or have additional three-dimensional wax structures, ranging from a few nanometers to micrometers. Epicuticular waxes might have developed by self-assembly as reported by Koch *et al.* (2004). The morphology and chemistry of epicuticular waxes are extremely diverse. Barthlott *et al.* (1998) established a classification of the most common types including thin wax films, filaments, differently orientated platelets, tubules and rodlet shapes, only to name a few examples. Furthermore, three-dimensional waxes can be either distributed randomly or arranged in a specific organisation, e.g. in parallel or around stomata. Moreover, there are also manifold structured hairs, trichomes, glands and papillas sitting on the surfaces, acting either as hydrophobic or hydrophilic structures (Neinhuis & Barthlott, 1997) (Figure 17).
The chemistry of epicuticular waxes is also an important key-issue that might decide whether the surface has general hydrophobic or hydrophilic properties. There are also plant species bearing a lot of hairs, papilla or porous cells acting as superhydrophilic surfaces (e.g. the peat mosses (*Spahgnum*)) (Koch *et al.,* 2008).

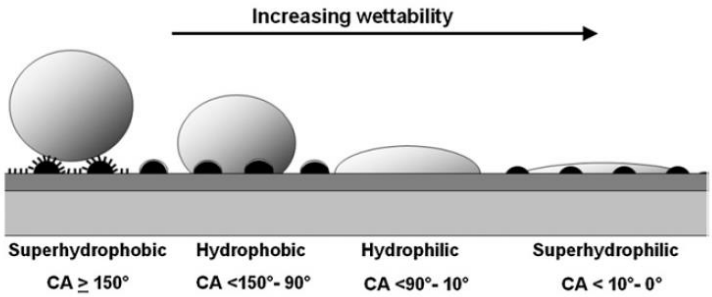

Figure 17: The wettability of surfaces as a result of surface structures can be determined by the water contact angle (illustration derived from Koch *et al.,* 2008).

The characterisation of the wettability and therefore the hydrophobicity of the surface can be easily determined with the water contact angle measurement (Carrier & Bonn, 2015). A droplet is deposited on the substrate, and the equilibrium sessile contact angle is measured. Wenzel (1936) and later Cassie & Baxter (1944) first modeled the influence of surface roughness on the value of the contact angle. A more recent work investigated the initial spray droplet adhesion on hairy leaves (Nairn *et al.,* 2013). The categories of Wenzel (hairy leaves) and Cassie–Baxter (super hairy leaves) were distinguished by how the droplets penetrate the leaf' hairs. It is a general agreement that a contact angle lower than 90° indicates a surface that has a good wetting behaviour. In contrast, water contact angles higher than 90° are specific for more or less hydrophobic surfaces (Figure 17). Especially, many crops belong to the family of *Poaceae* and are of high economical interest, are so-called *'difficult-to-wet-species'*. Resulting water contact angles are often immeasurably high (>150°) and a ranking in order to characterise the wettability of these species is difficult (Taylor, 2011).

Some physico-chemical considerations regarding the droplet retention

Considering surfactant solutions, the dynamic surface tension (DST) differs from the equilibrium value (STeq). Already small amounts of surfactants can cause alterations of the surface tension (Rein, 1993). The reason for this is the interface between the aqueous droplet and the surrounding gaseous phase, which is produced extremely quickly. Therefore, also the kinetics of the interface formation have to be kept in mind. The mobility of surfactant molecules becomes an important factor in the formation of the dynamic surface tension (Semenov *et al.,* 2015).

The diffusion of surfactants from the bulk solution to a liquid-air-interface is a retention determining factor. This diffusion occurs during drop formation, on the trajectory from the nozzle to the leaf surface, and during adherence (Wirth *et al.,* 1991). Therefore, the adsorption of amphiphilic surfactant molecules at the interface (spherical droplet periphery) results into a reduction of surface tension (Figure 18).

Obviously, the retention process is one which involves short time dynamics (Taylor, 2011). The time dependency is very essential for the retention process, because the time of flight of a droplet from the nozzle to the leaf surface typically ranges from 50 to 100 ms (de Ruiter *et al.,* 1990) depending on the height of the spray boom above the plant canopy and the velocity of the spray droplets. Wirth *et al.* (1991) defined the droplet impinging the surface between 100 to 400 ms, depending on the trajectory which is influenced by drift and evaporation. Accordingly, the interface saturation and so the surface tension lowering must occur during the first 100 ms for a successful retention (Figure 18, left). If the dynamic surface tension is not lowered significantly during this small time frame, the droplet will bounce off or shatter (Figure 18, right).

Basically, the process can be explained by the physical law that the adhesional force between droplet and solid must be greater than the kinetic energy of the droplet to prevent droplet rebound (Figure 18) (Taylor, 2011). When an incoming droplet is retained by the leaf surface, it first spreads out (expansion), and assuming that the droplet will not shatter, reaches a point of maximum spread before recoiling (retraction) due to surface tension occurs (Forster *et al.,* 2012) (Figure 18, top right). During both, the spreading and recoiling phases, the droplet loses energy. If the energy loss is small, there is sufficient energy remaining and the droplet will bounce off the leaf. If the energy losses are high enough, the droplet will adhere to the leaf surface (Figure 18, right) (Forster *et al.,* 2012).

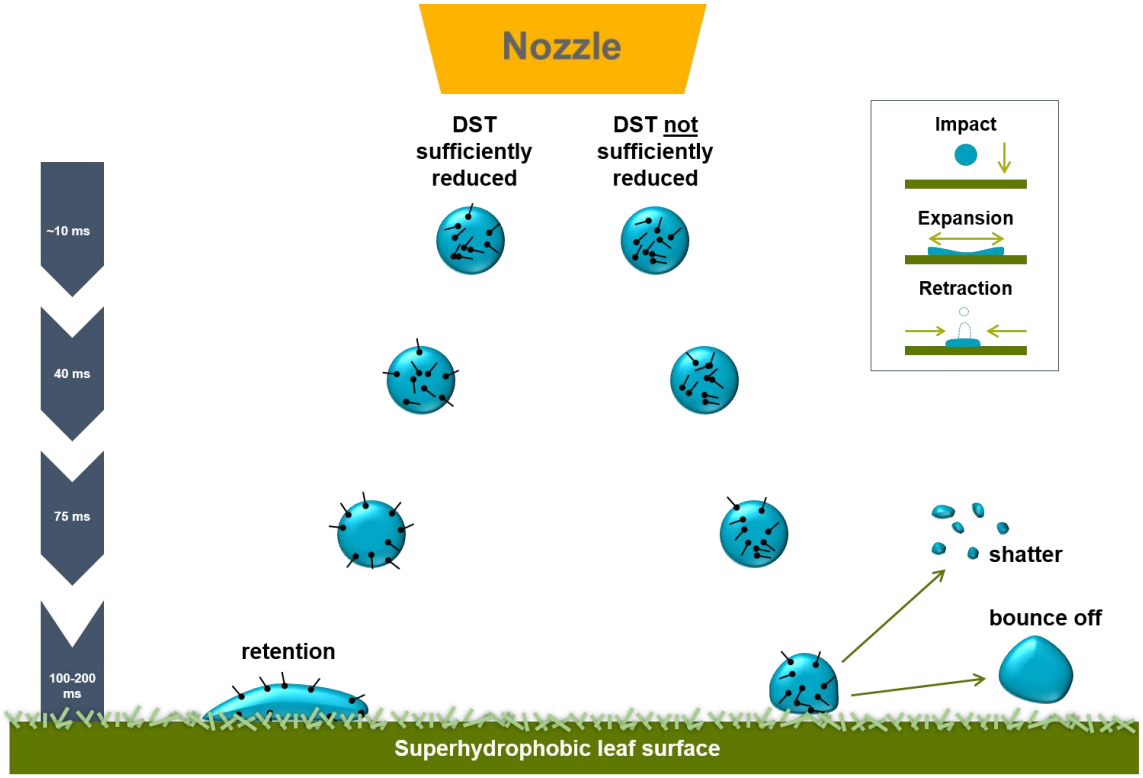

Figure 18: Droplet formation during the flight from the nozzle to a superhydrophobic leaf surface (illustration modified after a design by Daniel Schneider). The time of flight of a droplet from the nozzle to the leaf surface typically ranges from 50 to 400 ms (Wirth *et al.,* 1991; Butler Ellis *et al.,* 2004). If dynamic surface tension (DST) would not be sufficiently reduced by surfactants during this time frame, droplets might bounce off or shatter (right). A sufficient DST reduction may cause a successful adherence on the plant surface (left).

Application methodology

The retention characteristics of a droplet can be investigated exactly by laboratory spraying set-ups. Stevens *et al.* (1993) described the method where adhesion is measured under defined conditions. Starting with the selection of the surfactants and their concentrations in water, the droplet diameter, the fall distance, the droplet velocity at the moment of impact and the angle of incidence on the plant surface are recorded and varied (Watanabe & Yamaguchi, 1992; Forster *et al.,* 2012; Mercer *et al.,* 2010).

Other studies, like Wirth *et al.* (1991), Grayson *et al.* (1991), Holloway *et al.* (2000) and Butler Ellis *et al.* (2004) used a track sprayer to apply the formulated spray liquids to the plants. A convertible spray nozzle is attached to a speed track as it is used under field application conditions. Parameters like speed and pressure are variable due to track settings.

Both methods of application are important to understand the fundamental principles of the retention process. While the controlled application with the help of a droplet generator may elucidate the sensitive single variables in detail, the track sprayer may better reflect the situation in the field.

Objectives and research questions

The ideally consequence of impinging of droplets on the leaf surface is the droplet adherence. But it can also result either in bouncing off or in drop shattering. After the successful retention, the droplet begins to spread on the leaf. The reduction of interfacial tension is one of the most crucial physico-chemical properties of surfactants, which influence droplet retention and spreading characteristics on plants.

The dynamic surface tension of selected adjuvants was monitored over a certain short period of time to characterise the surface tension lowering behaviour of adjuvants, which is due to the velocity of monomers. When monomers are fully saturated on the droplet interface, a static or equilibrium surface tension value can be determined. This value was measured by ring and pendant drop method considering processes, like spreading or run-off effects. The influence of different adjuvants on the wetting process was characterised by studying time-dependent static contact angles and droplet spread areas on the superhydrophobic leaf surface of *Triticum aestivum*, which was used as a model crop. For further visualisation of surface structures of wheat and different adjuvant deposits scanning electron microscopy examinations were carried out.

The main objective was to investigate how selected adjuvants would have an influence on the retention and wetting process during spray application. Therefore, several laboratory studies were considered separately. To transfer findings from laboratory to spray application related to field conditions, retention and leaf coverage was measured quantitatively on wheat leaves by using a variable track sprayer.

2.2 Materials and methods

2.2.1 Chemicals

The non-ionic sorbitan fatty acid esters (Span 20 and Span 80) and their polyethoxylated derivatives (Tween 20, Tween 40, Tween 60, Tween 65, Tween 80, Tween 81 and Tween 85) were used for the following experiments.
Also oleyl alcohol ethoxylates (Genapol O050, Genapol O080, Genapol O100 and Genapol O200) and polyoxyethylene sorbitol hexaoleate (Atlas G1096) and Tris(2- ethylhexyl)phosphate (TEHP EW400) were used.
Isodecyl alcohol ethoxylate (900 g/l) (Trend 90) was selected as a control adjuvant, because it is known to have good retention aiding properties.
The chemical and physical properties of all adjuvants used for experiments are listed in Table 1. All substances were dissolved in water and had a concentration of 0.1% (w/v) of the respective adjuvant.

2.2.2 Equilibrium surface tension

Ring method

The surface tension of an aqueous surfactant solution was investigated with the help of the manual tensiometer K5 (Krüss GmbH, Hamburg, Germany) using the 'Du Noüy' ring method. The force, acting on an optimal wettable ring as a result of the tension of the withdrawn liquid lamella when removing the ring, is measured. A lamella is produced, when the platinum-iridium ring moves through the phase boundary between a liquid and gaseous phase (Harkins & Jordan, 1930). With a mechanical tensiometer, the maximum force F_{max} can only be determined by stretching the lamella until it detaches (ring tear-off method). This maximum force correlates with the surface tension σ according to the following equation (Krüss GmbH. Du Noüy ring method. 10.12.2015):

$$\sigma = \frac{F}{L * cos\theta} \qquad \text{(eq. 1)}$$

At least 10 replicates were measured per substance solution and a mean value was calculated. Between each measurement, the solution was left for at least 5 minutes to allow equilibration between vapor and liquid.

Pendant drop method

The surface tension of an aqueous surfactant solution was investigated with the help of the Drop Shape Analyser DSA100S (Krüss GmbH, Hamburg, Germany) using the pendant drop method (Ambwani & Fort, 1979).

The shape of a droplet suspended from a needle is determined by the surface tension and the weight of the drop. The surface tension can be ascertained by the image of the drop using drop shape analysis. An increased pressure is produced inside the drop as a result of the interfacial tension between inner and outer phase. The mathematical derivations of a pendant drop is based on the fundamental equation of capillarity (Ambwani & Fort, 1979). The pendant drop is deformed under the effect of gravity, as a hydrostatic pressure which affects the two radii of curvature being produced inside the drop due to the weight. As the hydrostatic pressure depends on height, the curvature of the drop interface also changes in the vertical direction. This results in the characteristic ‘pear’ or ‘tear’ drop shape of a pendant drop (Figure 19) (Ambwani & Fort, 1979; Krüss GmbH. Pendant drop. 10.12.2015). A detailed mathematical explanation of the geometric treatment of the pendant drop is given by Ambwani & Fort (1979).

Figure 19: Shadow image of a hanging ‘pear-shape’ droplet for determining the equilibrium surface tension (STeq).

2.2.3 Dynamic surface tension

DST experiments were investigated using the bubble pressure tensiometer BP100 from Krüss GmbH (Hamburg, Germany). The physical principle of dynamic surface tension corresponds to the specific device and is also explained by Krüss GmbH. The method of maximum bubble pressure allows to analyse the mobility of surfactants in water solutions for high speed processes like the spraying of plant surfaces. A gas bubble is produced by a capillary immersed in the liquid surfactant solution. Then the maximum internal pressure of a gas bubble formed in the solution is then measured. The Young-Laplace equation (eq. 2) establishes the mathematical relation between the internal pressure p of a spherical bubble (Laplace pressure), the radius of curvature r and the surface tension σ (Krüss GmbH. Bubble pressure tensiometer. 05.03.2016):

$$p = \frac{2\,\sigma}{r}$$

(eq. 2)

The curvature initially increases and subsequently decreases, when a gas bubble is produced at the tip of the immersing capillary. During this, a pressure maximum can be measured. The greatest curvature means the greatest pressure occurs when the radius of curvature is equal to the radius of the capillary, which must be known. So the surface tension can be related from the maximum pressure p_{max}. Since the capillary is immerged in the surfactant solution, the hydrostatic pressure p_0 given by the depth of capillary immersion and the liquid density must be subtracted from the maximum pressure p_{max} (Krüss GmbH. Bubble pressure tensiometer. 05.03.2016):

$$\sigma = \frac{(p_{max} - p_0) \ * \ r}{2}$$

(eq. 3)

The resulted surface tension corresponds to the specific value at a certain surface age (ms). This time dependence is the main difference for measuring the static surface tension. The surface age is the time from the start of the bubble formation to the occurrence of p_{max}. By varying the speed at which the capillary produces bubbles, the dependency of surface tension on surface age can be analysed (Krüss GmbH. Bubble pressure tensiometer. 05.03.2016).

2.2.4 Contact angle measurement

Surface material

Parafilm (Parafilm M, Bemis Company, Inc., Neenah, Wisconsin, USA) was used as an artificial, apolar control surface having no surface structures. The winter wheat cultivar *Triticum aestivum* cv. Arina was used as a model plant during growth stage BBCH 12 (2-leaf-stadium). The second leaf was sampled for contact angle measurements. The growing conditions consisted of a 10-h light period and 20/15 °C day/night temperature at 70% relative humidity.

Specimen slides were prepared with double-sided adhesive tape (Tesa double face; Beiersdorf Co., Hamburg, Germany). Plant material was carefully placed on specimen slides. All plant material was transported and stored in a box with a wet paper towel to prevent fast transpiration.

Time-dependent sessile contact angle

Contact angle measurements were performed with an optical contact angle measuring device OCA 15 plus (DataPhysics Instruments GmbH, Filderstadt, Germany). A 3 µl droplet was placed on the leaf surface by touching. At least 10 droplet replicates were measured per substance and surface.

The contact angle was determined from the shadow image of the sessile droplet and analysed with the drop shape analysis (DSA) software. A contour recognition was initially carried out based on a grey-scale analysis of the image. In the second step, a geometrical model describing the drop shape is fitted to the contour (Krüss GmbH. Drop shape analysis. 09.12.2015). The contact angle is considered by the angle between the calculated drop shape function and the sample surface.

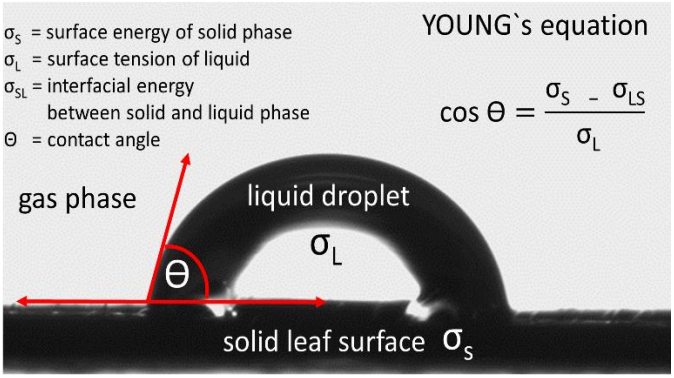

Figure 20: Droplet shape image as a schematic drawing of the contact angle measurement and the physical relationship between the contact angle and the surface tension.

Working with surfactant solutions, the amphiphilic molecules diffuse through the liquid phase (see Figure 6 and Figure 18) so the process becomes dynamic and time-dependent. Considering the CA of surfactant solutions on plant surfaces, the process of droplet spreading during the first 60 s was investigated. A droplet of 3 µl volume was placed on the leaf surface by touching the surface. A camera recorded the droplet spreading process with 1fps. Afterwards, the single droplet shadow images were analysed by the drop shape analysis (DSA) software of OCA 15 plus (DataPhysics Instruments GmbH, Filderstadt, Germany), as described above. The droplet states at different points of time at 0 s, 3 s, 5 s. 10 s, 20 s, 30 s and 60 s were evaluated.

All surfactant solutions were dissolved in water and had a concentration of 0.1% (w/v) of the respective adjuvant (see Table 1). Moreover, the strawberry-red azo dye Sanolin Ponceau 4RC 82 (also known as Acid Red 18, denoted by E number E124) (Clariant, Muttenz, Switzerland) was added in the concentration of 0.1% (w/v) to the surfactant solutions for further visualisation of the droplet residue. The dye was assured having no influence on the contact angle measurement compared to pure water.

2.2.5 Droplet spread area

After complete evaporation of water from the droplets used for contact angle measurements, areas of dry spray deposits were further analysed using a microscope (Leica DMR, Leica Microsystems Wetzlar GmbH, Wetzlar, Germany) which was equipped with a camera (AxioCam MRc, Carl Zeiss Microscopy GmbH,

Jena, Germany). The red dye was used as a marker for visualisation of the borders of the droplet residue. The determination of the droplet spread area was carried out with the software AxioVision Rel. 4.8 (Carl Zeiss Microscopy GmbH, Jena, Germany).

2.2.6 Visualisation of surface structures by SEM

Micromorphological investigations of surface structures and adjuvant residues on fresh leaf material were performed with a scanning electron microscopy (JEOL JSM-7500F, JEOL GmbH, Freising, Germany) equipped with a field emission gun and LEI and SEI detectors. Fresh leaf material of *Triticum aestivum* cv. Arina was used for SEM experiments. Plants were used in growth stage BBCH 12. To illustrate contact areas between the leaf surface and the surfactant solution, 0.1% aqueous surfactant solution droplets (0.2 µl) were carefully applied on the surface. Fresh plant material with droplet deposits was mounted on aluminium holders, carefully air dried on silica gel, then sputter-coated with ~ 3 nm platinum. For the visualisation of surfactant deposits, the LEI detector was used, as well as the SEI detector.

2.2.7 Track sprayer experiments

Plant material

For the track sprayer experiments, plant material from winter wheat (*Triticum aestivum* cv. Arina) was used. At the experimental set-up, plants were in growth state BBCH 12 (2-leaf-stadium). The growing conditions consisted of a 14-h light period and 18/17 °C day/night temperature at 70%/70% day/night relative humidity.The plants were treated with the growth regulator Chlormequatchloride (Bayer CropScience, Monheim, Germany). Chlormequat inhibits cell elongation which increases yields in cereals. The treatment has no influence on droplet retention.

Application

The retention tests were carried out at Syngenta CropProtection, Münchwilen AG, Münchwilen, Switzerland with technical assistance by the formulation-application department. All treatments were applied to the plants from a spray nozzle attached

to a variable speed track. The track sprayer was equipped with a Teejet XR11003VP flat fan nozzle. The pressure was set at 2 bar and the speed was 8 km/h. 10 Plants were cut at the bottom and placed carefully in the spray cabin. Therefore, tips were used to place the plants vertically (Figure 21). To prevent spraying shadows, plants were placed in two rows. A single plant was positioned separately from the other 9 plants and filmed with a high speed camera. A solution of the fluorescent tracer Helios SC500 (Novartis, Basel, Switzerland) was used to examine quantitatively the spray deposit on the plant surface.

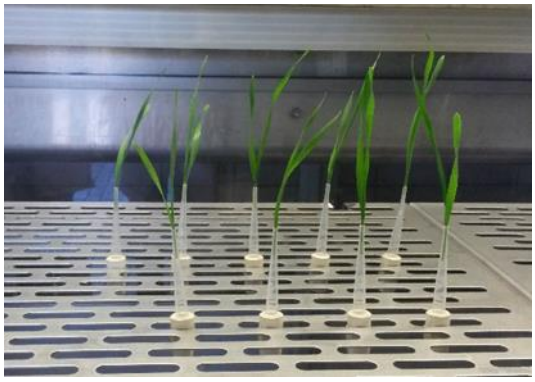

Figure 21: Arrangement of vertically placed wheat plants in the spray cabin in order to prevent spray shadows.

Determination of leaf coverage

The fluorescent tracer substance Helios SC500, which contains the active agent Tinopal OB CO (2,5-thiophenediylbis(5-tert-butyl-1,3-benzoxazole), (BASF SE, Ludwigshafen, Germany), was adopted as a tracer for quantifying the spray deposit on the plant surface. Tinopal OB CO is an optical brightener which can be excited by UV light which leads to its emitting of visible light. Helios is soluble in organic solutes but not in water. Therefore, Helios was formulated as SC500 (suspension concentrate containing 500 g l^{-1} Tinopal OB CO). The SC500 formulation has no influence on the treated plants. Helios SC500 was concentrated 0.2% in water (v/v). So the solution contained 0.1% UV tracer. All adjuvants were added in the concentration 0.1% (w/v) to the tracer solution.

Spray deposits were made visible with an UV lamp. Plants were separately placed on a red coloured surface and photographed on both sides with a camera (Figure 22). The determination of the leaf coverage was carried out with the software FluorSoft v0.1.

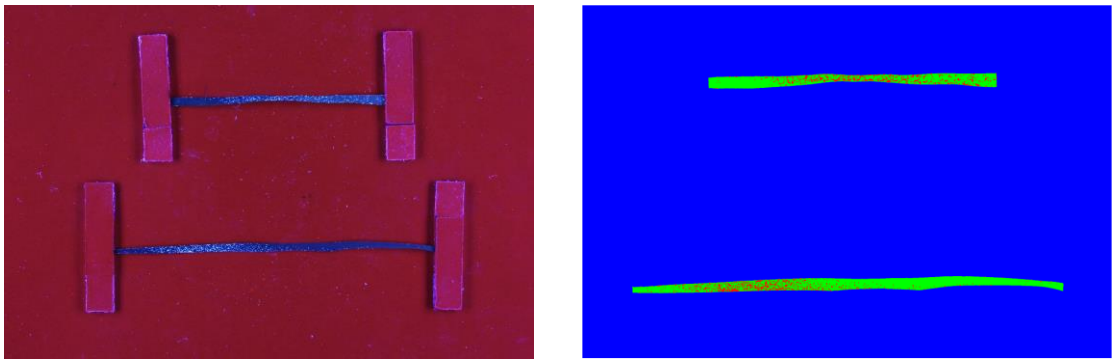

Figure 22: Leaves were fixed on a red coloured surface and photographed (left), pictures were processed into pseudocolour images and then analysed with the image processing program FluorSoft (right).

Determination of retention

After determination of the optical leaf coverage, the plants were placed separately into glass tubes. The tracer was washed with 8 ml acetonitrile for 30 s from the plant surface. The solution was then filtered into UV glass tubes. The concentration of Helios in the solution was measured fluorimetrically via the Fluorimeter 96 (proprietary development of Novartis, Basel, Switzerland). The excitation light was 375 nm and the emission light was 435 nm. All results were calculated as µg Helios per liter, including two technical replicates.

2.3 Results

2.3.1 Equilibrium surface tension

The equilibrium surface tension (STeq) of selected surfactants dissolved 0.1% in water (w/v) was determined by two different techniques using the ring method and the more recently developed pendant drop method (Table 2). Pure water (dest.) was used as a control. At room temperature (20 °C), the surface tension value for water was defined at 72.75 mN m^{-1} (Vargaftik *et al.,* 1983). The values of pure water established by either the ring method or the pendant drop were only slightly different, although the pendant drop method was with a value of 72.3 mN m^{-1} more close to the literature value. The differences between both methods, considering the surfactant solutions, varied between 0.1 mN m^{-1} for Genapol O200 and 9.3 mN m^{-1} for Tween 80. For further assumptions, values derived from the pendant drop method will be adopted.

Table 2: Comparison of methods determining the equilibrium surface tension (STeq) using the ring method and the pendant drop method

Surfactant solution 0.1% (w/v)	**STeq (mN/m) Ring method**	**STeq (mN/m) Pendant drop**
Water	71.2	72.3
Span 20	26.9	32.0
Span 80	30.7	29.3
Tween 20	33.4	38.0
Tween 40	/	43.8
Tween 60	/	44.5
Tween 65	/	42.7
Tween 80	36.7	46.0
Tween 81	38.7	37.0
Tween 85	44.4	43.0
Genapol O050	33.5	29.0
Genapol O080	/	30.0
Genapol O100	33.4	33.0
Genapol O200	39.9	40.0
Atlas G 1096	39.5	42.0
TEHP EW400	/	48.0
Trend 90	/	27.8

The lowest measured value was 27.8 mN m^{-1} for Isodecyl alcohol ethoxylate (900 g/l) (Trend 90), which was known to have surface tension lowering properties. Also for Span 80 a low STeq of 29.3 mN m^{-1} was observed (Table 2).

The highest value was measured for Tris(2- ethylhexyl)phosphate (TEHP EW400) (48.0 mN m^{-1}). The STeq for Tween 80 was with 46 mN m^{-1} much higher than Tween 20, having 38.0 mN m^{-1}. Overall, the majority of selected surfactant solutions resulted in a narrow distribution of STeq values, ranging between 30 to 45 mN m^{-1}.

2.3.2 Dynamic surface tension

The dynamic surface tension (DST) of surfactant solutions (conc. 0.1% in water (w/v)) was measured with the method of maximum bubble pressure. Single surface tension values (mN m^{-1}) were measured over a specific time period, ranging from 10 ms to 30000 ms surface age. Therefore, results can be interpreted as decreasing DST curves as a function of time (Figure 23).

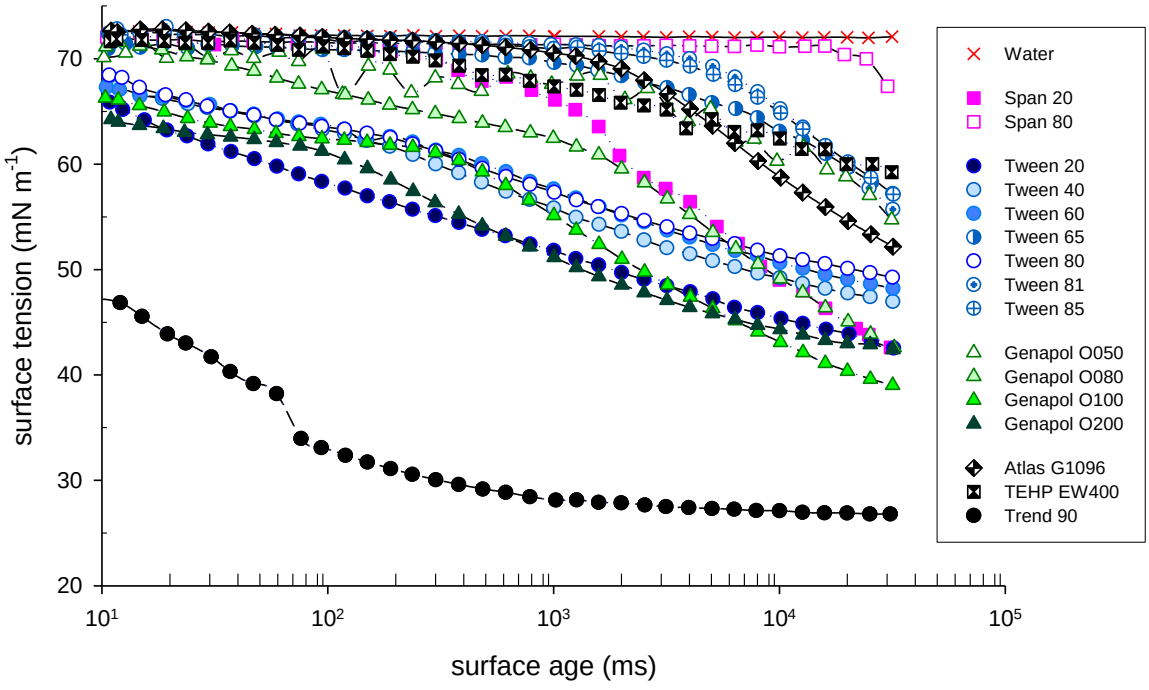

Figure 23: Results of DST measurements expressed as relation between surface age (ms) and surface tension (mN m^{-1}). Surfactants were dissolved 0.1% in water (w/v). Axis of surface age with logarithm scaling, ranging from 10 ms to 30000 ms.

Pure water (dest.) was used here as control experiment. During the complete time interval, no decrease of surface tension could be observed (Figure 23). DST remained constant at a value of about 72 mN m^{-1}.

All of the selected surfactants (conc. 0.1% in water (w/v)), with the exception of Trend 90, showed very high initial values of about 65 to 72 mN m^{-1} compared to pure water. During the first 1000 ms, several surfactants showed nearly no change in surface tension (ca. 70 mN m^{-1}). Then, the curves decreased steeply. This observation was true, for e.g. Span 80, Tween 65, Tween 81, Tween 85 or Atlas G1096 (Figure 23). The process of Span 20 was also smooth during the first 1000 ms but decreases abrupt at the end of measurement.

The shapes of the curves of Tween 20, Tween 40, Tween 60, Tween 80, Genapol O100, Genapol O200 decreased more smooth throughout the whole experiment and ended at the surface age of 30 s with comparable low values of about 40 to 50 mN m^{-1}.

Comparing to pure water, the majority of samples resulted in relatively high DST values with the exception of Trend 90, which produced the maximum decrease of DST. Already the initial DST value of Trend 90 (47 mN m^{-1}) was by far lower than the other samples. Moreover, the slope decreased steeply during the first 100 ms and ended at 30 s at about 27 mN m^{-1}. Trend 90 was selected in this experiment as a substance which was known to have strong surface tension lowering properties.

2.3.3 Contact angle measurement

The determination of time-dependent sessile contact angles (CA) was carried out to characterise the surfactant wetting and spreading potential on the one hand, but also to investigate surface properties of a plant surface of wheat leaves on the other hand. The process of droplet spreading during the first 60 s after droplet settling was studied.

Parafilm was used as an artificial control surface considering differences between selected surfactant samples (Figure 24). All samples were dissolved in water (0.1%, w/v). A red dye (0.1%, w/v) was added to all surfactant solutions for further visualisation of the droplet residue after water evaporation. Pure water (dest.) was adopted as control experiment. During the complete time interval of 60 s water CAs

remained constant at a value of about 107° (Figure 24). Between the surfactant selections of Spans, big differences became visible (Figure 24, A). Span 40, Span 60 and Span 65 produced high CAs around 110° which did not decrease during the first minute. No CA lowering effect compared to pure water could be observed. Span 85 resulted in a mean CA of around 104° also without changing over time. In contrast, Span 80 showed the highest decrease in CA during the first minute after droplet application. Already the initial CA value of Span 80 (98°) was lower, compared to the pure water. Moreover, the CA decreased steeply during the first 20 s and ended at about 74°. Therefore, the CA difference for Span 80 was more than 20° during one minute.

In general, the majority of Spans resulted in high CA values (≥100°) with the exception of Span 80 and particularly Span 20, which produced the maximum decrease of CA. The initial CA value of Span 20 was with 73° comparable to the final value of Span 80 after one minute. The initial CA of Span 20 was by far lower than all other surfactant samples (Figure 24). The CA value after 60 s (56°) was the minimum value which could be observed. For the Tween family, all selected surfactant solutions resulted in a narrow distribution of values ranging between 95° and 70° (Figure 24, B). Substantial differences compared to pure water were visible. The maximum CAs (around 90°) produced by Tween 60, which did not decrease over time. CA values of Tween 20 and Tween 80 were also around 90° to 85° and decreased during the first seconds. The lowest CAs (about 70°) were produced by Tween 81, which strongly decreased during the first 5 s. The results of CA values of Genapol O and Atlas G1096 showed a high CA development during the first 5 to 10 s after droplet settling (Figure 24, C). Especially Genapol O050 produced an initial CA of about 93° and decreased to a value of 70°.Temporal differences of the CA decreasing between Spans and Genapol O could be observed. While Span 80 showed a more linear decline in CA, Genapol O decreased mainly during the first 5 to 10 s. Genapol O080 and Genapol O100 resulted in the steepest development in CA during the first seconds and therefore ended with low CAs between 75° and 60°. In general, the majority of samples resulted in medium to high CA values (around 90°) with the exception of Span 80 and Span 20. Especially the initial CA of Span 20 (73°) was by far lower, compared to all other samples.

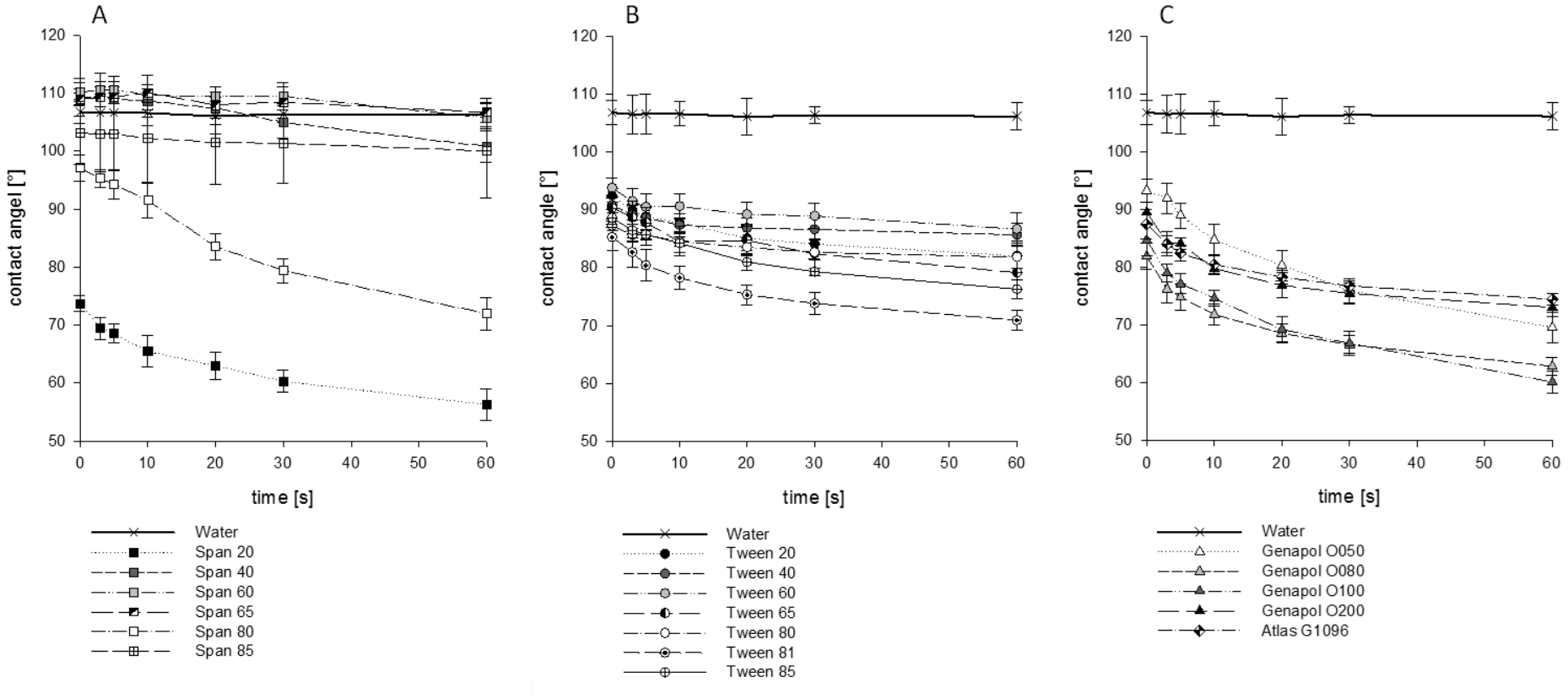

Figure 24: Time-dependent sessile contact angle development on parafilm during the first 60 seconds after droplet application for Spans (A), Tweens (B) and Genapol O and Atlas G1096 (C), conc. 0.1% in water (w/v). Pure water (dest.) was used as a control. Symbols represent mean values and error bars illustrate the standard deviation, n≥10.

The determination of time-dependent sessile CAs was also carried out to characterise the wetting capability of surfactants considering the plant surface of *Triticum aestivum* cv. Arina. Therefore, CAs of selected surfactants on both, the adaxial (Figure 25) and the abaxial side (Figure 26) were distinguished. Pure water (dest.) was used again as control experiment. On the upper side of the leaf, water CAs remained constant at a high value of about 152° during the one minute (Figure 25). All surfactants had the ability to lower the CA compared to water, even on a low level. The majority of surfactants, with the exception of Span 20, Genapol O080 and Genapol O100, resulted in no decrease of CA during time. While Span 20 produced a final CA of 125°, Genapol O100 had the minimum CA of 120° in this experiment. Also the shape of the CA development was steepest for Genapol O100. All Tween surfactants showed no decline in CA values over time. While Tween 65 produced the highest CA (around 150°), Tween 20, Tween 40 and Tween 60 showed nearly the same CA value (around 130°).

The water CA on the abaxial side of the leaf was slightly lower than on the upper side (lower side: 145°, upper side: 152°) (Figure 26). Furthermore, CA results of all selected surfactants were slightly smaller than the upper side experiment but had generally the same characteristics.

The differences of the initial and final CA considering Span 20, Genapol O080 and Genapol O100, were more emphasised (Figure 26, A and C). The minimum CAs were observed for Span 20 and Genapol O100 (around 107°). For the class of Tweens, a narrow distribution of CA values ranging between 135° and 120° could be observed, while Tween 81 showed a small decrease of CA at the end of the experiment. Compared to the results generated on parafilm, the ability of surfactant solutions to decrease the CA on the surface of wheat was non-existent or very low during the first seconds of measurement.

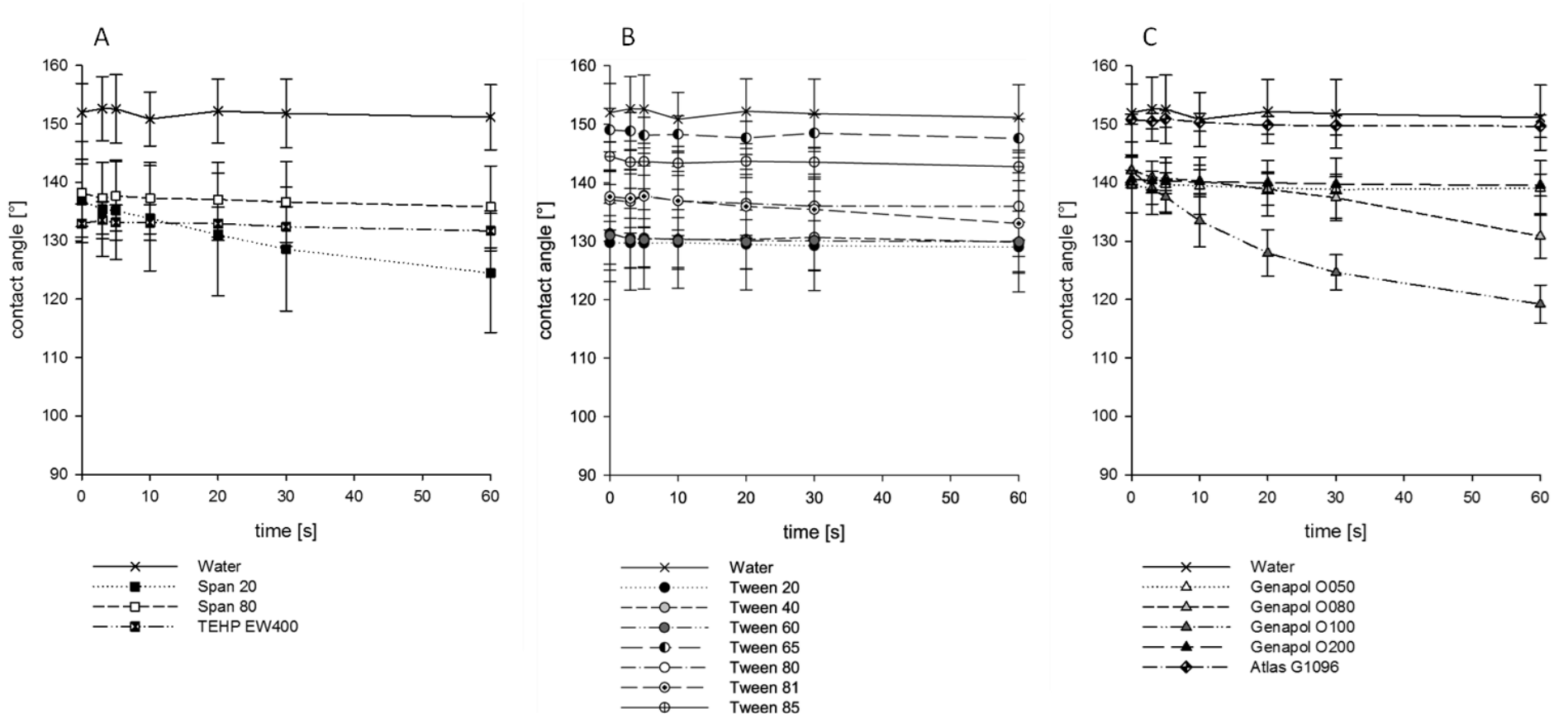

Figure 25: Time-dependent sessile contact angle development on the adaxial side of wheat cv. Arina during the first 60 seconds after droplet application for Spans (A), Tweens (B) and Genapol O and Atlas G1096 (C), conc. 0.1% in water (w/v). Water was used as a control. Symbols represent mean values and error bars illustrate the standard deviation, n≥10.

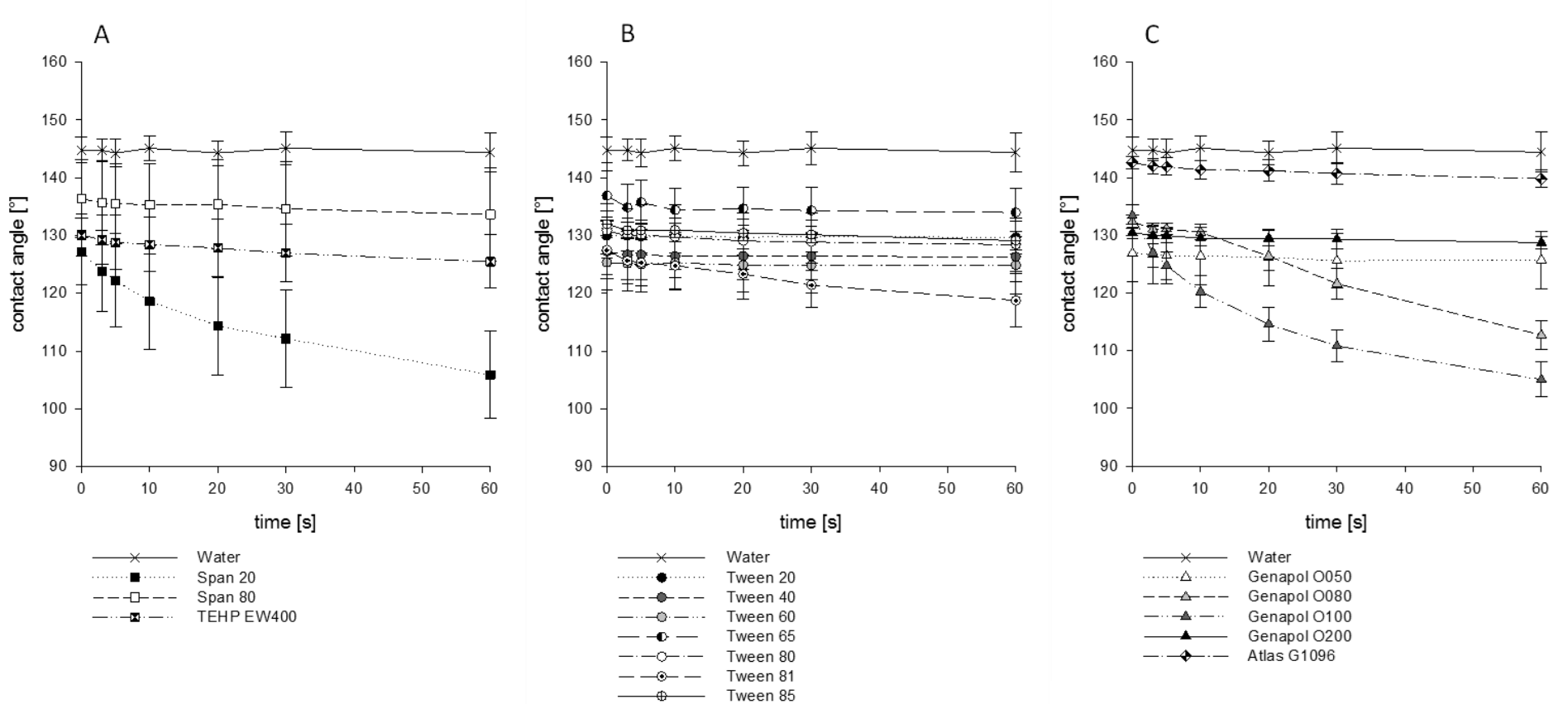

Figure 26: Time-dependent sessile contact angle development on the abaxial side of wheat cv. Arina during the first 60 seconds after droplet application for Spans (A), Tweens (B) and Genapol O and Atlas G1096 (C), conc. 0.1% in water (w/v). Water was used as a control. Symbols represent mean values and error bars illustrate the standard deviation, n≥10.

2.3.4 Droplet spread area

After the complete evaporation of water from 3 µl droplets, measured in contact angle experiments, the remaining dry and red deposits from the strawberry-red azo dye Sanolin Ponceau (which was added to all surfactant solutions (0.1%, w/v)) were used for further visualisation of the droplet spread area on adaxial and abaxial leaf surfaces of *Triticum aestivum* cv. Arina by microscope (Figure 28). The different drying times of droplets were not recorded.

Water droplets were used here as a control and resulted in a minimum covered leaf area (0.6 $mm^2 \pm 0.3$) (Figure 27 and Figure 28). In comparison to water, all surfactant solutions had an increasing effect on the covered leaf area, although differences between the adaxial and abaxial side of the wheat leaf were not visible.

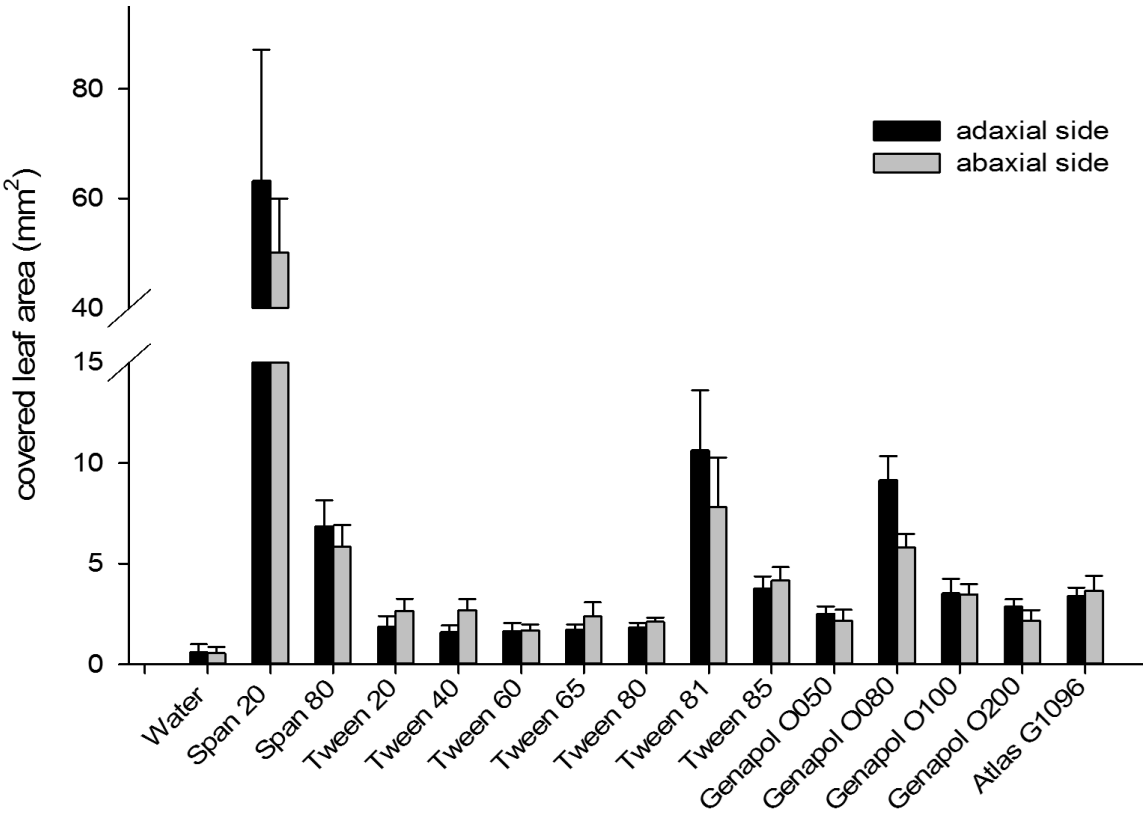

Figure 27: Covered leaf area in mm^2 of 3 µl volume surfactant droplets (conc. 0.1% in water (w/v)). Comparison between adaxial (black) and abaxial side (grey) of *Triticum aestivum* cv. Arina leaves. Water was used as a control. Bars represent mean values and error bars illustrate the standard deviation, n≥10, paired samples from contact angle experiments.

By far the maximum covered leaf area was measured for Span 20 (upper side: 63.2 mm^2 ± 23.9; lower side: 50.2 mm^2 ± 9.7) (Figure 28). Tween 81, Genapol O080 and Span 80 had a leaf area ranging from 5.8 to 10.6 mm^2. All other selected surfactants resulted in areas lower than 4 mm^2. Also Tween 20 and Tween 80 produced a small covered leaf area (about 2 mm^2) compared to Span 20.

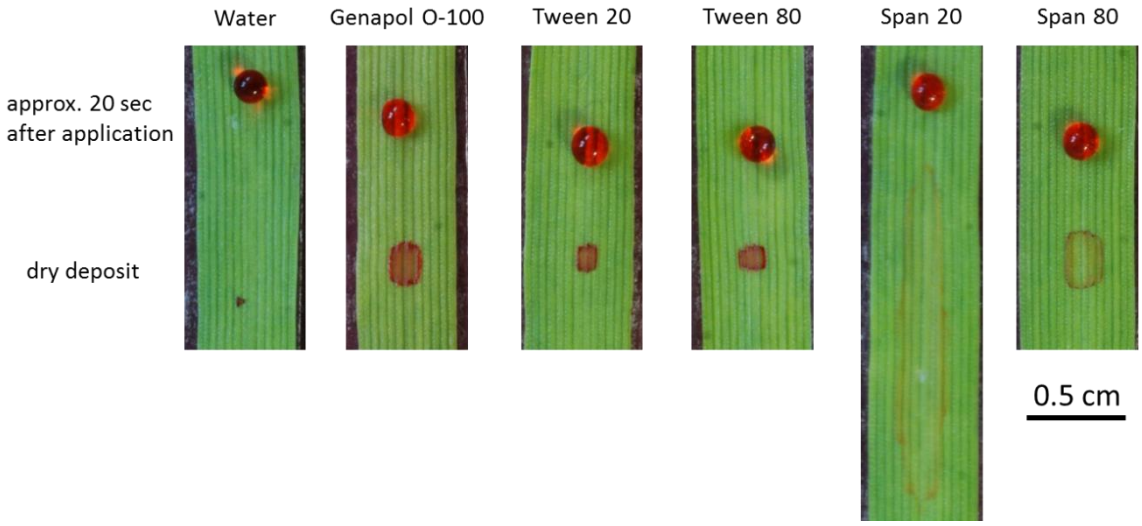

Figure 28: Comparison of freshly settled droplets (3 µl volume) and droplet residue after water evaporation of selected surfactant solutions on adaxial *Triticum aestivum* cv. Arina leaves.

2.3.5 Visualisation of surface structures by SEM

Investigations of surface analysis by scanning electron microscopy (SEM) should visualise microstructures of plant surfaces and might display differences between the surfactant samples used for wetting experiments.

Parafilm was used as a synthetic surface for contact angle measurements, considering basic differences between surfactant samples. Parafilm is known to be strong apolar and free of any surface structures. The SEM picture showed no or only very small surface imperfections (Figure 29).

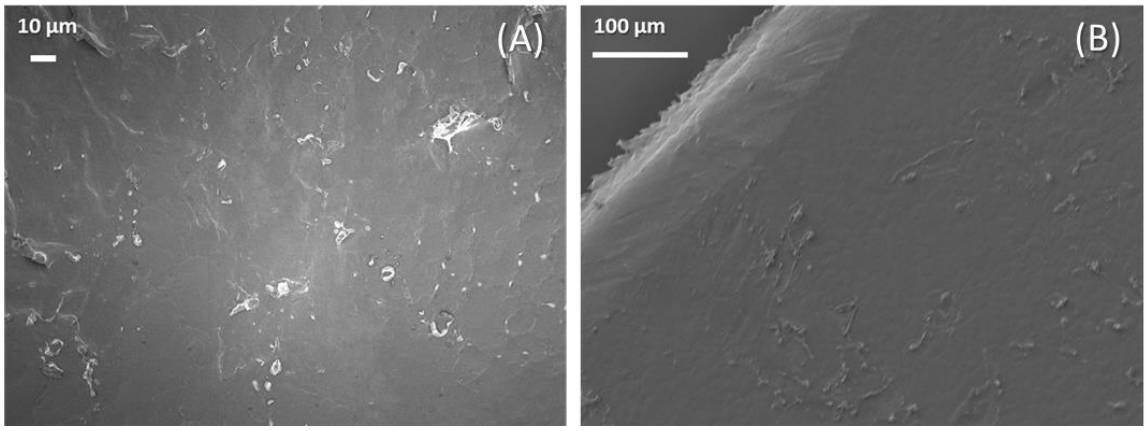

Figure 29: Dominant surface structures of parafilm are absent (higher magnification (A), lower magnification (B)).

Differences between both sides of *Triticum aestivum* cv. Arina leaves were observable in a low magnification (50x, Figure 30, A and B). Non-glandular trichomes were orientated in parallel on both sides. The upper side hairs are longer than the lower side ones (not measured). However, the hair density of around 10 trichomes per mm^2 is half as much compared to the abaxial side, having around 20 hairs per mm^2. The surface of trichomes on both sides is free of any epicuticular wax crystals (Figure 30, C and D). Though, epicuticular wax crystals are the predominant microstructural element on the wheat surface on both sides of the leaf (Figure 30, E and F). The density of wax crystals seems to be slightly higher on the adaxial side, because of more free 'gaps' in the wax crystal coverage on the abaxial side.

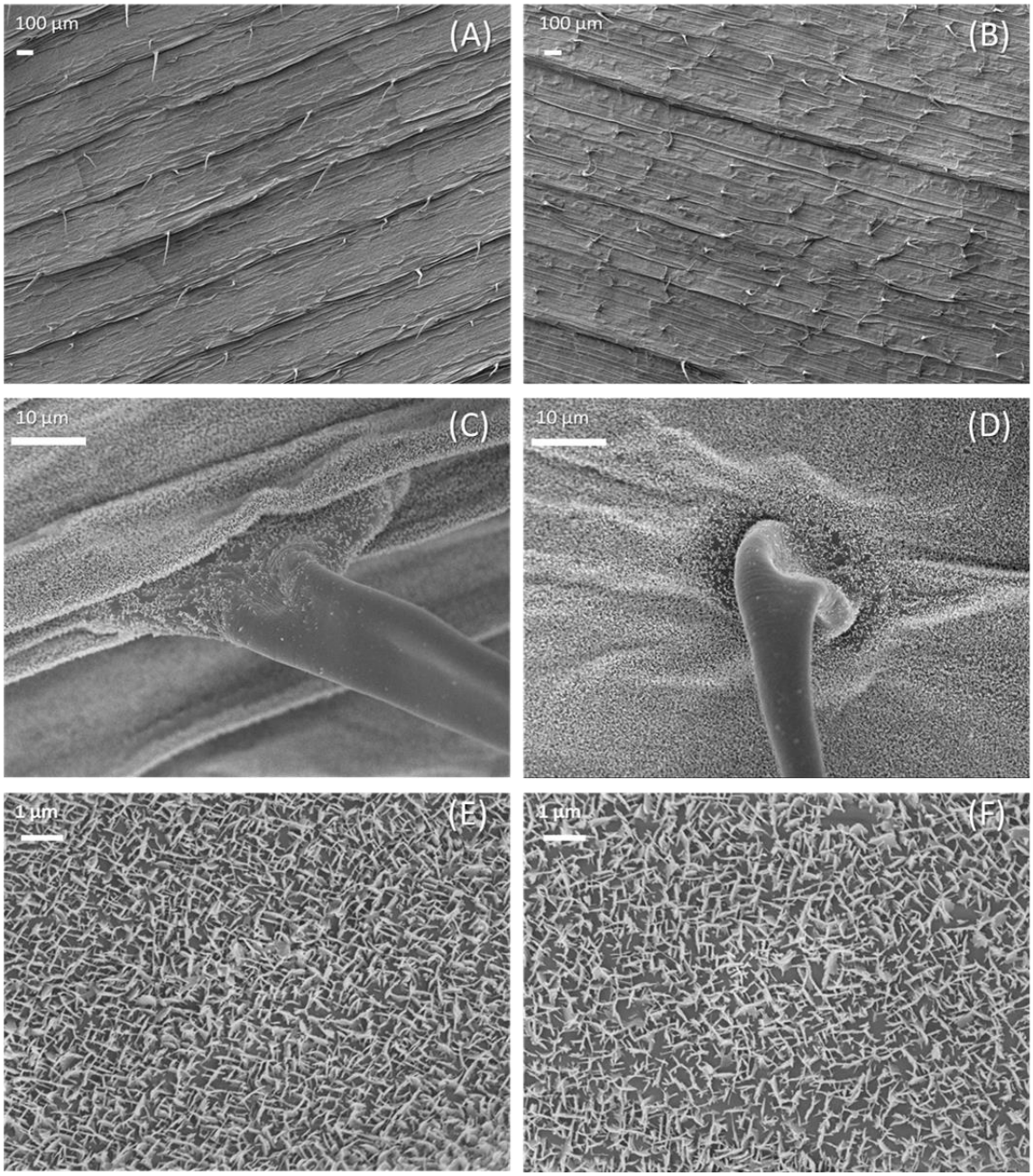

Figure 30: Comparison of surface microstructures of the adaxial (left) and the abaxial (right) side of *Triticum aestivum* cv. Arina. Magnification increases from top to bottom. Non-glandular trichomes were orientated in parallel on both sides of the leaf (A and B). Surface structures on these trichomes reveal no wax crystals in a higher magnification (C and D). Epicuticular wax crystals are also present on both leaf sides (E and F).

Leaf material of *Triticum aestivum* cv. Arina was also used to show differences between selected surfactant samples (conc. 0.1% in water (w/v)) by applying small droplets on the adaxial surface. The residue was not washed or cleaned after application, because the dry surfactant deposit was studied. Therefore, the borders between the droplet and the non-treated areas were visualised. The influence of trichomes was not investigated in these experiments. SEM pictures were selected to display a representative result of several observed impressions.

The treatment with Tween 20 seemed to result in a disappearance of wax crystals (Figure 31, A and B). The border between the droplet and the treated area is not visible as a sharp line. In contrast, the application of Tween 80 caused a formation of a smooth, amorphous deposit which covered the surface including the epicuticular wax crystals. The peaks of wax crystals stick out of the deposit layer. The borderline is clearly visible in the center of both images (Figure 31, C and D). The treatment with Genapol O050 also resulted in a formation of an amorphous film which covered the surface inclusive of the epicuticular wax crystals. The peaks of wax crystals stick out of the deposit layer as it was true for Tween 80. The border between the droplet and the treated area was clearly visible as a sharp line. At the borderline of the crusted layer, a lifting or detaching could be observed by a shadow (Figure 31, E and F).

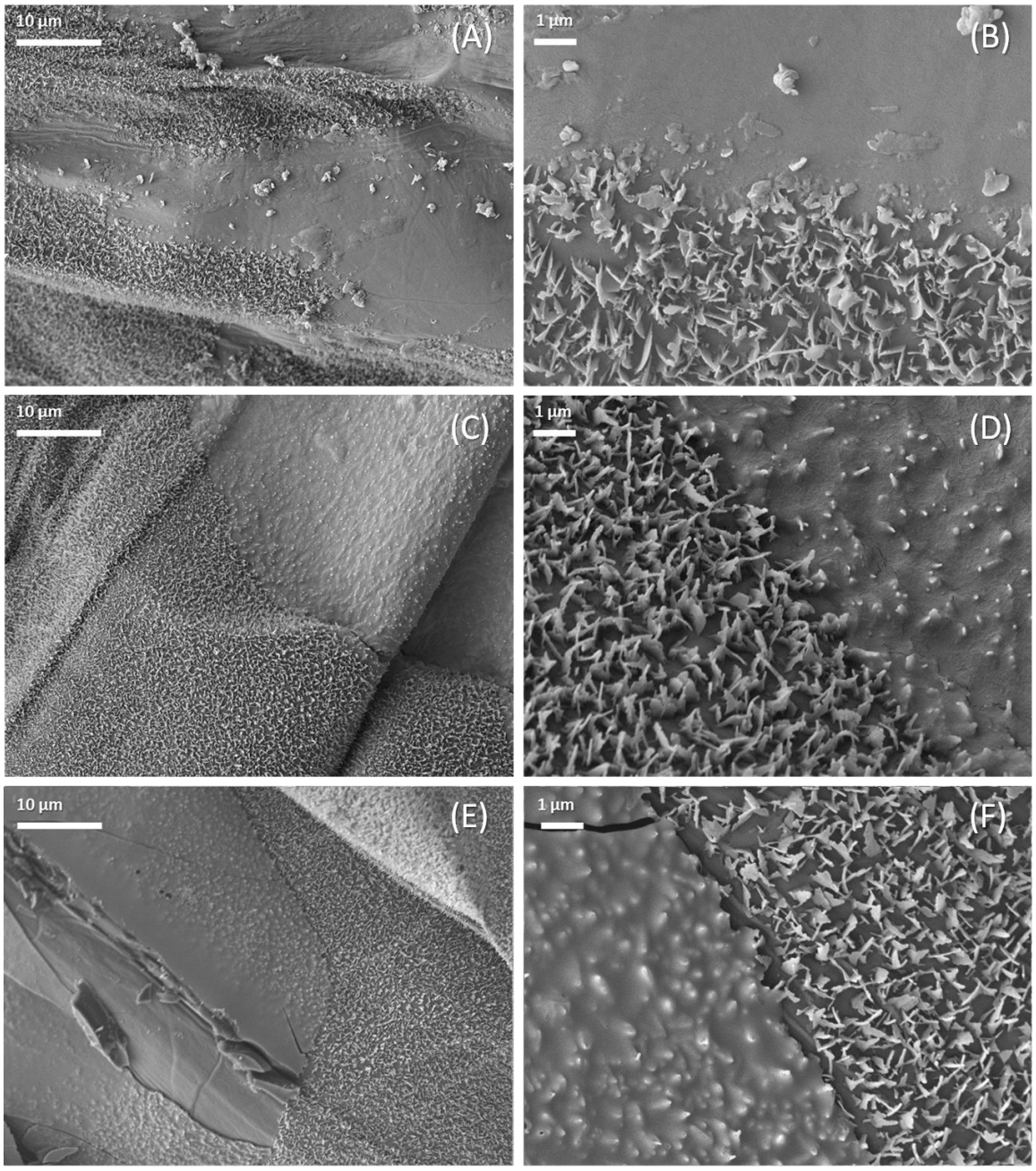

Figure 31: Droplet residues of Tween 20 (A and B), Tween 80 (C and D) and Genapol O050 (E and F) solutions (conc. 0.1% in water (w/v)) on *Triticum aestivum* cv. Arina leaves. Magnification increases from left to right.

2.3.6 Track sprayer experiments

Spray droplet adhesion results of track sprayer experiments are separated into the percentage of leaf coverage and the determination of droplet retention which based on the experimental design involving an optical and a fluorimetrical set-up. The mean leaf coverage and their standard deviation is expressed in % and the mean retention and their standard deviation is shown in ng Tinopal OB (UV marker) per mm^2 leaf area (Table 3).

Table 3: Results of mean leaf coverage (%) and mean retention (ng Tinopal OB per mm^2 leaf area), standard deviation is shown in brackets; n=10

Tradename	Mean leaf coverage (%)	Mean retention (ng Tinopal OB per mm^2 leaf area)
Water	0.96 (1.04)	0.20 (0.15)
Span 20	4.49 (1.05)	0.28 (0.08)
Span 80	2.23 (0.74)	0.18 (0.03)
Tween 20	5.31 (2.19)	0.82 (0.25)
Tween 40	5.17 (2.57)	0.55 (0.30)
Tween 60	2.90 (1.16)	0.30 (0.10)
Tween 65	2.18 (0.71)	0.20 (0.08)
Tween 80	5.34 (1.52)	0.57 (0.14)
Tween 81	2.79 (0.86)	0.22 (0.05)
Tween 85	2.72 (0.95)	0.26 (0.12)
Genapol O050	2.94 (1.37)	0.25 (0.14)
Genapol O080	4.47 (1.02)	0.33 (0.08)
Genapol O100	7.32 (1.23)	0.57 (0.13)
Genapol O200	4.50 (0.79)	0.64 (0.13)
Atlas G1096	2.22 (0.67)	0.25 (0.09)
TEHP EW400	2.97 (0.74)	0.40 (0.12)
Trend 90	13.70 (4.27)	0.95 (0.22)

Pure water was used as a negative control and resulted in a leaf coverage of 0.96% ± 1.04 of the whole leaf area (Table 3). In general, the leaf coverage for all measured surfactants, except Trend 90 and Genapol O100, was equal or less than 5%.

Spray droplets with Span 20 obtained almost a double leaf coverage as compared to Span 80 (4.49% ±1.05). For the class of Tweens, the results of leaf coverage are distributed into higher values of about 5% and lower values of ca. 2.5%. Tween 20, Tween 40 and Tween 80 resulted in the higher leaf coverage compared to Tween 60, Tween 65, Tween 81 and Tween 85. The lowest leaf coverage was visible for Tween 65 which had a leaf coverage of 2.18% ± 0.71.

The results of leaf coverage for the class of Genapol O were more diverse. While Genapol O050 resulted in the lowest leaf coverage value (2.94% ± 1.37), Genapol O100 had the highest coverage (7.32% ± 1.23) compared to the classes of Span, Tween and Genapol O. Genapol O080 and Genapol O200 showed almost the same coverage results (about 4.5%).

Atlas G1096 and TEHP EW400 also resulted in a low leaf coverage level. Though, by far the highest leaf coverage (13.70% ± 4.27) was reached by the retention aiding adjuvant Trend 90.

The fluorimetrically measured values for the retention results were generally related to the results of leaf coverage. The results spread between 0.18 and 0.95 ng Tinopal OB per mm^2 leaf area. Comparing the retention results with the leaf coverage of Tween 20 and Trend 90, Trend 90 showed only a little more retention than Tween 20, whereas Tween 20 had almost half of the leaf coverage of Trend 90. Genapol O200 also resulted in about twice as much ng Tinopal OB per mm^2 leaf area compared to Genapol O080. However, both surfactants displayed the same leaf coverage.

2.4 Discussion

2.4.1 Surface tension measurements

Dynamic surface tension (DST) experiments were performed to analyse selected surfactant solutions considering their ability to lower the physical value of surface tension during this critical time frame. Therefore, the method of maximum bubble pressure was performed which allows to study the mobility of surfactants from a very early surface age of 10 ms. Then, the experiment was continued for 30 s.

During foliar application in the field, the majority of spray droplets impact the leaf surface after about 50 to 400 ms (Wirth *et al.,* 1991; Butler Ellis *et al.,* 2004), (Figure 18). Because DST results are a function of time and the critical time frame of droplet impact might be averaged at about 100 ms (de Ruiter *et al.,* 1990), the specific DST value of 94 ms will be selected for further assumptions (value depends on the measurement procedure of maximum bubble pressure method) (Table 4). During this time frame, the DST values of surfactant solution should reach the critical value of about 55 to 60 mN m^{-1} (Taylor, 2011).

Table 4: Results of DST measurements at 94 ms surface age

Tradename	Chemical name	DST at 94 ms surface age
Water		72.2
Span 20	Sorbitan monolaurate	71.2
Span 80	Sorbitan monooleate	71.6
Tween 20	Polyoxyethylene sorbitan monolaurate	58.4
Tween 40	Polyoxyethylene sorbitan monopalmitate	63.3
Tween 60	Polyoxyethylene sorbitan monostearate	63.8
Tween 65	Polyoxyethylene sorbitan tristearate	70.9
Tween 80	Polyoxyethylene sorbitan monooleate	63.6
Tween 81	Polyoxyethylene sorbitan monooleate	72.0
Tween 85	Polyoxyethylene sorbitan trioleate	71.9
Genapol O050	Oleyl alcohol polyglycol ether	70.9
Genapol O080	Oleyl alcohol polyglycol ether	68.9
Genapol O100	Oleyl alcohol polyglycol ether	62.4
Genapol O200	Oleyl alcohol polyglycol ether	61.2
Atlas G1096	Polyoxyethylene sorbitol hexaoleate	72.1
TEHP EW400	Tris(2-ethylhexyl)phosphate	71.2
Trend 90	Isodecyl alcohol ethoxylate (900 g/l)	33.1

Especially the comparison of DST results at the specific surface age of 94 ms showed little variation among the range of surfactants. With the exception of Trend 90, which was half as low as the majority of samples, Tween 20 resulted in the lowest value of 58.4 mN m^{-1}. All other samples ranged between values of 61 and 72 mN m^{-1}. Accordingly, the lowering of surface tension compared to pure water was maximum about 10 mN m^{-1}.

During the complete time interval, no decrease of surface tension of pure water could be observed and the DST remained constant at a value of about 72 mN m^{-1} (Figure 23) which is defined as literature surface tension value for pure water at 20 °C (Vargaftik *et al.,* 1983). This result confirms, that there are no surface active contaminations in the water which serves as the solvent medium for all other surfactant solutions.

All experiments were performed using a surfactant concentration of 0.1% in water. This concentration was selected, because it is in-between the typical range of commonly used surfactant concentrations for agricultural spray formulations and more important, this value is high above the critical micelle concentration (cmc) of all selected surfactants. Therefore, the formation of micellar aggregates in the bulk phase of the water solvent is ensured. With this, the complete saturation of the water-air interface with surfactant monomers is guaranteed and an equilibrium state can be reached constantly.

None of the selected surfactant samples, except Trend 90, were able to decrease the surface tension to the critical value of about 55 to 60 mN m^{-1} (Taylor, 2011), during the first 100 ms. Most samples reached this critical range much later, after 1000 to 1500 ms. Tween 20 and Genapol O200 decreased DST values most rapidly and reached 55 mN m^{-1} already at about 140 ms.

The diverse shapes of curves of DST of the surfactants are produced due to the nature of their chemical structures (Rosen, 1989). Especially, differences between decreasing DST curves of Span 20 and Span 80 with regard to their chemical structure (Figure 7 and Figure 8) can be discussed exemplary. The alkyl chains of the sorbitan fatty acid esters are mainly reasonable for influencing physico-chemical properties like DST (Peltonen & Yliruusi, 2000). Span 20 carries a saturated lauric acid (C_{12}) which causes the whole molecule having a straight-chain lipophilic tail. In contrast to this, Span 80 carries an unsaturated oleic acid rest

($C_{18:1}$) as lipophilic part of the amphiphilic surfactant molecule. The hydrophilic head remains similar across the class of sorbitan fatty acid esters. The introduction of a cis-double bond causes a branching of the lipophilic tail, with the result that the whole molecule becomes more bulky, compared to Span 20. Branching of the lipophilic tail causes a looser packing of the surfactant molecules at the interface, compared to almost straight-chain homologues (Rosen, 1989, chapter 1). Thereby, the cis-isomer is particularly loosely packed and the trans-isomer would be packed almost as closely as the saturated and straight-chain homologues (Rosen, 1989, chapter 1). Additionally, branched-chain and ring-containing surfactants are basically more soluble in both, water and hydrocarbons and more important, they show a lower viscosity in aqueous media than straight-chain surfactants (Rosen, 1989, chapter 1). Accordingly, the interfacial properties concerning Span 20 and Span 80, especially apparent in DST results, might change.

Peltonen & Yliruusi (2000) calculated the molecular area per molecule for Span 20 and Span 80. This value can be explained as the area of a molecule that is accessible to a surrounding solvent, like in this case water. The unsaturated Span 80 had a larger accessible surface area per molecule (46 $Å^2$) than the saturated Span 20 (40 $Å^2$) (Peltonen & Yliruusi, 2000).

This fact might be the explanation why DST curves of Span 80 (unsaturation) decrease only very late, at the end of the experiment. Span 20 (saturation) has a smaller molecular area and the movement of molecules might be faster, which is confirmed by the earlier decrease of DST. Once the surface saturation has begun (starting of surface tension decrease), the larger Span 80 molecules cover the interfacial area faster than the smaller Span 20 with their linear shape. Consequently, the drop of DST curve was more abrupt for Span 80. This conclusion coincides with the results from Peltonen & Yliruusi (2000) who found out, comparing Span 20, Span 40, Span 60 and Span 80 that the *'unsaturation of the hydrocarbon chain seemed to be more dominant in determining the interfacial properties […] than in determining the hydrocarbon chain length'.*

Another value explaining DST behaviours of surfactants would be the calculation of diffusion coefficients (*D*) of the molecules. Most of the selected surfactants are highly polydisperse, so that these calculations would only result in a very unprecise value. Other factors like contaminations of organic material in the surfactant batch

would exert also great influence on surface tension properties. This could also be the reason why differences among the Tween family are not so clearly visible and explainable as compared to the less polydisperse Span or Genapol classes. Nevertheless, the calculation of *D* is an important physico-chemical information which would be required for further evaluations.

Two methods, the 'Du Noüy' ring method and the pendant drop method (Good, 1979), were used for analysing the static or equilibrium surface tension (STeq). Both methods have their advantages, but due to technical equipment, the ring method was not executed any further. The automatic determination of surface tension with the Drop Shape Analyser DSA100S (Krüss GmbH, Hamburg, Germany) was preferred to the tensiometer K5 (Krüss GmbH, Hamburg, Germany), which could be only operated manually. Therefore, results gained by the pendant drop method were more reliable, consistent and reproducible.

The majority of selected surfactants resulted in a narrow distribution of STeq values ranging between 30 and 45 mN m^{-1}. Nevertheless, all surfactants were able to considerably decrease the surface tension compared to pure water (72.3 mN m^{-1}). The high surface tension value of pure water reflects the high intermolecular attractions of water molecules (Rosen, 1989, chapter 6). As the surface tension of water is a function of temperature (Vargaftik *et al.,* 1983), the literature value of water (72.75 mN m^{-1} at 20 °C (Vargaftik *et al.,* 1983)) is closely comparable to the results in this experiment. According to Singh *et al*. (1984) the influence of the water hardness on the surface tension is negligible.

The lowest measured value was 27.8 mN m^{-1} for Isodecyl alcohol ethoxylate (Trend 90). This tank-mix adjuvant is added to formulations because of its surface tension lowering properties to improve retention effects for spraying superhydrophobic plant surfaces (Koch & Barthlott, 2009). Several other tank-mix adjuvants which were also commonly used for improving physico-chemical properties were compared by Janku *et al.* (2012). They ascertained for Trend 90 an equilibrium surface tension value of 26.6 mN m^{-1} at a concentration of 1.24 g kg^{-1} which was indicated as critical micelle concentration (cmc). Regarding slightly different concentration levels, findings from Janku *et al.* (2012) coincide with results in this study.

Also for Span 80, a comparatively low STeq value of 29.3 mN m^{-1} could be observed. As mentioned in the previous section, the DST of unsaturated Span 80 decreased only at a very late stage of the experiment. The relationship between DST and STeq is the time dependence of the movement of surfactant molecules through an aqueous phase. Only when the water-air interface is fully saturated with surfactant molecules, STeq values were achieved. This time-dependent process is mainly influenced by the chemical nature of the surfactant and can last between several milliseconds and minutes (Venzmer, 2015). The comparison of DST curves of saturated Span 20 and unsaturated Span 80 revealed a late but steep drop of Span 80 and in contrast, an earlier but more linear decline of Span 20. Regarding STeq values which can be considered as temporal continuation of the experiment, Span 80 reached a lower value (29.3 mN m^{-1}) than Span 20 (32.0 mN m^{-1}). This finding confirms again the particular importance of temporal aspects, considering the surface tension lowering properties of surfactants and therefore, the spraying process as a whole.

2.4.2 Wetting characteristics of selected surfactants

The term *'wetting agent'* is applied to any substance that increases the ability of water or an aqueous solution to displace air from a solid surface. This surface property is shown by all surface active agents, although the extent to which they exhibit this phenomenon varies greatly (Rosen, 1989, chapter 6). The water contact angle (CA) test is generally applied as a simple and easy to measure method of evaluating the wettability of different plant species. Therefore, the CA is a unit for the wettability of surfaces (Koch *et al.,* 2008). A low water CA of <10°-0° is indicative of a superhydrophilic surface, CAs <90° would characterise surfaces that are hydrophilic or easy to wet. Results up between 90 and 150° are regarded as difficult-to-wet or hydrophobic and CAs over 150° are extremely difficult-to-wet or superhydrophobic surfaces (Figure 17) (Brutin, 2015; Koch *et al.,* 2008).

As the water CA on parafilm had a relatively high value (107°), the surface must be assessed to be apolar. On the plant surface of *Triticum aestivum* cv. Arina, the adaxial and abaxial leaf surface was distinguished. The adaxial side had a higher CA (152°), than the abaxial side (145°). Both values are very high and indicate a

very hard to wet surface, whereas the adaxial surface has to be classified as superhydrophobic.

In the literature, there are some critical debates about the best way to characterise wettability of difficult-to-wet species, like *Poaceae*. Resulting water CAs are often immeasurably high to be able to rank these species for wettability (Taylor, 2011). Gaskin *et al.* (2005) have recommended the use of a 20% acetone in water solution (v/v) as a test solution to characterise these plant surfaces.

The observation of plant surfaces having hydrophobic characteristics is based on the lipophilic wax surface of the plant cuticle. Investigations of the chemical wax composition of *Triticum aestivum* cv. Arina coincided with literature data and revealed a main component class of primary alcohols with the predominant octacosanol (C28 alcohol) (>70%) (data not shown) (Bianchi *et al.,* 1980; Koch *et al.,* 2006). Scanning electron microscopy (SEM) analyses also showed hierarchical organised micro-structures like convex epidermal cells (not shown) with epicuticular wax crystals sitting on their surface (Figure 30). Moreover, both leaf sides of wheat showed a high number of non-glandular trichomes, whereas the density on the adaxial side was half as much than on the abaxial side. In general, trichomes have a strong influence on leaf wettability. Brewer *et al.* (1991) showed *'that leaves with trichomes were more water repellent, especially where trichome density was greater than 25 mm^{-2}'*. But they also observed that some hairy species are able to entrap droplets with their trichomes (Brewer *et al.,* 1991). Neinhuis & Barthlott (1997) found out that wetting of plants covered with hairs strongly depends on the presence or absence of epicuticular wax crystals on their surface. Leaves covered with non-waxy hairs were only water repellent for a short time after a water droplet had been applied. In contrast, leaves with waxy trichomes were extremely water repellent, although the trichomes were up to 2 mm high and only loosely distributed over the leaf surface (Koch *et al.,* 2008). The results found for *Triticum aestivum* cv. Arina support this theory. The abaxial side showed twice as much non-waxy hairs and resulted in lower CAs in general, compared to the adaxial side covered by less trichomes. The trichomes might be evaluated as 'hydrophilic peaks' sitting on an extremely hydrophobic surface.

The optical estimation of SEM samples revealed that the wax crystal density was slightly higher on the adaxial side, because of more free 'gaps' in the wax crystal

coverage on the abaxial side. This finding also supports the conclusion of the abaxial side having better wetting characteristics than the adaxial side, although it is only slightly better.

As already mentioned, the CA analysis can be generally applied as a simple and easy to measure method. There exist several methods derived from the original reflections by Thomas Young (1805). The tilting angle, also the advanced and receding angle can be used to characterise the self-cleaning property of surfaces considering the angle when a water droplet rolls off (Koch *et al.,* 2008). This tilting angle must not be mixed up with the dynamic sessile angle, where a liquid is pumped in and out of a droplet (Carrier & Bonn, 2015). In this work, the hysteresis angle is regarded as a sessile droplet which was observed to spread over a surface during a certain time period. The change of the CA of this sessile droplet was therefore recorded with a camera. Since evaporation of water should be avoided during CA analysis, the droplet volume was set at 3 µl and the measurement was persisted for maximal one minute. The information about CA change might give evidence about spreading properties of surfactants. Some publications do not provide any details about the exact point in time of CA recording, they measured the CA when the droplet was initially applied to the surface, which is sometimes very complex (Guo & Liu, 2007). In this study, most surfactant droplets, as it was observed for the Tween and Genapol O family (conc. 0.1% in water, w/v), mainly decreased the CA during the first 5 to 10 seconds on parafilm. After about 10 seconds spreading was finished and a CA decline was no longer observed. However, the initial CA was reduced compared to the water CA which did not change over time.

An exception was Span 80, resulting in a comparatively high initial CA which declined very steep during the first 20 seconds. In comparison, Span 20 started already with a very low initial value (73°) and spread only moderate during the first 10 seconds. For Span 20 and Span 80 CA development did not reach an equilibrium value during the first minute.

Since spreading of droplets with surfactants is mainly influenced by the surface tension, measuring the time-dependent sessile CA development on parafilm might be considered as a continuation of DST experiments. Therefore, findings gained from both measurements coincide. DST results revealed a very late decrease in

surface tension of Span 80 explained by its unsaturation. After several seconds, spreading on parafilm was continued. On the other hand, Span 20 showed in DST experiments a faster but linear surface tension decrease and accordingly the initial CA on parafilm was already lower and did not spread as strong as compared to Span 80. Nevertheless, the final CA after one minute of spreading was much lower for Span 20.

The further spreading which lasted much longer than one minute was analysed by the droplet spread area after the evaporation of water. The diameter of the residue of the added red dye was measured by microscope. The covered leaf area was about six-times higher for Span 20 (63.2 mm^2) on the adaxial side, than for the next best-spread surfactant Tween 81 (10.6 mm^2). From the CA results, one would suggest the abaxial side to be better to wet than the adaxial side because of already discussed reasons. Contrastingly, results of droplet spread area showed slightly lower values for the abaxial side, but differences may not be statistically significant. The reasons for Span 20 to result in such a maximum spread area cannot be explained only by data gained in the performed experiments and need to be discussed in an extensive manner.

A comprehensive work about the ‘Droplet Wetting and Evaporation’ was published by Brutin (2015) who summarised in detail the numerous influencing factors on a sessile droplet. For example, super-spreading is a fascinating phenomenon which refers to the quite surprising action of a droplet of a diluted solution of some special trisiloxane surfactants on hydrophobic substrates as plant surfaces (Nikolov *et al.,* 2002). Despite numerous studies, the elucidation of the MoA of these organosilicone surfactants, concerning the super-spreading behaviour, is still ongoing (Venzmer, 2015). Even though, Span 20 does not belong to the family of silicone surfactants and the term ‘super-spreading’ would be inappropriate, the wetting potential, especially after one minute, was enormous. One explanation for the special wetting properties of Span 20 might be complex interactions at the interface (Venzmer, 2015). Spreading action can be pre-determined by the surface free energy of solids and liquids (Ivanova & Starov, 2011). Therefore, the surface free energy of both, the liquid and the solid, must be well characterised with the help of contact angle measurements with liquids of different polarities. When polar and dispersive fractions of the liquid and the surface are equal, the interfacial

tension would be zero. Accordingly, adhesion work would be very high. In this unrealistic case, the droplet would spread completely, producing a CA of zero (Volpe & Siboni, 1997; Owens & Wendt, 1969). This concept considers only smooth surfaces, for example the painting and coating of metal and synthetic polymer surfaces. However, the model disregards highly structured rough surfaces, like most plant surfaces. Fernández & Khayet (2015) were the first apply the concept 'OWRK' of (Owens & Wendt, 1969) on plant surfaces by comparing different methods, regardless of the surface roughness.

Moreover, so-called *'Marangoni effects'* are generally believed to be the cause for super-spreading accounting for trisiloxane surfactants and could be another reason for the well wetting properties of Span 20 (Venzmer, 2015).

The driving force, caused by a surface tension gradient between the apex of the droplet and the expanding contact area, has been proposed for the action of trisiloxane surfactants (Nikolov *et al.,* 2002). An alternative driving force has to be suggested for a droplet during evaporation. It was proved, that evaporation is higher at the droplet contact line (Starov & Sefiane, 2009). So the droplet may be warmer near this zone (periphery) and colder in the inner of the droplet (Hu & Larson, 2005). This temperature gradient (thermodynamic reasons), induced within the droplet, also causes a Marangoni effect and could be another reason for the well wetting action. However, it seems likely, that an interaction of these different physical phenomena is the reason for the surprisingly observed wetting action of Span 20.

In summary, the CA of a liquid on a surface depends on molecular forces that affect the physical property of surface tension of an involved liquid, solid surface and the surrounding gaseous phase (Young, 1805). Consequently, wetting depends on the ratio between the energy that is necessary for the enlargement of the surface and the gain of energy due to adsorption (Adamson & Gast, 1997). The behaviour of liquids is different when they are applied to smooth or structured surfaces (Koch *et al.,* 2008). So the main causes for the CA hysteresis are surface roughness and heterogeneities (Carrier & Bonn, 2015). When the surface area to be wet is small, like wetting of smooth and nonporous solids, then conditions close to the equilibrium can be attained during the wetting process. Free energy changes that are involved in the process determine the degree of wetting are attained. On the

other hand, when the surface to be wet is large, as it is the case for superhydrophobic structured plant surfaces like most *Poaceae*, equilibrium conditions are not often reached during the time allowed for wetting. Then, the degree of wetting is determined by kinetics rather than thermodynamics of the wetting process (Rosen, 1989, chapter 6). Therefore, the wetting of highly complex organised, rough and lipophilic surfaces, like the surface structure of wheat, cannot be predicted precisely by experiments like CA and surface tension measurements. The wetting process of surfactants will last for a longer time, including the droplet evaporation. Nevertheless, CA and surface tension analyses form the basis and help to understand and estimate the wetting behaviour of a surfactant.

2.4.3 Spray droplet retention experiments

Investigating the retention characteristics of surfactant droplets, laboratory track sprayer experiments were carried out. Measurements distinguished between determinations of droplet retention which based on the experimental design, involving a fluorimetrical set-up and also the optical quantification of percentage of leaf coverage when the droplets had already dried.

The relation of both experiments revealed a broad distribution of results gained from individual leaf values (Figure 32). Thus, both results, retention and leaf coverage, are not correlated positively. For example, results with a mean retention value of about 0.8 ng Tinopal OB per mm^2 leaf area range in their leaf coverage between 3 and 15%. The reason for this is that the measuring of the optical leaf coverage also includes the droplet spreading on the leaf surface (extensively discussed in the section before). Factors like different spreading properties of surfactants and the complex surface of *Triticum aestivum* are involved in the process of wetting. A distinct relationship between retention and wetting would not be expected, because droplets containing the same marker concentration, can show a different spreading result. The experiment to quantify the exact concentration of the UV tracer was conducted afterwards. Therefore, the fluorimetrical set-up serves therefore as a value, characterising the droplet retention without including spreading effects.

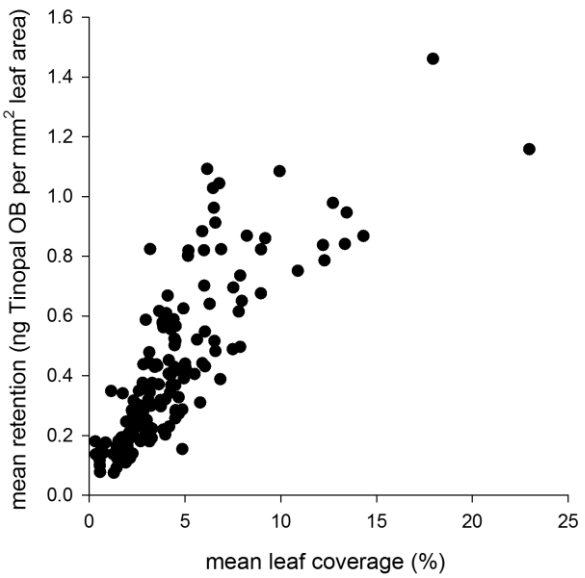

Figure 32: Correlation mean leaf coverage (%) and mean retention (ng Tinopal OB per mm^2 leaf area). Dots represent individually measured values.

Since the retention process involves short time dynamics, it is well-known that the spray retention on a plant surface is not correlated to the equilibrium but to the dynamic surface tension (de Ruiter *et al.,* 1990; Wirth *et al.,* 1991; Holloway *et al.,* 2000; Taylor, 2011; Green & Green 1991; Anderson & Hall, 1989). Nevertheless, there is a discussion in literature regarding the correlation of retention results and the dynamic surface tension at a certain surface age. Stevens and Kimberly (1993) criticised publications based on retention correlations using the surface tension values at fixed and arbitrarily selected surface ages or the selection of the best fit from correlations. Because the critical timeframe of droplet impact might be defined as about 50 to 100 ms (de Ruiter *et al.,* 1990), the specific DST value of 94 ms was selected for further assumptions (value depends on the measurement procedure of maximum bubble pressure method). Plotting both results, gained from the track sprayer experiments and the DST results, showed decreasing coverage or retention results with increasing DST values (Figure 33 and Figure 34).

In order to focus on retention results, a plateau appears at DST values below ca. 60 mN m^{-1} (Figure 34). The lack of surfactant species bearing DST values between 33.1 mN m^{-1} (Trend 90) and 58.4 mN m^{-1} (Tween 20) complicates the exact determination of the plateau. Nevertheless, it could be shown that there is not a linear relationship between retention on *Triticum aestivum* cv. Arina and DST at a certain surface age (Figure 34). In fact, it seems likely that retention would not be further improved at very low DST values.

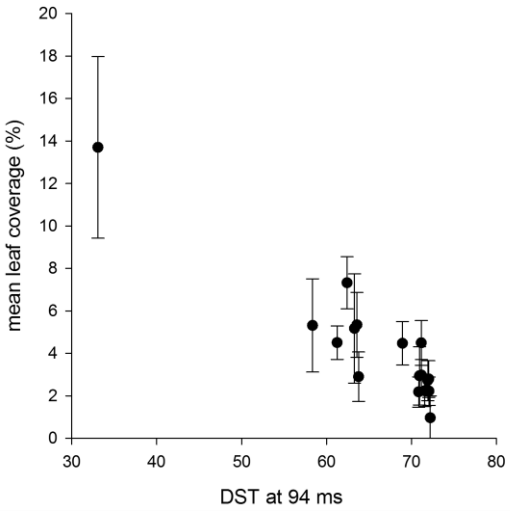

Figure 33: Relation between mean leaf coverage (%) and DST at 94 ms surface age. Dots indicate mean values and error bars represent SD, n=10.

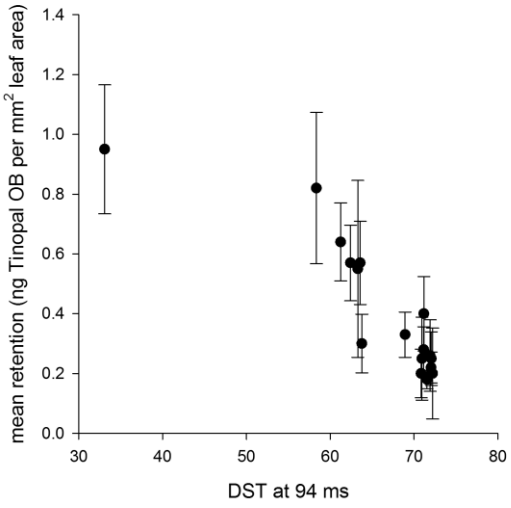

Figure 34: Relation between mean retention (ng Tinopal OB per mm^2 leaf area) and DST at 94 ms surface age. Dots indicate mean values and error bars represent SD, n=10.

These considerations are contrary to Wirth *et al.* (1991) who ascertained a satisfactory linear correlation between leaf retention on *Zea mays* of a large number of spray liquids and DST values at 100 ms (surfactants covered a wide range of 25 to 72 mN m^{-1}).

Different reasons why retention and DST correlations show a plateau at low DST values have to be considered. One possible reason could be the phenomenon of droplet shattering when the surface tension is very low, e.g. as it would be the case for Trend 90. Droplet shattering is also an effect of surface characteristics. It was shown that shattering is reduced when smooth and polished surfaces are studied (Rein, 1993). Levin & Hobbs (1971) found out that the droplet splashing is promoted at the collision, especially on rough surfaces, like on *Triticum aestivum*

which was used in this work. The shattering of droplets is an unwanted side effect which is important to be reduced by different measures. Not only cost aspects, but also regulatory risks are adverse consequences when the retention is decreased and the spray liquid is lost to the ground. Tiny, splashed droplets can easily drift and pollute neighbouring fields, waters and preserved areas (Rein, 1993).

Another reason for explaining the low retention results of Trend 90 would be the droplet run-off because of a very low surface tension (Fernández, 2013). A strong recoiling of the successfully adhered droplet, due to a low surface tension, can lead to a bounce-off and therefore to a reduced retention (Mercer *et al.,* 2010). Unfortunately, such phenomena could not be observed by recording the spray process with the help of the high-speed camera. Other influencing factors might be of minor relevance. For example, Wirth *et al.* (1991) identified that the orientation of the leaf had only little influence on the retention result. Stevens *et al.* (1993) stated that the reduction of DST of aqueous spray droplets with surfactants is more important than factors like droplet size, droplet velocity or angle of incidence on the leaf.

Contrastingly, Taylor (2011) mentioned the surface tension and CA of the droplet as it impacts on the leaf surface controlling the work of adhesion of the droplet on the surface. The adhesional force between the droplet and the surface must be higher than the kinetic energy of the droplet to prevent the drop from bouncing off the leaf. He also advocates systematic studies looking at each individual process when a droplet impacts and try to develop a mathematical model (Mercer & Sweatman, 2006; Mercer *et al.,* 2010; Gaskin *et al.,* 2005; Stevens *et al.,* 1993). Stevens *et al.* (1993) first described the method where adhesion is measured under defined conditions. Starting with the selection of the surfactants and their concentrations in water, spray liquid viscosity, droplet diameter, fall distance, droplet velocity at the moment of impact and the angle of incidence on the plant surface are recorded and varied. From a theoretical point of view, the droplet impact velocity is an elementary physical parameter that can easily be changed in laboratory set-ups (Rein, 1993). So mathematical models based on the physical processes involved in the bounce or adhesion or shatter of droplets can be established (Schou *et al.,* 2011). These process-based retention models have been recently implemented within an experimental set-up of the spray application

simulation software ‘AGDISP’ (Forster *et al.,* 2012). Taylor (2011) values this outstanding model as being extremely promising having the advantage of providing a fundamental understanding of the retention process in contrast to empirical models.

Both methods of application are important to understand the fundamental principles of the retention process. While the controlled application with the help of a droplet generator may elucidate the sensitive single variables in detail, the track sprayer may reflect the situation on the field better. Both types of studies are needed. It is also very important to keep in mind that the trajectory of the spray droplets and also the plant surfaces are well defined under laboratory conditions and not equivalent to the canopy structure and the plant density on the field. For a certain application procedure, retention characterisation should therefore be also carried out under field conditions.

3 CHAPTER II: THE HUMECTANT PROPERTIES OF ADJUVANTS

This chapter is based on the following publication:

Asmus, E., Popp, C., Friedmann, A.A., Arand, K., Riederer, M. (2016). Water Sorption Isotherms of Surfactants: A Tool to Evaluate Humectancy. *Journal of Agricultural and Food Chemistry* (doi: 10.1021/acs.jafc.6b01378)

Statement of individual author contributions in the manuscripts:

Publication (complete reference) Asmus, E., Popp, C., Friedmann, A.A., Arand, K., Riederer, M. (2016). Water Sorption Isotherms of Surfactants: A Tool to Evaluate Humectancy. *Journal of Agricultural and Food Chemistry* (doi: 10.1021/acs.jafc.6b01378)					
Participated in	**Author Initials,** Responsibility decreasing from left to right				
Study Design	E.A.	K.A.	M.R.	C.P.	A.F.
Data Collection	E.A.	K.A.	M.R.	C.P.	A.F.
Data Analysis and Interpretation	E.A.	K.A	M.R.	C.P.	A.F.
Manuscript Writing	K.A.	E.A.	M.R.	C.P.	A.F.

All figures and tables included in this chapter, except Figure 35 and Figure 36, are also illustrated in the publication.

I confirm that I have obtained permission from both the publishers and the co-authors for legal second publication and the correctness of the above mentioned assessment.

I also confirm my primary supervisor's acceptance.

Elisabeth Asmus 29.06.2016 Würzburg

_____

Doctoral Researcher's Name Date Place Signature

3.1 Introduction

Spray application is a key process determining the effectiveness of a foliar applied active ingredient (AI) (Rodham 2000). The activity of adjuvants is influenced by environmental factors like rainfall, light levels, temperature and humidity (Kirkwood 1993; Rodham 2000). Spraying at low humidities at sunny days causes an aqueous droplet to dry very fast within a few seconds to minutes. Accordingly, the active ingredient precipitates as a crystalline deposit on the plant surface and is not available anymore for the following permeation process. Accordingly, the efficacy of agrochemicals is strongly influenced by relative humidity, with an optimal at humid conditions (Kudsk & Kristensen, 1992). Particularly, the uptake of highly water-soluble active ingredients is enhanced under a high relative humidity (Ramsey *et al.,* 2005). It is commonly believed, that the humidity effect is basically related to the rate or extent of droplet drying which may reduce the availability of certain active ingredients due to crystal precipitation (Kudsk & Kristensen, 1992; Ramsey *et al.,* 2005; Price, 1982; Cook *et al.,* 1977). Increased AI uptake and efficacy were shown to be associated with gel-like or amorphous residues without crystalline deposits (Hess & Falk, 1990; Macisaac *et al.,* 1991).

Hygroscopic substances are used in tank mix formulations to delay the droplet drying by remaining a liquid deposit on the surface and keeping the active ingredient bioavailable. By maintaining the herbicide in solution, the AI is more available for uptake into the plant. These adjuvants are urgently required, particularly in warm and dry areas where relative humidity is significantly lower than 50%.

Consequently, a large variety of substances, so-called '*humectants'*, are used to increase the '*equilibrium water content and increase the drying time of an aqueous spray deposit*' (ASTM, 1999) on the leaf surface (Price, 1982). Humectants absorb and retain moisture from the surrounding atmosphere. A general known organic humectant is glycerol which is commonly used in pharmaceutical, cosmetic (Björklund *et al.,* 2013) and food products to give them the desired flexibility, softness and shelf life (Soaps and Detergents Association, 1990).

In the context of plant protection agents, the humectancy of adjuvants is believed to be related to a high ethylene oxide (EO) content, since surfactants with a high EO content enhance the cuticular uptake of water soluble active ingredients

(Stevens & Bukovac, 1987b; Baur *et al.,* 1997b; Gaskin & Holloway, 1992; Stock & Holloway, 1993). In most ethoxylated surfactants, the hydrophilic moiety is composed of polyoxyethylene (POE) chains. Ethoxylated surfactants are thought to improve the uptake of hydrophilic and lipophilic herbicides by different modes of action (Stock & Holloway, 1993). Low EO content surfactants having a comparably high lipophilicity enhance the uptake of lipophilic herbicides by entering the plant cuticle (Burghardt *et al.,* 1998; Riederer *et al.,* 1995; Burghardt & Riederer, 1996) and altering the cuticular wax fluidity (Schönherr, 1993a; Schönherr, 1993b). Surfactants with a high EO content have been suggested to have humectant properties and thereby delay droplet drying and AI crystallization (Stevens & Bukovac, 1987b) or enhance cuticular swelling (Coret & Chamel, 1993). Stevens and Bukovac (1987a) could show within one distinct class of ethoxylated octylphenol surfactants (also known as Triton X series) that water absorption increases with increasing EO content, at least at relative humidities above 70%. Unfortunately, due to the limitation on only one surfactant class studied only at high humidity levels (80%, 90% and 100% RH), it gets difficult to draw further conclusions about the essential mechanism of humectancy. An extrapolation of results from Stevens and Bukovac (1987a) reveals that there would be almost no water sorption of ethoxylated octylphenol surfactants below 70% RH (Ramsey *et al.,* 2005). Therefore, Ramsey *et al.* (2005) valued the suggestion that surfactants with long EO chains would have humectant properties as misleading because all studies were performed only at high humidity levels which would prevent a rapid droplet drying *a priori*. Controversy, Baur *et al.,* (1997b) found a linear relationship between the mass fraction of polyethylene glycol 400 (PEG400) and relative humidity between 11% and 93%. These two basically contrasting studies reveal that the physical process of water sorption of surfactants is not completely understood, yet.

Objectives and research questions

After the successful retention on the plant canopy, the droplet begins to spread on the surface. Since an increased surface extension and warm and dry environmental conditions promote the already rapid water evaporation, the AI impends to precipitate as a crystalline deposit on the surface and is not available anymore for uptake into the plant. Therefore, precipitation must essentially be avoided by a prolongation of droplet drying or re-hydration of the deposit, with the help of humectants. Although, humectants are known to absorb and retain moisture from the surrounding atmosphere, a clear definition including a rigorous quantification, does not exist.

Therefore, the water absorption and also desorption potential of pure selected adjuvants was investigated comprehensively. Since adjuvants used in this study represent non-ionic polydisperse surfactants with differing EO content and variable aliphatic chains, a fundamental structural analysis was conducted. From the obtained water sorption isotherms, relationships between the molecular structure and the water sorption behaviour may be assumed.

This knowledge may help to predict the humectant potential of a broad range of adjuvants used in agrochemical spray formulations in order to obtain an integrative understanding of how surfactants can influence the foliar uptake of AIs.

3.2 Materials and methods

3.2.1 Chemicals

Non-ionic sorbitan fatty acid esters (Spans) and their polyethoxylates (Tweens), oleyl alcohol ethoxylates (Genapol O) and polyoxyethylene sorbitol hexaoleate (Atlas G1096, Figure 36) were used in water sorption experiments (Table 1). Anhydrous glycerol was also studied as a reference chemical (Figure 35).

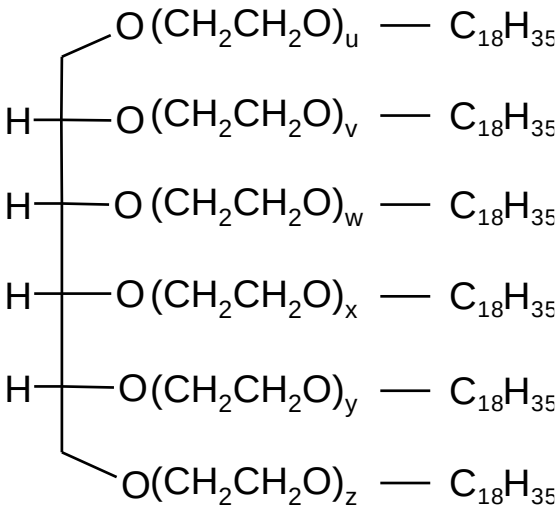

Figure 35: Generalised chemical structure of polyoxyethylene sorbitol hexaoleate (Atlas G1096) carrying an unsaturated alkyl chain (18:1).

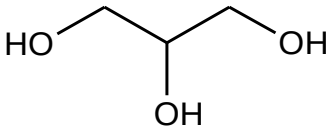

Figure 36: Chemical structure of propane–1,2,3- triol (glycerol).

3.2.2 Calculation of hydrophilic-lipophilic balance (HLB) values

Surfactants are characterised by their amphiphilic properties, combining a nonpolar lipophilic and a polar hydrophilic portion in one molecule (Semenov *et al.,* 2015). The hydrophilic-lipophilic balance (HLB) is a fractional ratio of the hydrophilic to the hydrophobic part in a surfactant molecule (Griffin 1954). Based on the mean saponification values of the ester (S) and the acid value of the fatty acid (A), Griffin (1954) calculated HLB values of non-ionic surfactants.

$$HLB = 20\ (1 - \frac{S}{A})$$

(eq. 4)

The values range from 1 to 20 in which water solubility increases and lipid solubility decreases with increasing HLB. However, the HLB value is a property that has not been rigorously defined and we recalculated the HLB values according to Pasquali *et al.* (2008). For all surfactants, values corresponded to Pasquali *et al.* (2008).

3.2.3 Water sorption isotherms

Water sorption isotherms were determined using a gravimetrical sorption test system (SPS11-10µ, ProUmid GmbH & Co. KG, Ulm, Germany). The sorption test instrument automatically determines the water uptake/release of up to 10 samples in parallel in a test atmosphere with controlled temperature and relative humidity.
The device is equipped with an analytical microbalance (precision ± 10 µg) determining the change in sample mass at regular time intervals. When all samples are in equilibrium with the water vapour partial pressure of the test chamber, the sample masses remain stable. Subsequently, the relative humidity was increased/decreased to the next level (Figure 37). The relative equilibrium water sorption (% of the dry weight) of a specific surfactant is highly specific and independent from the initial weight, but a higher net weight requires more time for equilibration (Figure 37).
Approximately 100 mg of pure substance were evenly spread over the bottom of the sample dishes to assure a flat surface and a film thickness comparable among all compounds. Powdery surfactants were previously melted at 50 °C. Before measurement, all samples were dried under a flow of nitrogen until they reached a

constant weight. Equilibrium water sorption (mass %) was determined by increasing relative humidity in 10% intervals from 0% to 60% and at 5% intervals from 60% to 95% and in the same way back to 0%. Individual equilibrium values for each humidity were used to generate water sorption isotherms.

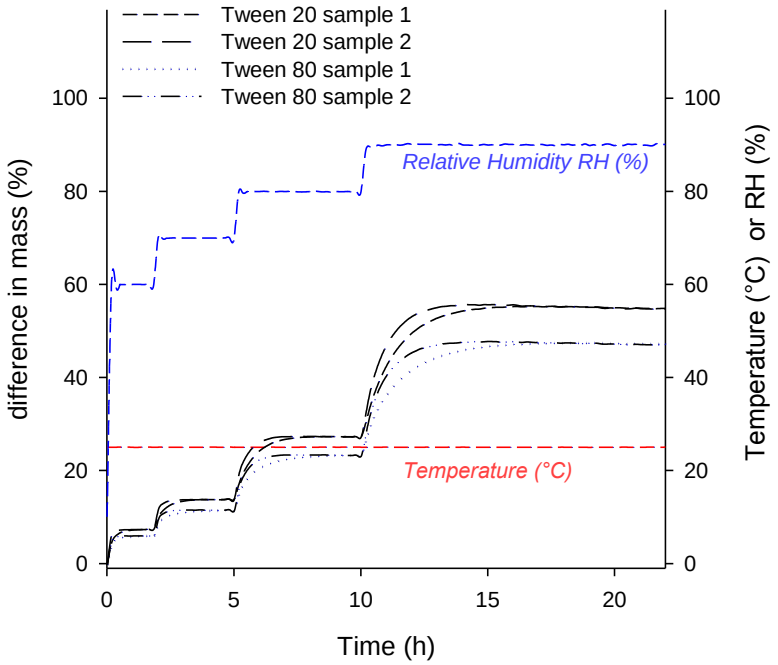

Figure 37: Typical sequential sorption measurement for two samples (with different initial dry weight) of Tween 20 and Tween 80 at controlled temperature of 25 °C (red). The sample weight increased with moisture absorption. When equilibrium with the surrounding atmosphere was reached, the sample weight remained stable and humidity (blue) was raised to the next level.

3.3 Results

The majority of surfactant samples significantly increased when the RH in the surrounding atmosphere was increased from 0% to 95% (Figure 37). When the RH was subsequently decreased again from 95% to 0%, sample weights decreased without hysteresis. The resulting moisture sorption isotherms showed an exponential shape with a steeper increase starting at 60% to 70% RH (Figure 38). As an exception, two Spans (Span 65 and Span 85) exhibited no significant increase in weight at 95% RH. Water sorption only reached 1.7% and 1.2% of the initial mass.

In general, water sorption was low for Spans (Figure 38, A) and much more distinct for the polyethoxylated surfactants (Tweens and Genapol O series, Figure 38, B and C). Even at 95% RH, none of the surfactants sorbed more water than their initial dry weight and therefore, the maximum mass increases were below 100%. In the group of sorbitan fatty acid esters, Span 20 reached a maximum water sorption of 42% of the initial dry weight at 95% RH (Figure 38, A). In comparison, the water sorption at 95% RH was about twice as high for the polyethoxylated surfactants Tween 20 (80%, Figure 38, B) and Genapol O200 (76%, Figure 38, C). The water sorption isotherm of Atlas G1096 was comparable to that of Span 20 (Figure 38, D). The water absorption (mass %) of glycerol was much more distinct than that of any surfactant investigated here. It reached a value of about 350% of the initial dry weight at 95% RH (Figure 38, D). The investigated water sorption isotherms of Span 20, 40, 60 and 80 (Figure 38, A) and of the Genapol O series (Figure 38, C) clearly differ. Water sorption at 95% RH decreases from 42% for Span 20 to 10% for Span 80, while Span 40 and 60 have intermediate values (Figure 38, A).

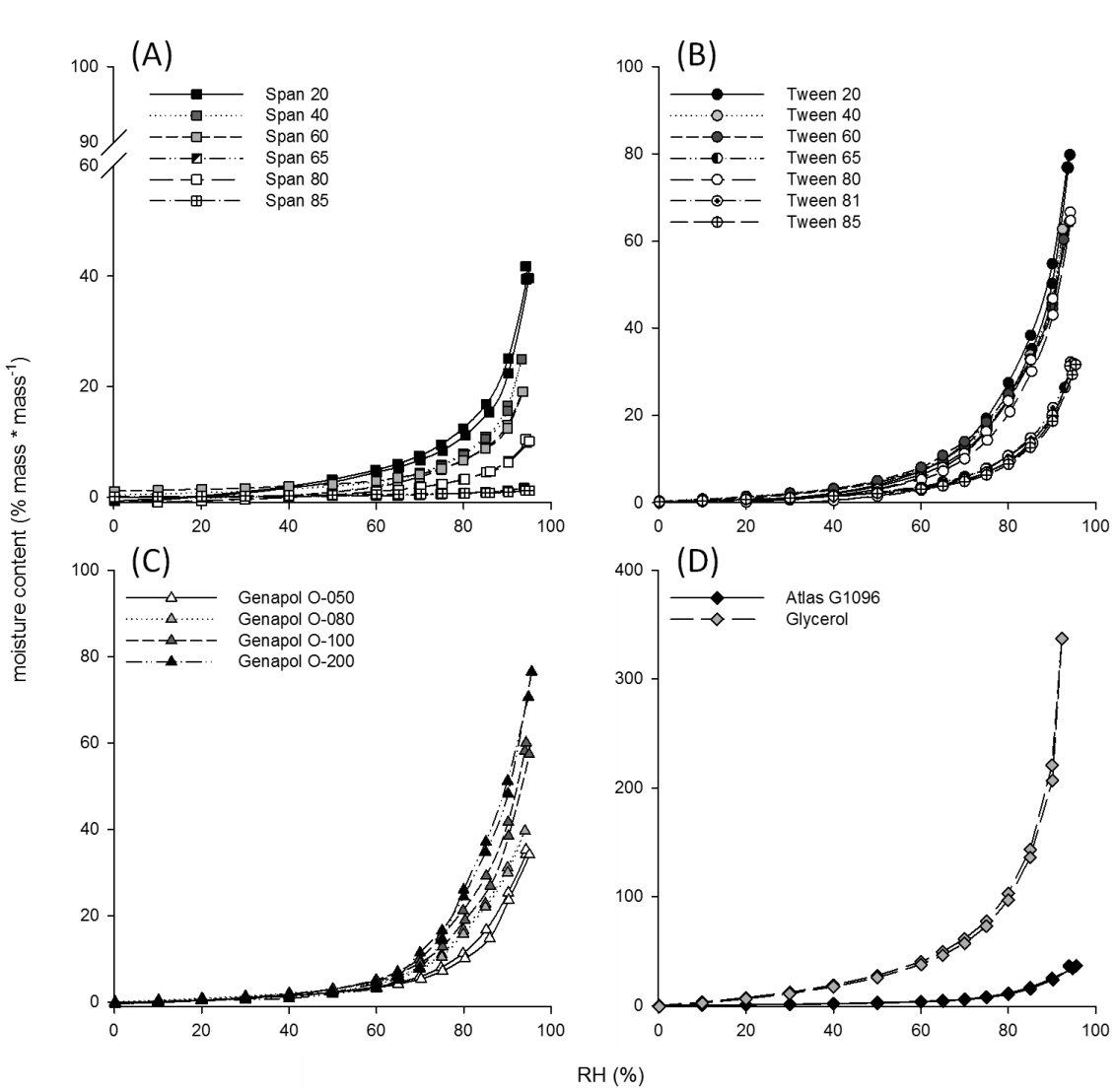

Figure 38: Water sorption isotherms for Span series (A), Tween series (B), Genapol O series (C), polyoxyethylene sorbitol hexaoleate (Atlas G1096) and glycerol (D) represented as moisture content (mass %) vs. relative humidity RH (%).

Within the Genapol O series, water sorption systematically increases from Genapol O050 (35.3% at 95% RH) to Genapol O200 (70.7%) (Figure 38, C).

Similar relationships could not be observed within the group of Tweens. Water sorption isotherms for Tween 20, Tween 40, Tween 60 and Tween 80 cluster together while Tween 65, Tween 81 and Tween 85 showed a significantly lower water sorption (Figure 38, B).

3.4 Discussion

Comprehensive experimental data about the water sorption ability of commonly used non-ionic polydisperse surfactants with differing EO content at different humidities had been investigated to test whether they might act as humectants.

None of the measured surfactant samples showed any hysteresis (Figure 38). This fact indicates that structural and conformational rearrangements, which would alter the accessibility of energetically favourable sites, do not occur in surfactants during water sorption (Caurie, 2007).

The typical exponential shape of resulting isotherms is known to account for a solvent or a plasticiser above the glass transition temperature (Andrade *et al.,* 2011). Brunauer (1940) characterised five different isotherm types in physical adsorption, according to their shape. In our experiments, water sorption isotherms of surfactants (Figure 38) can be clearly assigned to Brunauer's type 3, also known as *'Flory-Huggins isotherm'* (Brunauer *et al.,* 1940).

Non-ionic polyethoxylated surfactants are postulated to have the ability to sorb and retain water (Baur *et al.,* 1997b; Stevens & Bukovac, 1987a) helping to keep the active ingredient in the spray deposit in a physical state which favours its uptake into the leaf (Hazen, 2000; Stock & Briggs, 2000). Therefore, the present work studied the humectant potential of selected non-ionic surfactants in a systematic approach.

Comprehensive experimental data about the water sorption ability of commonly used non-ionic polydisperse surfactants at the full range of relative humidities up to 95% are presented. Most studied surfactants absorb water from the atmosphere, although to different extents. The sorbitan esters (Span series) lacking any EO, have a significantly lower water sorption ability than the corresponding ethoxylated polysorbates (Tween series) and the oleyl alcohol polyoxyethylene ethers (Genapol O series; Figure 38). This indicates that the EO content plays a significant role for the water sorption ability of surfactants. In several experiments, cuticular uptake and efficiency of water soluble active ingredients were enhanced by high EO content surfactants (Gaskin & Holloway, 1992; Coret & Chamel, 1994; Stevens & Bukovac, 1987b). Therefore, it was hypothesised that humectancy is related to a high EO content. Indeed, within the class of ethoxylated octylphenol surfactants (Triton X series), with EO contents ranging from 5 to 40, the moisture content

(mass %) increases with the EO content, at least at high humidities (Stevens & Bukovac, 1987a). This effect was also observed for the Genapol O series where the water sorption also increases with the EO content (Figure 39).

Statistical parameters, describing the linear regression in Figure 39, are shown in Appendix 1. The moisture content (mass %) of several polysorbates with identical EO content strongly differs, and the moisture content (mass %) of Atlas G1096 is always significantly lower than expected from its EO content.

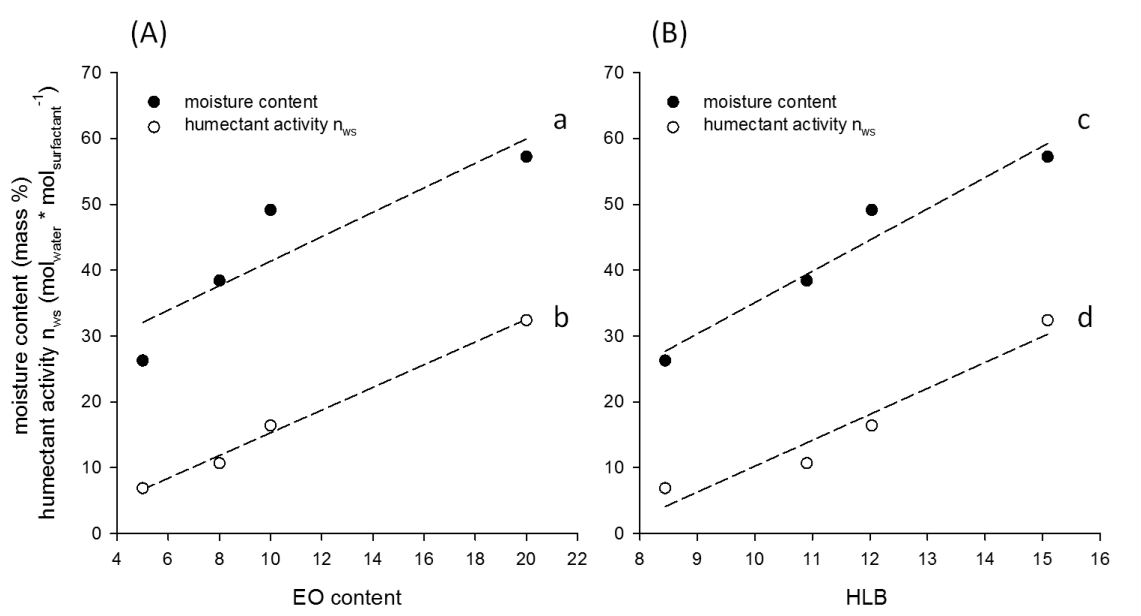

Figure 39: Correlation between the moisture content (mass %) or the humectant activity (n_{ws}) (mol_{water} $mol_{surfactant}^{-1}$) and the EO content (A) or HLB (B) of different oleyl alcohol polyglycol ethers (Genapol O series) at 90% RH. For parameter of the regression lines refer to Appendix 1.

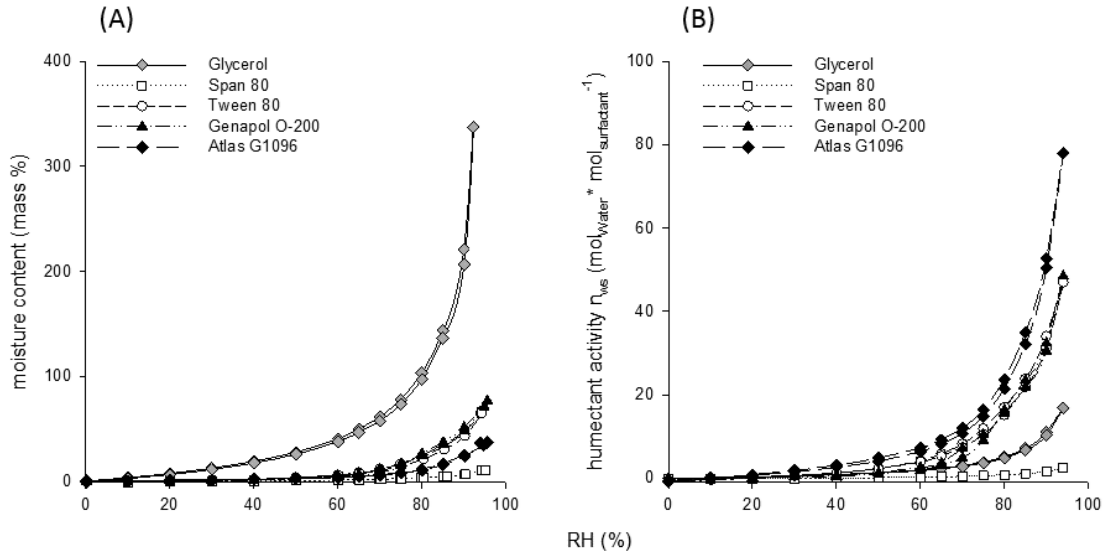

Figure 40: Comparison of water sorption isotherms for selected surfactants from different classes based on moisture content (mass %) (A) or humectant activity n_{ws} (mol_{water} $mol_{surfactant}^{-1}$) (B).

The sorption isotherms of surfactants from different classes, all bearing one or more octadecyl chains, but differing in their EO content, were also compared (Figure 40, A). The water sorption (mass %) of Atlas G1096, which has the highest EO content (50 EO units), was lower than of Tween 80 and Genapol O200, which only have 20 EO units (Figure 40, A). Glycerol displayed by far the highest increase in mass (about 350% at 95% RH). This leads to the assumption that the water sorption capacity cannot be predicted solely by the degree of ethoxylation, but instead the entire molecule has to be taken into account. Therefore, the calculation of the so-called *'humectant activity'* (n_{ws}) from the number of mols of water sorbed per mol of surfactant (mol fraction) (Cohen *et al.,* 1993; Sagiv & Marcus, 2003) was carried out to correct the significant variation in molecular size among the studied surfactants. The ranking of the mol fraction based sorption isotherms (Figure 40, B) differed from the respective mass based isotherms (Figure 40, A). Atlas G1096 has a low mass-based moisture content (mass %) (Figure 40, A) but shows the highest humectant activity (n_{ws}) with 78 mol of water per mol surfactant being sorbed at 95% RH (Table 5). This is about 1.6fold higher than for Tween 80 and Genapol O200 and even 4.6times more than for glycerol. Atlas G1096 indeed takes up the most water (Figure 40, B), as it would have been expected from the 50 EO units.

Table 5: Humectant activity (n_{ws}) and humectant activity per oxygen content (n_{ws}/n_o) at five different humidity levels.

Tradename	Mean O content	30% RH		50% RH		80% RH		90% RH		95% RH	
		n_{ws}	n_{ws}/n_O	n_{ws}	n_{ws}/n_O	n_{ws}	n_{ws}/n_O	n_{ws}	n_{ws}/n_O	n_{ws}	n_{ws}/n_O
Glycerol	3	0.52	0.17	1.30	0.43	5.08	1.69	11.00	3.67	16.84	5.61
Span 20	6	0.05	0.01	0.10	0.08	2.23	0.37	4.65	0.78	7.43	1.24
Span 40	6	0	n.d.	0.17	0.02	1.64	0.27	3.56	0.59	5.44	0.91
Span 60	6	0	n.d.	0.06	0.03	1.54	0.26	3.06	0.51	4.51	0.75
Span 65	8	0	n.d.	0.09	0.01	0.33	0.04	0.61	0.08	0.84	0.10
Span 80	6	0	n.d.	0.15	0.02	0.76	0.13	1.56	0.26	2.42	0.40
Span 85	8	0.05	0.01	0.10	0.02	0.36	0.04	0.48	0.06	0.64	0.08
Tween 20	26	0.69	0.03	2.77	0.11	18.72	0.72	37.34	1.44	52.40	2.02
Tween 40	26	1.24	0.05	3.25	0.13	17.50	0.67	33.24	1.28	44.52	1.71
Tween 60	26	1.22	0.05	3.24	0.12	17.13	0.66	32.92	1.27	43.76	1.68
Tween 65	28	0.18	0.01	1.54	0.06	10.24	0.37	20.02	0.72	26.11	0.93
Tween 80	26	0.46	0.02	2.25	0.09	16.98	0.65	34.03	1.31	47.03	1.81
Tween 81	11	0	n.d.	0.57	0.05	3.85	0.35	7.83	0.71	11.44	1.04
Tween 85	28	0.50	0.02	1.70	0.06	8.91	0.32	19.63	0.70	31.36	1.12
Genapol O050	6	0.26	0.04	0.63	0.11	3.07	0.51	6.89	1.15	9.28	1.55
Genapol O080	9	0.40	0.04	1.00	0.11	5.71	0.63	10.67	1.19	13.61	1.51
Genapol O100	11	0.38	0.03	1.18	0.11	8.36	0.76	16.41	1.49	22.89	2.08
Genapol O200	21	0.21	0.01	1.06	0.05	16.37	0.78	32.39	1.54	48.47	2.31
Atlas G1096	56	1.81	0.03	4.80	0.09	23.65	0.42	52.68	0.94	78.00	1.39

n_{ws}, humectant activity, number of mols of water sorbed per mol surfactant
n_{ws}/n_O, humectant activity per oxygen content of surfactant

In surfactants in equilibrium with dry air, the hydrophobic and hydrophilic moieties align (Hoffmann *et al.,* 2005). In straight-chain and non-branched surfactants this results in a lamellar phase where the hydroxyl functional groups or the ethoxy oxygens of adjacent molecules are in close proximity (Hoffmann *et al.,* 2005). Single water molecules absorbed in this lamellar phase can cross-link two adjacent oxygen atoms. However, the probability for a water molecule to settle far away from the alkyl chain is higher than to interact with oxygens close to the lipophilic domain (Hoffmann *et al.,* 2005). One water molecule per two surfactant molecules attached to the facing ends of the polar chains is required to totally cross-link the network. When the surfactant sorbs more water, the water molecules either attach to different locations along ethoxy chains or associate with other water molecules already hydrogen-bound to polar groups. The latter leads to the growth of a 'free' water domain (Hoffmann *et al.,* 2005).

This process is expressed by the exponential shape of the isotherms. The flat slope at the beginning accounts to the phase where single water molecules cross-link single surfactant molecules. At higher humidity levels and thus higher water contents of the surfactant, the steep increase is induced by the growth of the 'free' water domain and the hydration of the inner oxygen atoms which are closer to the lipophilic end. All surfactants used in this study represent complex three-dimensional polar heads, but it is likely that molecules will arrange in the same way as the straight surfactants, with an alignment of the hydrophilic and the lipophilic domains, respectively.

The architecture of the lipophilic portion of the surfactant molecules will strongly contribute to the availability of polar sites for hydration. Within the Span series, the oxygen content remains constant (with the exception of Span 65 and Span 85) while the lipophilic domain changes. With increasing chain length of the fatty acid, the humectant activity (n_{ws}) of the Span surfactants and also the humectant activity per oxygen content (n_{ws}/n_o) decreases (Table 5). For example, at 95% RH each oxygen atom in Span 20 (containing a dodecylic acid) is on average associated with 1.24 water molecules which is 1.65 times more than in Span 60 (0.75) with an octadecenoic acid (Table 5). Though, the increasing lipophilicity of the alkyl chain impairs the accessibility of the adjacent oxygen atoms. The introduction of a double bond leads to a cis conformation of the $C_{18:1}$ fatty acid in Span 80. This results in a

further decreased humectant activity of the oxygen atoms (0.4) compared to Span 60 (0.75) with a straight conformation of the $C_{18:0}$ fatty acid. Span 65 and Span 85 only sorb very small amounts of water (Table 5) presumably because their oxygen atoms are shielded by the three fatty acids.

In the group of Genapol O, where the lipophilic portion remains constant ($C_{18:1}$), the humectant activity (n_{ws}) clearly increases with the EO content (Figure 39) and also with increasing oxygen content (Table 5). Most members of the Tween series possess a huge polyethoxylated polar head group with 20 EO groups on average resulting in a high humectant activity. Even at 30% RH, the values for Tween 20, 40 and 60 are higher than for glycerol (Table 5). Modification of the single fatty acid domain (e.g. elongation or unsaturation) does not remarkably influence the humectant activity. However, introducing additional fatty acids, probably decreases the humectant activity due to a shielding effect (Figure 38, B).

The hydrophilic-lipophilic balance (HLB) is a basic proxy for the relative importance of hydrophilic and lipophilic domains in surfactant molecules (Griffin, 1954). For an aliphatic alcohol series with a constant hydrophobic tail and differing EO content (Stock & Holloway, 1993) and also for the Genapol O series (Figure 39), the HLB correlates with the degree of ethoxylation. However, when different surfactant classes are considered, the HLB value does not correlate with the level of ethoxylation, because both, the lipophilic and the hydrophilic domains, change in different ways. Two surfactants with the same level of ethoxylation can possess a different HLB as two surfactants with a widely varying molecular structure could possess the same HLB.

From these findings, Stock and Briggs (2000) concluded that humectancy is related to the EO content rather than to the HLB. In contrast to this, in the present study, the moisture absorption (mass %) across a broad range of surfactants correlates well with their HLB values (Figure 41, C) and not with the EO content (Figure 41, A). (Statistical parameters describing the linear regressions in Figure 41 are presented in Appendix 2 and Appendix 3).

This means that the HLB can be used to rank the water sorption ability (mass %) of surfactants amongst different classes. Nevertheless, it is important to keep in mind, that the HLB value does not consider sterical effects within the surfactant molecules. For example, Atlas G1096 strongly differs from the other surfactants in

size and architecture, because the lipophilic domain consists of six fatty acids. Therefore, Atlas G1096 does not fit in the correlation when humectant activity is plotted versus HLB over all surfactant classes (Figure 41, D).

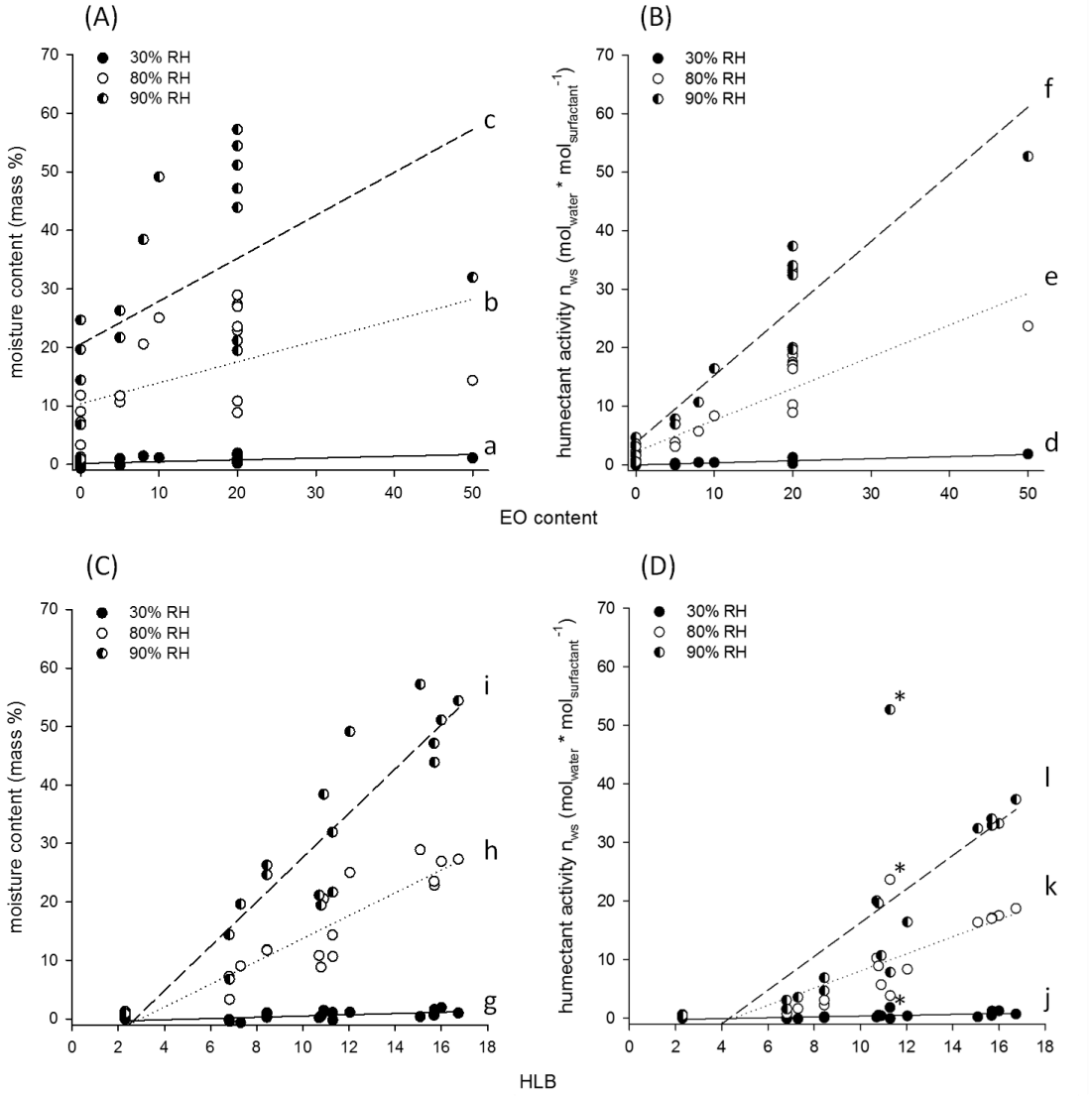

Figure 41: Correlation between the moisture content (mass %) (A) or the humectant activity n_{ws} (mol_{water} $mol_{surfactant}^{-1}$) (B) and the mean EO content for all surfactants at different RH. Parameter of the regression lines are given in Appendix 2.Correlation between the moisture content (mass %) (C) or the humectant activity n_{ws} (mol_{water} $mol_{surfactant}^{-1}$) (D) and the hydrophilic-lipophilic balance (HLB) for all surfactants at different RH. Parameter of the regression lines are given in Appendix 3. Symbols indicated with * represent polyoxyethylene sorbitol hexaoleate (Atlas G1096) as an outlier.

Obviously, the water sorption of surfactants used in this work is relatively low, and one would not expect the humectant potential. Glycerol is known to be a very efficient humectant, but even at very low relative humidities (30%) some members of the Tween series, Atlas G1096 and, with increasing relative humidity, also members of the Genapol O series, show a higher humectant activity (n_{ws}) than glycerol.

As discussed above, the exponential shape of the moisture sorption isotherms of the surfactants studied here, indicates that water sorption results in the formation of 'free' water domains. This is relevant to the properties of a spray droplet residue on a leaf surface and its consequences for the availability of the active ingredient for the uptake into the leaf. The formation of aqueous phases within the deposit might prevent the active ingredient from crystal precipitation. Thus, several surfactants used in this study are supposed to enhance the uptake of water soluble active ingredients by their humectant activity.

Nevertheless, further work is required, investigating the water sorption of an actual spray deposit as it would occur on the field and comparing it to the cuticular uptake. Beside physico-chemical factors like surface tension or lipophilicity, the humectant activity of the spray droplet has a strong influence on the uptake of active ingredients. The method for measuring water sorption isotherms introduced in this paper could be applied to complex mixtures of agrochemical formulation products in order to evaluate the process of water evaporation and rehydration of the foliar deposit. A comprehensive understanding of the underlying mechanism will help to improve spray formulations to optimise the uptake and the efficiency of plant protection agents.

4 CHAPTER III: EFFECTS OF ADJUVANTS ON PINOXADEN PENETRATION THROUGH CUTICULAR MEMBRANES AND INTO INTACT PLANTS

4.1 Introduction

Quantitative descriptions of cuticular transport

Since the plant cuticle is the initial contact zone between a foliar applied agrochemical and the plant, it is the main barrier that has to be penetrated (Riederer, 1991). Therefore, penetration of an active compound through the plant cuticle is the rate-limiting step. Most agrochemicals have a more or less lipophilic nature (Schreiber, 2005). Considering the penetration of these lipophilic compounds across plant cuticles, it requires three steps: the sorption into the cuticular lipids, the diffusion across the cuticular membrane and finally the desorption into the apoplast of epidermal cells (Buchholz, 2006).

The diffusion of water and organic solutes over small molecular distances is a physical process. Diffusion is the net movement of molecules from an environment of high concentration to a lower concentration environment until both concentrations reach an equilibrium state (Cussler, 2009). The simplest case would be the diffusion across a stagnant liquid film where the film and the adjacent solutions are chemically and structurally identical (Schönherr & Baur, 1994). In the case of the diffusion across a cuticular membrane the aqueous compartment with a high solute concentration, like a spray droplet, is called *'donor'* and the compartment of lower concentration, like the apoplast, is called *'receiver'*. The amount (M) of a substance that diffuses per time (t) is defined as flow of molecules (F) (eq. 5). It depends on the properties of the barrier and on the driving force acting across it. Frequently used units are mol per second or mass per second.

$$F = \frac{M}{t}$$

(eq. 5)

The so-called *'flux'* (J) occurs over a defined area (A) across which penetration takes place and can be determined if the particular area is known (eq. 6). Since in some cases the exact determination of the penetration area is not possible, the flux (J) cannot be obtained. The flux is the normalised flow, also called flow density and

is independent from the barrier area. Typically the flux (J) is expressed in the unit mol m^{-2} s^{-1} (Schreiber & Schönherr, 2009, chapter 2).

$$J = \frac{M}{A \cdot t} = \frac{F}{A}$$

(eq. 6)

For the diffusion of molecules, there must be a driving force (Fick's first law). This force is the difference in concentrations (Δc) (eq. 7). The concentration gradient is determined by the concentration difference of the aqueous donor and receiver phases.

$$\Delta c = c_{Donor} - c_{Receiver}$$

(eq. 7)

The flux is proportional to the difference in solute concentration between both media. If the concentration difference is constant, a linear relationship is considered. The slope of this correlation is often called *'permeance'* or *'permeability coefficient'* (P). The permeance has the unit of a velocity m s^{-1} (eq. 8).

$$J = P \cdot \Delta C \quad \rightarrow \quad P = \frac{F}{A \cdot \Delta C}$$

(eq. 8)

The solubilities of a solute in the membrane and in adjacent solutions usually differ and this necessitates the introduction of an additional parameter. This parameter is the *'cuticle-water partition coefficient'* (K_{CW}) which is the ratio of the equilibrium concentrations of a solute in the cuticle (C_C) and in water (C_W) (eq. 9).

$$K_{CW} = \frac{C_C}{C_W}$$

(eq. 9)

Simulation of foliar penetration

In this study, the cuticular penetration of a model compound was measured by using an experimental set-up called ‘simulation of foliar uptake/penetration’ (SOFU/SOFP) (Schönherr & Baur, 1994). Since the cuticle represents a purely physical system, it does not actively interact with water and solutes. For this, the term ‘uptake’ is not appropriate, as it implements an active mass transfer in plants, comparable to transmembrane proteins (Schreiber & Schönherr, 2009, chapter 2). Accordingly, the term *‘simulation of foliar penetration’* (SOFP) will be further used. Isolated cuticular membranes (CM) obtained from the adaxial sides of hypostomatous leaves or fruits were used (Riederer & Schreiber, 2001) to monitor the solute penetration. In SOFP experiments, droplets containing an active ingredient–surfactant-solution are applied on the outer (waxy) surface of the cuticular membrane. These droplets or the hydrated surfactant deposit after the water evaporation serves as a donor for the penetration across the CM. Active ingredients and surfactant molecules diffuse through the CM into a receiver solution, facing the inner (non-waxy) surface of the CM (for detailed experimental descriptions, please refer to ‘materials and methods’).

In SOFP experiments volatile solvents (also water) evaporate from the donor droplet and both solutes and surfactants penetrate into the CM during this evaporation to an unknown extent, leaving a surface deposit (Baur *et al.*, 1997a). Accordingly, there are at least two steps in series during the penetration process. First, from the surface deposit into the lipophilic wax layer and second, from the CM into the apoplast (or receiver medium). The first step cannot be first-order since the solvent volume, and hence the concentration of the penetrants, changes with time (Baur *et al.*, 1997a).

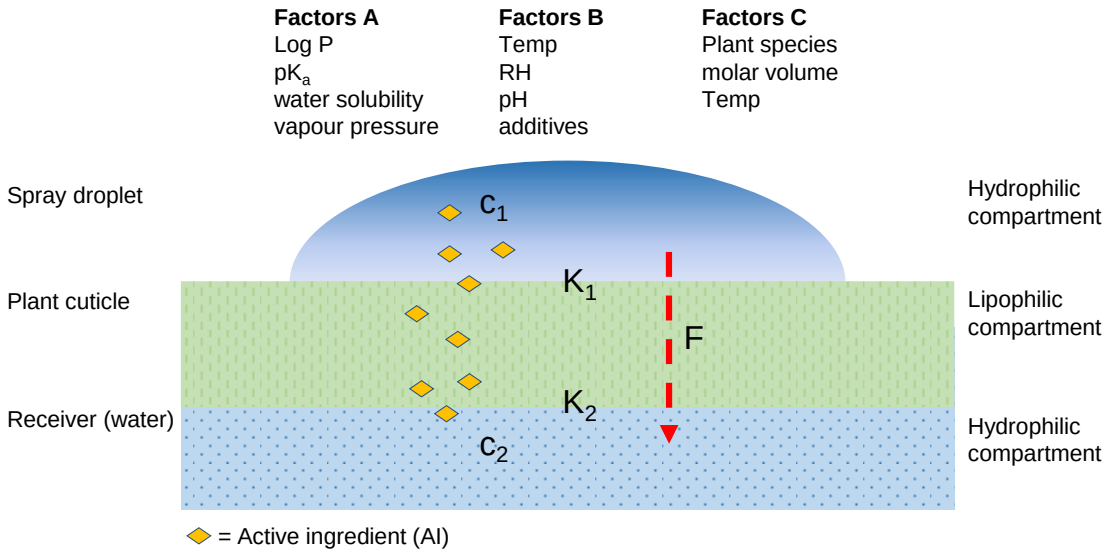

Figure 42: Generalised schematic illustration of a spray droplet on the cuticular membrane (CM) and the adjacent receiver medium (water) as it would be the set-up in SOFP experiments. Three factors affecting cuticular penetration via the lipophilic pathway can be distinguished: Factor group A: physico-chemical properties of the AI; Factor group B: environmental conditions and those coming from the spray solutions; Factor group C: parameters affecting the solute mobility in the plant cuticular membrane (CM).
c_1 = concentration of AI in the formulation deposit; c_2 = concentration of AI in water (either receiver medium or apoplast); K_1 = partition coefficient wax/formulation deposit; K_2 = partition coefficient cutin matrix/water; F = flow rate of the AI; (The figure is not to scale) (illustration modified from Buchholz, 2006).

Particularly, the sorption process is affected by several factors which change continuously during droplet drying and rewetting. All these factors can rarely be analysed individually. Figure 42 tries to illustrate the most relevant factors considering SOFP experiments with a lipophilic model compound (Buchholz, 2006).

Physico-chemical properties of the AI (Factors A) affect the driving force, e.g. a low water solubility of the (lipophilic) AI causes a low concentration of dissolved molecules in the water (C_1) and will result in minor sorption in cuticular wax (K_1), although partitioning could be high.

After partitioning into the cuticle, the driving force, considering the partition coefficient between the cutin matrix and water in the apoplast (receiver water) (K2) becomes important. The potential access to the plant's symplast after crossing the bio-membrane determines the translocation into plant tissues (not further investigated). A rapid distribution (K_2) will result in a low concentration underneath the spray droplet and will again enlarge driving forces. To summarise, it is the

challenge to maximise the penetration rates in order to increase c_1 and therefore also K_1.

As an example for this, the water solubility of the lipophilic AI is increased by including adjuvants and other spray additives (e.g. emulsifiers, dyes, buffers, etc.) to the spray solution (Hess, 1999; Penner, 2000; Tu & Randall, 2003) (Factors B). It is commonly known that adjuvants affect solubility properties and partitioning of the AI (Foy, 1993; Kirkwood, 1993; Baur *et al.,* 1997a) (those individual mechanisms coming from the adjuvant are not further respected in Figure 42).

Especially environmental factors on the field like relative humidity and temperature, can rapidly change during the application process, determine the dynamic processes. Because of this, SOFP experiments were performed under constant relative humidity levels (low, medium, high) in this study. The knowledge of both, the humectant character of surfactants (chapter II) and the effect on cuticular penetration, might help to understand the influence of relative humidity or water available in the formulation deposit.

The individual parameters affecting the solute mobility in the cuticle (Factors C) are, of course, the plant species itself, the solute size (molar volume) and temperature effects. Solute mobilities in cuticles vary considerably between plant species (Schönherr *et al.,* 1999). Moreover, no clear relationship has been found between the cuticular wax composition and the respective cuticular permeability of water (Haas & Schönherr, 1979; Riederer & Schneider, 1990). Epicuticular waxes have considerable influence on the wetting of leave surfaces (chapter II), but they may rarely affect the penetration of organic solutes into the leaf (Baur, 1998) and the water transpiration (Zeisler & Schreiber, 2016).

Prunus laurocerasus (cherry laurel) as a model cuticle

It was shown that enzymatic isolation does not affect the transport properties of CMs (Kirsch *et al.,* 1997), but it is feasible only with a limited number of species. One important prerequisite for enzymatically isolation is the presence of a continuous pectinaceous layer (Buchholz, 2006), which makes the CM mechanical stable (e.g. for some perennial plants like *Rosaceae (Malus domestica, Pyrus communis)*, or evergreen species). Investigators preferentially use leaf CM from *Citrus aurantium*, *Hedera helix* or *Prunus laurocerasus* for transport experiments.

Those CMs have an average mass of 250- 400 µg cm^{-2}. The thickness of CMs significantly varies between 30 nm (*Arabidopsis thaliana*) and 30 µm (*Malus domestica*) (Schreiber & Schönherr, 2009, chapter 1).

As transport experiments through CMs require the absence of stomatal pores, the selection is restricted to the adaxial sides of hypostomatous leaves (or fruits). Since *Poaceae* belong to the plant family which are of high economical interest for the agrochemical market, the usage of crops (e.g. wheat, corn) or grass-weed CMs would be preferred. Unfortunately, the isolation und usage of *Poaceae* model CMs (after Orgell, 1955) is not feasible, also because they have stomatal pores on both leaf sides.

Many work has been done investigating the water and solute transport with the help of the model plant *Prunus laurocerasus* (Gutenberger *et al.,* 2013; Kirsch *et al.,* 1997; Schreiber, 2002; Schreiber *et al.,* 1995; Stammitti *et al.,* 1995; Schreiber, 2001). Its chemical wax composition was also extensively studied (Jetter *et al.,* 2000; Zeisler & Schreiber, 2016). Moreover, Jetter & Schäffer (2001) analysed in detail the ontogenetic characteristics of the epicuticular wax film on adaxial surfaces of *Prunus laurocerasus* leaves.

Pinoxaden as a model compound

The active ingredient (AI) Pinoxaden (PXD) is a cereal selective post-emergent graminicide belonging to Group A, according to the HRAC classification of mode of action lipid synthesis inhibition (inhibition of ACCase) (Muehlebach *et al.,* 2009; Muehlebach *et al.,* 2011). In the year 2006, Syngenta Crop Protection has released the product *'Axial'* which is mainly used for agrochemical applications in wheat and barley (Ruchs *et al.,* 2006). PXD is applied flexible, from the two-leaf stage up to the flag leaf stage of grasses, and has a broad spectrum that covers a wide range of key annual grass weeds like *Alopecurus myosuroides* (blackgrass), *Apera spica venti* (silky bent grass), *Avena* spp. (wild oats), *Lolium* spp. (ryegrass) *Phalaris* spp. (canary grass), *Setaria* spp. (foxtails) and other monocotyledonous weeds commonly found in cereals (Hofer *et al.,* 2006). The product formulation is an emulsifiable concentrate (EC) containing 100 g l^{-1} PXD and 25 g l^{-1} of the crop safener cloquintocet-mexyl which induces the synthesis of herbicide degrading enzymes in the crops (Hofer *et al.,* 2006).

PXD is applied post-emergence at rates of 30-60 g AI ha^{-1}. Methyl oleate, as adjuvant, was first introduced to enhance the levels of activity without impairing crop safety (Wenger *et al.,* 2012). Later, TEHP EW400 was introduced to have better penetration increasing effects by being also crop compatible.

The pivalate group of PXD (Figure 43, left) is hydrolysed within a very short time to 'PXD acid' (Figure 43, right) which is rapidly further hydrolysed to the major metabolite analysed in sprayed plants (not illustrated). So PXD is a 'pro-cide' which becomes active *in planta* only under hydrolysed conditions. All PXD metabolites except the herbicide (Figure 43, right) were inactive when tested on plastidic wheat ACC *in vitro* and showed no phytotoxic effect on emerged grasses and cereals in greenhouse trials, even when applied at higher rates (Wenger *et al.,* 2012).

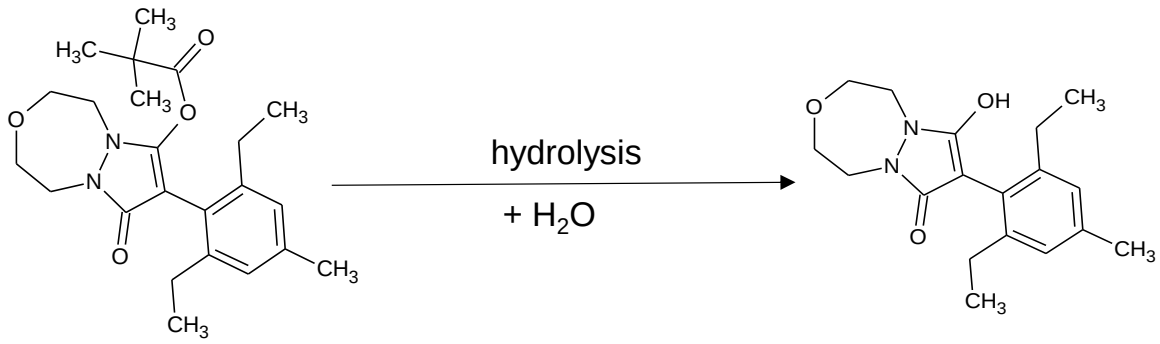

Figure 43: Chemical structure of Pinoxaden (PXD). PXD is a 'pro-cide' (left). The pivalate group is rapidly hydrolysed *in planta.* Only the herbicide 'PXD acid' (right) is active *in planta*.

The demands of a model AI for a comprehensive study, determining cuticular penetration as well as the AI uptake effects into living plants, had to be concerned. The physico-chemical characteristics of a low water solubility and a high octanol-water partition coefficient were decisive for working with PXD as a model compound. With these characteristics the results in this study may be comparable to other important lipophilic compounds with similar characteristics (not only herbicides, but also insecticides, for example). Furthermore, PXD is known to significantly respond to adjuvants (personal communication Christian Popp), which was a prerequisite for the AI selection for this work.

Many studies, as well as recently published, are dealing with cuticular penetration experiments by still using the same prominent but early developed ^{14}C-labelled compounds such as benzoic acid, salicylic acid, metribuzin, atrazine and most frequently, 2,4-D and its derivatives (Forster & Kimberley, 2015; Kirsch *et al.,* 1997; Burghardt *et al.,* 1998; Schönherr, 1993; Baur *et al.,* 1997a; Riederer *et al.,* 1995; Schönherr *et al.,* 2001). In contrast, PXD is a relative novel compound of the newly discovered 'DEN' derivatives (HRAC classification) and is therefore also of relevance for the agrochemical market. Moreover, the low toxicity ensures safe handling during the work in the laboratory.

Objectives and research questions

After the successful retention and spreading on the leaf surface, the cuticular membrane (CM) is the first barrier for agrochemicals to be passed during foliar application. Therefore, cuticular penetration experiments were conducted to study *in vitro* penetration of a lipophilic plant protection agent (PXD) through an astomatous model cuticle. In order to understand the influence of different adjuvant MoA, experiments were also performed under three different humidity levels.

Another central objective in this study was to evaluate, if results obtained in *in vitro* cuticular penetration experiments, can be transferred to spray application studies on living plants. Greenhouse trials, focussing on the adjuvant impact on *in vivo* action of PXD, were evaluated and tested on five different grass-weed species. Since agrochemical spray application and its following action on living plants includes also translocation processes and species dependent physiological effects, this investigation might help to simulate the situation on the field as realistic as possible. These two fundamental different studies, the cuticular penetration and the greenhouse trials were both performed in order to compare adjuvant effects on both, *in vitro* and also *in vivo,* systems.

4.2 Materials and methods

4.2.1 Chemicals

Axial 100 EC (Pinoxaden)

The ACCase inhibiting herbicide of the chemical subgroup of phenylpyrazolines Pinoxaden (PXD) (IUPAC name: 2,2-dimethyl-propionic acid 8-(2,6-diethyl-4-methyl-phenyl)-9-oxo-1,2,4,5-tetrahydro-9H-pyrazolo[1,2-d][1,4,5] oxadiazepin-7-yl ester) was used as a lipophilic model compound. The octanol/water partition coefficient was log $K_{O/W}$ 3.2. The molecular mass was 400.5 g mol^{-1}.

Because of the low water solubility of about 0.2 g l^{-1}, experiments were performed using the formulated product Axial 100 EC, containing 100 g l^{-1} PXD. The formulation contained no additionally adjuvants. Axial 100 EC was acquired from Syngenta Crop Protection AG, Stein, Switzerland.

Adjuvants

Anhydrous glycerol, a choice of non-ionic sorbitan fatty acid esters (Spans), and their polyethoxylates (Tweens), oleyl alcohol ethoxylates (Genapol O), polyoxyethylene sorbitol hexaoleate (Atlas G1096) and Tris(2- ethylhexyl)phosphate (TEHP EW400) were used for the following experiments. For substance information on physical and chemical properties refer to Table 1.

Chemicals for analytical procedures

Acetonitrile (ULC/MS quality), methanol (ULC/MS quality) and formic acid were purchased from Biosolve (BV, Valkenswaard, Netherlands).

4.2.2 Cuticular membranes

Cuticular membranes (CM) were obtained from the upper, astomatous leaf surfaces of fully expanded *Prunus laurocerasus* cv. Herbergii plants growing in the Botanical Garden of the University of Würzburg. Enzymatic isolation was carried out as described previously (Schönherr & Riederer, 1986).

4.2.3 Cuticular penetration experiments

The cuticular penetration of Pinoxaden (PXD) was measured using an experimental set-up called '*simulation of foliar uptake/penetration'* (SOFU/SOFP) (Schönherr & Baur, 1994). Cuticular membranes (CM) were mounted on chambers made of stainless steel with the physiological outer side facing the atmosphere (Figure 44). A 5 µl droplet of a mixture of the emulsified PXD product Axial 100 EC (without additional adjuvants) and one selected surfactant in water (2 µg μl^{-1} PXD, 4 µg μl^{-1} surfactant) was pipetted onto the outer, waxy surface. All selected adjuvants were purely added to the non-adjuvanted Axial 100 EC formulation and used in the ratio 1:2 (PXD : adjuvant).

The pure Axial 100 EC product dissolved in water (2 µg μl^{-1} PXD) without surfactant was used as control experiment. The water was evaporated from the 5 µl droplets after around 45 min leaving an amorphous surfactant deposit. After the droplet drying, chambers were inverted and 1 ml of deionised water was added as receiver solution. Chambers were placed in closed plastic cups where RH was controlled at 25 °C using different glycerol-water mixtures to achieve 30%, 50% or 80% RH (Forney & Brandl, 1992). The humidity was controlled by using a hygrometer. The penetration of PXD was investigated from a re-hydrated formulation residue. At approx. 24 h time intervals, 10 µl aliquots were sampled from the receiver solution and PXD concentrations were quantified by UPLC-MS. Plotting the amount of penetrated PXD as a function of time, the resulting slope of the linear section represents the flow rate (F) in µg s^{-1}.

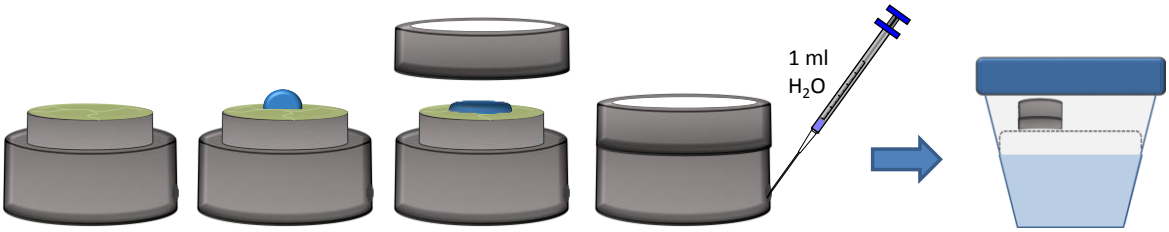

Figure 44: Simulation of foliar penetration (SOFP) experiment at adjusted humidity.

4.2.4 Analytical analysis of Pinoxaden

Quantification of PXD was carried out with UPLC-MS (ACQUITY UPLC H-Class, with ACQUITY QDa Detector, Waters, Eschborn, Germany). A sample volume of 2 µl was injected on an Acquity UPLC HSS C18 column (2.1 x 50 mm, 1.8 µm particle size, Waters GmbH, Eschborn, Germany) and gradient elution was performed within 2.5 min at a flow rate of 0.5 ml min^{-1} starting with 0.2% (v/v) formic acid in water and acetonitrile (50% v/v). The acetonitrile concentration was increased to 95% within 1.7 min and decreased again to 50% within 0.3 min, then held for 0.5 min. The ESI source of the detector was operated in positive ionization mode, cone voltage was set at 15 V and single ion record frequency was 10 Hz to detect the primary ion of PXD (401.3 m/z). For quantification, peak areas were automatically compared to a linear calibration curve of PXD using the program TargetLynx (Waters, Eschborn, Germany). For quantification a linear calibration curve was used. A correlation coefficient greater than 0.99 was achieved for a concentration range from 0.001 to 1.0 µg ml^{-1}.

4.2.5 Adjuvant impact on *in vivo* action of Pinoxaden

Plant material

Foliar uptake experiments were carried out at Syngenta Jealott's Hill International Research Centre Bracknell (UK), with technical assistance of the screening department for cereals. Plant material from one crop species *Triticum aestivum* (winter wheat cv. Horatio) and five grass-weed species (family *Poaceae*) *Avena fatua* (wild oat), *Lolium multiflorum* (italian rye-grass), *Setaria viridis* (green foxtail), *Phalaris paradoxa* (awned canary-grass) and *Alopecurus myosuroides* (black grass) were used (Figure 45). Plants were sown together in bio troughs on normal soil. At the application experiment, the plants were in growth state BBCH 12 (2- leaf-stadium). After application the growing conditions consisted of a 16-h light period and 20/17 °C day/night temperature at around 65% RH.

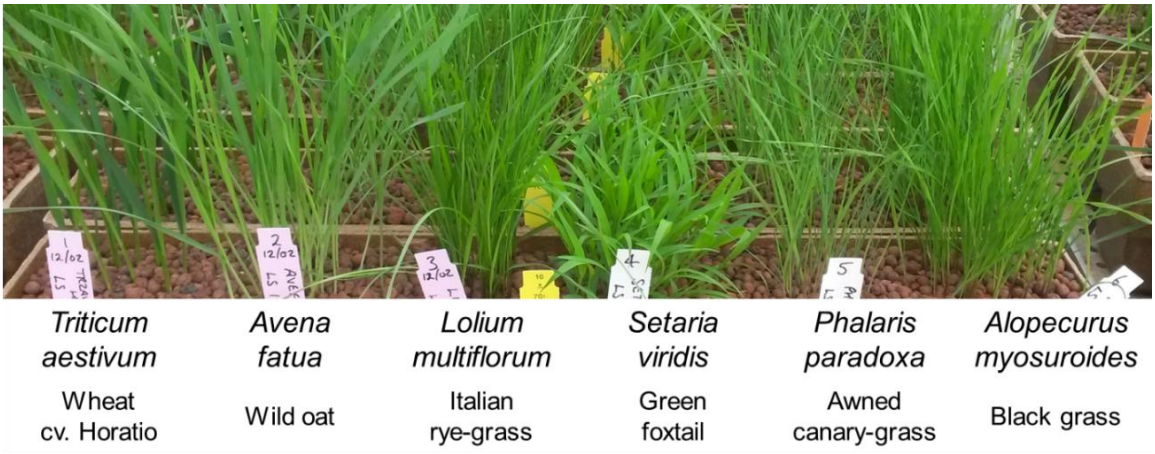

Figure 45: Plant material (*Poaceae*) used for greenhouse spray tests. The crop *Triticum aestivum* (left) was used as a negative control, because of crop selectivity achieved with safener technology. Plants were grown together in plant troughs on normal soil for each spray treatment. Plants were in growth stage BBCH 12 when sprayed.

Experimental set-up

The cereal selective post-emergent herbicide PXD was used as the non-adjuvanted Axial 100 EC formulation to test the *in vivo* effect of different adjuvant treatments. Non-adjuvanted Axial 100 EC contained, beside the ACCase inhibiting herbicide PXD, different emulsifiers, solvents, surfactants (different from those used in this study) and the safening substance cloquintocet-mexyl, which was added in order to achieve an herbicide selectivity of the monocotyledonous crops (e.g. wheat and barley). The greenhouse experiment was conducted with six different adjuvant treatments using one negative control where the non-adjuvanted Axial 100 EC (0.1% dissolved in water) was used, one positive control with 0.5% TEHP EW400 and also with selected adjuvants like 0.1% Tween 20, 0.1% Tween 80, 0.1% Span 20 and 0.1% Span 80. To distinguish between the adjuvant effects, five different PXD concentration rates at 1.875, 3.75, 7.5, 15 and 30 g AI ha^{-1} were conducted. All treatment combinations were sprayed on a selection of six different monocot species. Three replicates were made. The experiment was fully randomised.

Application

Spray application to the plants was carried out from a spray nozzle attached to a variable speed track (Syngenta Jealott's Hill International Research Centre Bracknell, UK).The track sprayer was equipped with a Teejet XR11002VP flat fan

nozzle. The pressure was set at 2 bar and the speed was 90 cm s^{-1}. The calibration of the track sprayer resulted in an output quantity of around 200 l ha^{-1}. This value will naturally vary with small fluctuations in pressure, spray volume, viscosity and plant position across the swath. All three repetitions were sprayed simultaneously.

Assessment

The plant assessment was conducted 14 days after application (DAA). The herbicide damage in percent was estimated visually. Expected symptoms of plants treated with an ACCase inhibiting herbicide are yellowish chloroses at the new growing meristems. For estimating the herbicide damage in percent, the treated plants were compared to non-treated (= non-sprayed) plants. Effects of loss of biomass, e.g. a prevented tillering of treated plants, were also taken into account in order to estimate the herbicide damage. The plant assessment was carried out by an experienced senior assistant of the screening department for cereals at Syngenta Jealott's Hill International Research Centre Bracknell (UK).

4.3 Results

4.3.1 Cuticular penetration experiments

The cuticular penetration of Pinoxaden (PXD) was studied from a re-hydrated formulation deposit. Differences in spreading behaviour of single droplets were not further monitored.

Certain samples, especially when flow rates were particularly low at the beginning of the experiment, kinetics showed a start-up-phase during the first one or two sampling intervals. These start-up phases are characterised by lower penetration rates compared to the following linear kinetic. For calculating flow rates, only the linear phases of penetration kinetics were adopted.

Flow rates of the cuticular penetration of PXD, which was dissolved in water/ACN (50% v/v), from a 10 µl droplet containing 1 µg μl^{-1} PXD, were compared to the cuticular penetration from a 5 µl droplet residue of non-adjuvanted Axial 100 EC containing 2 µg μl^{-1} PXD. Experiments were conducted at low (30%), medium (50%) and high (80%) RH, although the 30% RH analysis was not performed for PXD dissolved in water/ACN (Figure 46, left).

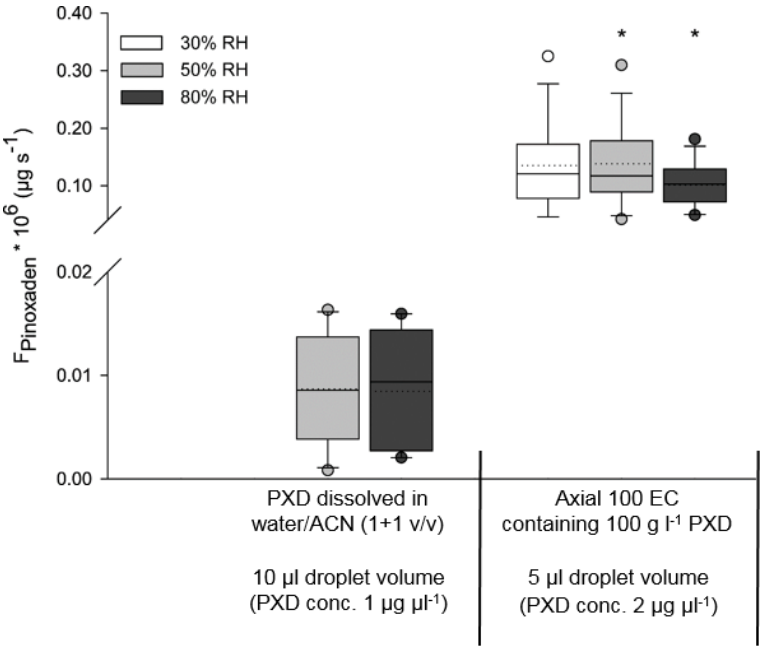

Figure 46: Comparison of cuticular penetration methods. Box-plots illustrating cuticular flow F (µg s^{-1}) of Pinoxaden (PXD) from a droplet residue of 10 µl PXD dissolved in water/ACN (1+1 v/v) (1 µg $µl^{-1}$ Pinoxaden) at 50% or 80% RH at 25 °C and PXD from a droplet residue of 5 µl Axial 100 EC in water (2 µg $µl^{-1}$ Pinoxaden) at 30%, 50% or 80% RH at 25 °C. Continuous lines represent the median and dotted lines the average. Whiskers illustrate 5th to 95th percentiles and dots minimum and maximum values. Box-plots indicated with * are significantly different from their corresponding humidity experiment (Kruskal-Wallis Test with Dunn's Test, $p < 0.05$).

The cuticular penetration of PXD from a droplet residue of PXD dissolved in water/ACN (50% v/v) was very low and independent of RH (Figure 46). Using Axial EC 100 instead of water/ACN (50% v/v) as a solvent for PXD, resulted in flow rates at least one order of magnitude higher for 50% RH (0.12×10^{-6} µg s^{-1}) and 80% RH (0.10×10^{-6} µg s^{-1}) (for detailed information of median values of F_{PXD}, see also Appendix 4). Both experiments were independent from humidity.

Comprehensive details about statistical analyses of significant differences between humidity levels of each adjuvant treatment (P- values calculated from Kruskal-Wallis One Way Analysis of Variance of Ranks) and adjuvant effects can be found in Appendix 4.

Further results show the influence of adjuvants on PXD penetration. Non-adjuvanted Axial 100 EC was adopted as the respective negative control. These results of control experiments are equivalent to Figure 46 (right) and are also illustrated in further box-plots displaying a direct comparison to the corresponding adjuvant and humidity tests.

Concerning Span 20 and Span 80, the flow of PXD was not statistically significant different to their humidity-corresponding control (Figure 47). The cuticular flow was low, median values of Span 20 and Span 80 ranged between 0.08×10^{-6} (Span 20 at 30% RH) and 0.36×10^{-6} µg s^{-1} (Span 80 at 80% RH). Thereby, cuticular penetration even slightly decreased by adding Span 20 at 30% RH was, although not in a significant manner (Figure 47). However, effects of Span 80 at 80% RH were increased by the factor of four.

Moreover, no statistically significant differences could be observed considering humidity levels.

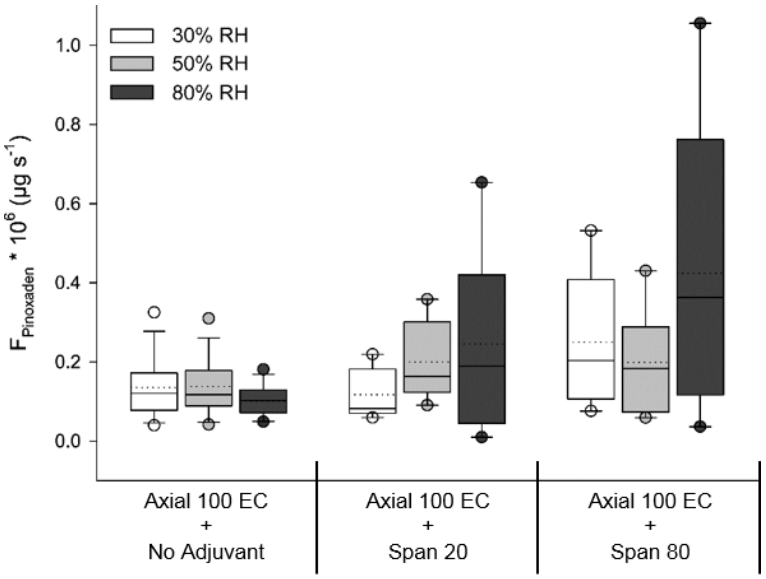

Figure 47: Box-plots illustrating cuticular flow F (µg s^{-1}) of Pinoxaden from a droplet residue of 5 µl Axial 100 EC in water without or with Span surfactants (2 µg $µl^{-1}$ Pinoxaden, 4 µg $µl^{-1}$ surfactant) at 30%, 50% or 80% RH and 25 °C. Continuous lines represent the median and dotted lines the average. Whiskers illustrate 5th to 95th percentiles and dots minimum and maximum values (Kruskal-Wallis Test with Dunn's Test, $p < 0.05$).

The cuticular penetration of PXD was generally increased by adding selected Tween surfactants at all three humidity levels (Figure 48).

PXD flow rates influenced by adding Tween 40, Tween 60 and Tween 65 resulted in a low increase ranging between 0.20×10^{-6} (Tween 60 at 50% RH) and 1.29×10^{-6} µg s^{-1} (Tween 65 at 30% RH) But, the increase was not statistically significant and also differences considering humidity levels could not be identified. The highest increase by the factor 11 was observed for Tween 65 at low RH.

The PXD penetration effected by Tween 80, Tween 81 and Tween 85 increased statistically significant at all humidity levels. The highest effects were observed for Tween 80 at a high humidity (effects ranging from 23 to 36). Adding Tween 81 resulted in almost constant median flow values between 1.60×10^{-6} and 2.18×10^{-6} µg s^{-1}. Significant differences due to humidity levels could not be observed.

By adding Tween 20, the PXD flow rates changed significantly (2.00×10^{-6} at 30% RH, 4.74×10^{-6} at 50% RH and 0.32×10^{-6} µg s^{-1} at 80% RH) (Figure 48). While PXD penetration with Tween 20, compared to the non-adjuvanted Axial 100 EC control, reached a maximum effect increased by factor 40 at medium RH, only low effects increased by factor three were measured at high RH levels. Therefore, the penetration enhancing effect of Tween 20 compared to pure Axial 100 EC suddenly disappeared at a high humidity. Accordingly, penetration effects at 80 % RH also significantly decreased, compared to Tween 20 treatments at 30% and 50% RH. The PXD penetration decreased by around one order of magnitude between high and medium RH. For further detailed information about statistical tests, median values of F_{PXD} and effect values, the reader is referred to Appendix 4.

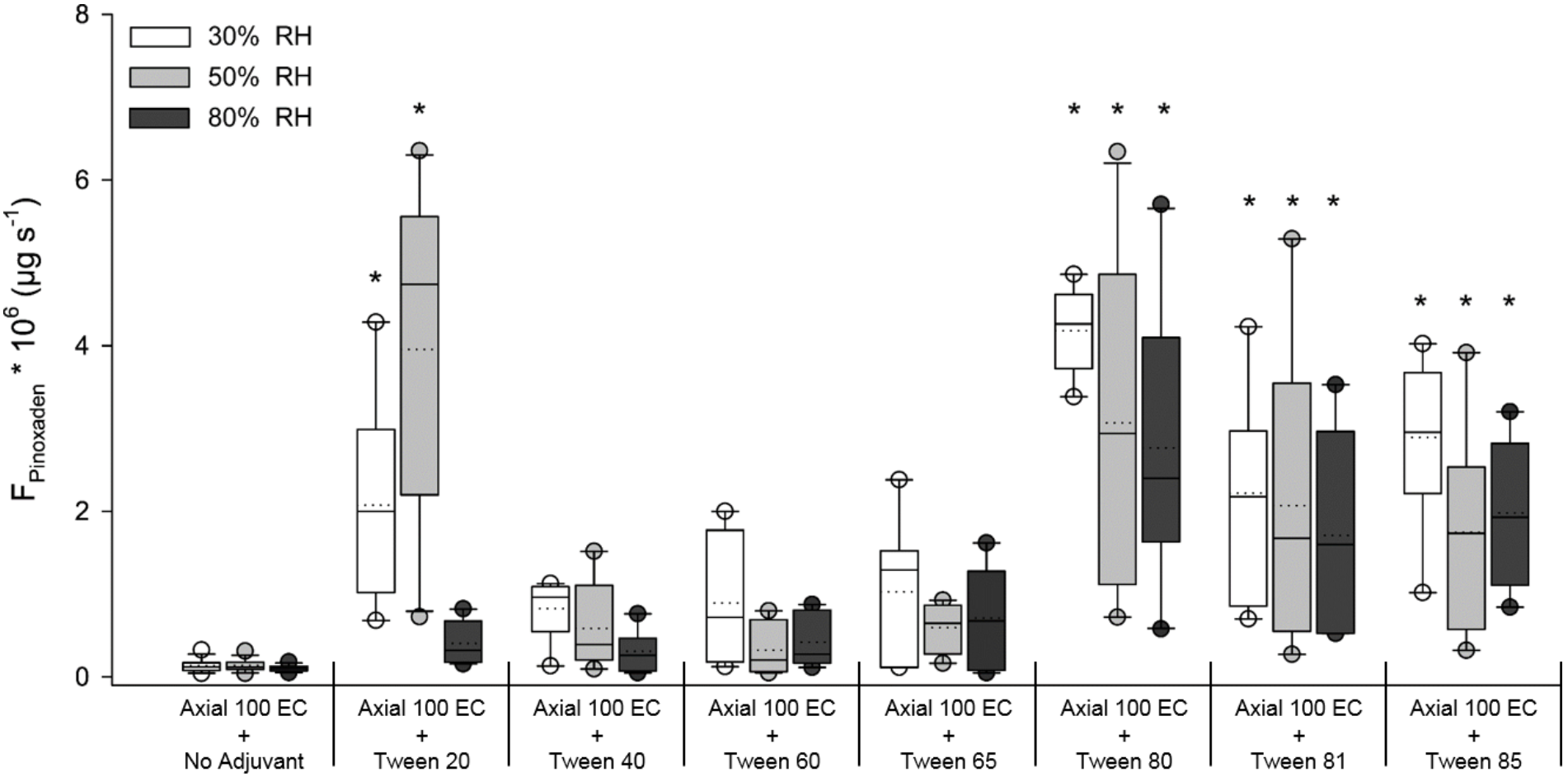

Figure 48: Box-plots illustrating cuticular flow F (µg s^{-1}) of Pinoxaden from a droplet residue of 5 µl Axial 100 EC in water without or with Tween surfactants (2 µg $µl^{-1}$ Pinoxaden, 4 µg $µl^{-1}$ surfactant) at 30%, 50% or 80% RH and 25 °C. Continuous lines represent the median and dotted lines the average. Whiskers illustrate 5th to 95th percentiles and dots minimum and maximum values. Box-plots indicated with * are significantly different from their corresponding non-adjuvanted control (Kruskal-Wallis Test with Dunn's Test, $p < 0.05$).

With the different Genapol O surfactants tested, the PXD penetration at 30% RH increased significantly by an average factor of 20, compared to the non-adjuvanted penetration experiments (Figure 49).

With Genapol O050 the PXD flow was statistically independent of RH levels, but it significantly increased compared to the control. Effects ranged between 14 at low RH levels and 42 at a high humidity. Furthermore, the addition of Genapol O080 resulted in no significant differences for the PXD penetration considering humidity effects. At 80% RH flow rates slightly decreased, compared to Genapol O050 at 80% RH.

Contrastingly, cuticular flow significantly decreased by about two-thirds at 80% RH with Genapol O100 and Genapol O200, compared to Genapol O050 and Genapol O080. Also compared to 30% and 50% RH, flow rates at 80% RH significantly decreased for both Genapol O100 (0.71×10^{-6} µg s^{-1}) and Genapol O200 (0.83×10^{-6} µg s^{-1}) (Figure 49).

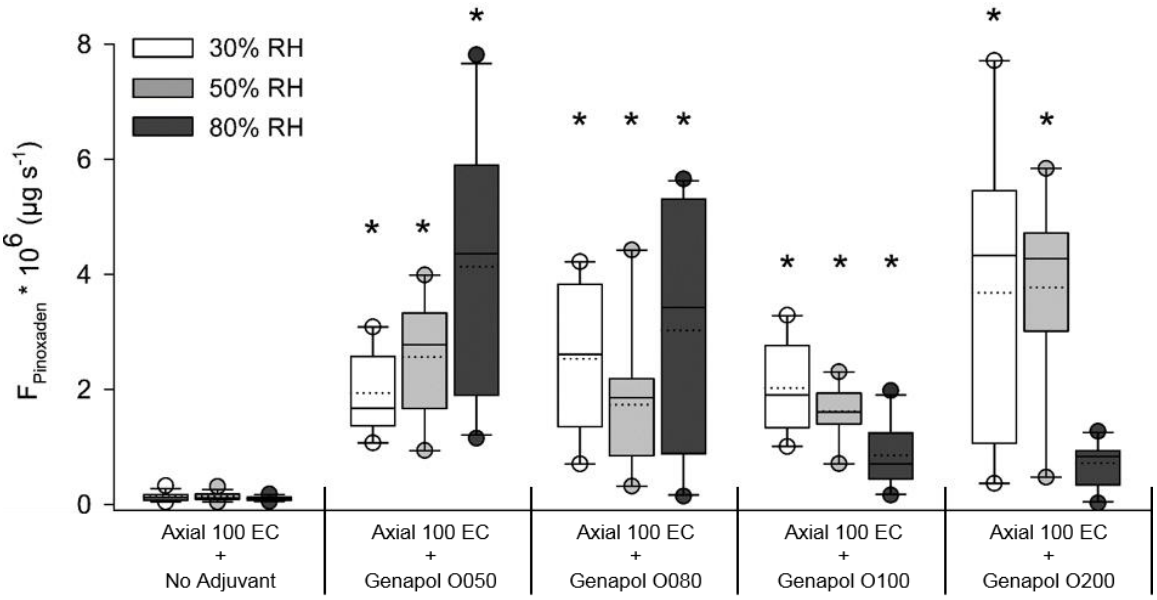

Figure 49: Box-plots illustrating cuticular flow F (µg s^{-1}) of Pinoxaden from a droplet residue of 5 µl Axial 100 EC in water without or with Genapol O surfactant (2 µg $µl^{-1}$ Pinoxaden, 4 µg $µl^{-1}$ surfactant) at 30%, 50% or 80% RH and 25 °C. Continuous lines represent the median and dotted lines the average. Whiskers illustrate 5th to 95th percentiles and dots minimum and maximum values. Box-plots indicated with * are significantly different from their corresponding non-adjuvanted control (Kruskal-Wallis Test with Dunn's Test, $p < 0.05$).

After having added glycerol to Axial 100 EC, the PXD penetration significantly increased only at 50% and 80% RH. At 30% RH flow rates also slightly increased but were not statistically different to the control (all humidity levels averaged at around 0.94×10^{-6} µg s^{-1}) (Figure 50). No further statistically significant differences could be detected as a result of humidity.

The addition of Atlas G1096 resulted only in a small, but not statistically significant increase of penetration rates by a factor of four, compared to the control. At all humidity levels, penetration was almost constant and no significant differences could be observed considering RH (Figure 50).

The cuticular penetration of PXD was effected at a maximum degree by TEHP EW400 (ca. 24×10^{-6} µg s^{-1}). The PXD flow increased significantly by more than two orders of magnitude (effects ranging from 192 to 242). However, the results were again independent of the humidity factor.

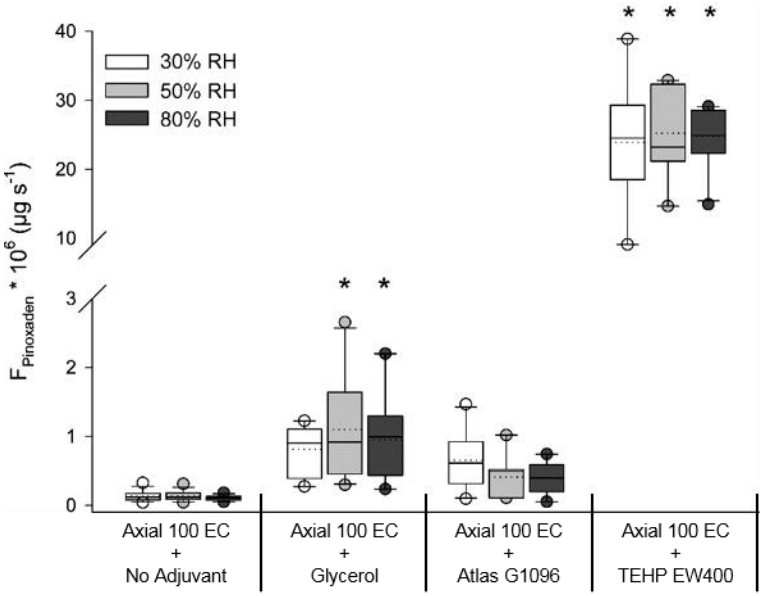

Figure 50: Box-plots illustrating cuticular flow F (µg s^{-1}) of Pinoxaden from a droplet residue of 5 µl Axial 100 EC in water without or with glycerol, Atlas G1096 or TEHP EW400 (2 µg $µl^{-1}$ Pinoxaden, 4 µg $µl^{-1}$ surfactant) at 30%, 50% or 80% RH and 25 °C. Continuous lines represent the median and dotted lines the average. Whiskers illustrate 5th to 95th percentiles and dots minimum and maximum values. Box-plots indicated with * are significantly different from their corresponding non-adjuvanted control (Kruskal-Wallis Test with Dunn's Test, $p < 0.05$).

4.3.2 Adjuvant impact on *in vivo* action of Pinoxaden

Typical ACCase symptoms were clearly visible only on grass-weed species (Figure 51Figure 51). Particular damages could be observed at the meristematic younger tissue. Newer leaf tissue turned slowly yellow (chlorotic) or brown leaf spots got visible (necrotic). Symptoms appeared slowly after five to eight days, depending on the treatment. The new growing leaf meristems could be pulled out of the plants easily because of injuries causing a strong twisting of leaves.

Figure 51: Typical ACCase symptoms at 14 DAA. Plants from left to right: *Triticum aestivum, Avena fatua, Lolium multiflorum, Setaria viridis* and *Phalaris paradoxa.*

Optical estimations of weed damage were conducted 14 DAA. Differences could be observed due to adjuvant treatment, PXD concentration level or between the plant species (Figure 52). For photographic illustrations only the concentration level of 15 g PXD ha^{-1} was selected. At this medium-high concentration level, different damage responses became best visible, comparing plants and adjuvant treatments.

The assessment of the grass-weed species *Phalaris paradoxa* could not be conducted, because of the occurrence of a considerable amount of a rogue species in it. Therefore, results could not be established. No damages on *Triticum aestivum* (TRZAW) could be observed (Figure 51; Figure 52, plants on the left side of the troughs). Comparing plant species, most damage was visible for *Setaria viridis* (Figure 52, fourth from the left) at all adjuvant treatments. The adjuvant treatment which resulted in the maximum damage rates for grass-weed species was TEHP EW400 0.5% (Figure 52, bottom right).

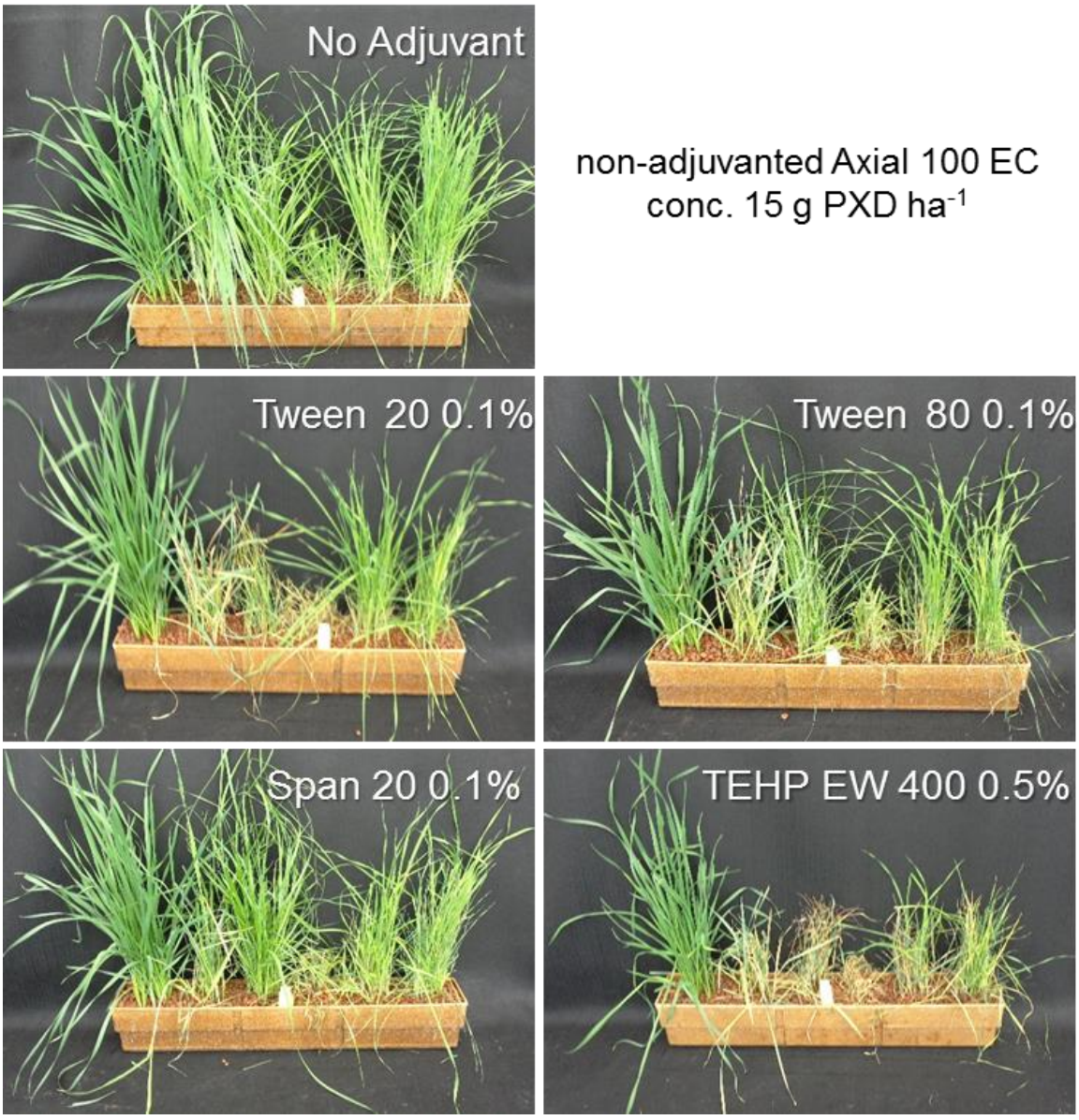

Figure 52: Photographs of plant troughs 14 DAA. Plants sprayed with non-adjuvanted Axial EC 100 treatment containing 15 g PXD ha^{-1} and the respective adjuvant treatment (Span 80 0.1% photograph is not illustrated). 'No Adjuvant' treatment (top) contained water 0.1% instead of an adjuvant. Plants from left to right: *Triticum aestivum, Avena fatua, Lolium multiflorum, Setaria viridis* and *Phalaris paradoxa, Alopecurus myosuroides.* No damages on *Triticum aestivum* (left) could be observed. Most weed damage was visible for *Setaria viridis* (fourth from left).

Due to the wide variations between the different weed species, statistical considerations were conducted using results from every single plant species (Figure 53, *Setaria viridis* (SETVI) (A), *Lolium multiflorum* (LOLMU) (B), *Alopecurus myosuroides* (ALOMY) (C) and *Avena fatua* (AVEFA) (D)). Therefore, results were not averaged over all plants.

The mean of weed damage (%) for the respective plant species was averaged over three replicates and is illustrated for each PXD dosage. With increasing PXD concentration, weed damage (%) increased for all plant species and for all adjuvant treatments. The general ranking of adjuvants relating to weed damage was almost similar for all plant species. The negative control (no adjuvant) resulted in a minimum damage. Span 20 0.1% and Span 80 0.1% showed only small differences but a higher damage than the non-adjuvanted control. Tween 80 0.1% resulted in a lower damage rate than Tween 20 0.1%. The maximum weed damage was observed for TEHP EW400 0.5%. Since TEHP EW400 is used as accelerating adjuvant in the product formulation of Axial and the selected adjuvant concentration of 0.5% was five-time higher than the other adjuvant concentrations, TEHP EW400 0.5% serves as a positive control treatment. Depending on the plant species, a high weed damage of 80% was already reached at medium PXD concentrations at 7.5 g PXD ha^{-1} (Figure 53).

Most statistically significant differences between all concentrations and adjuvant treatments could be observed for SETVI (Figure 53, A1). Results for AVEFA (D1) showed less statistically significant differences comparing adjuvant treatments. Here, the negative control achieved by far the lowest damage, compared to the adjuvant treatments.

Further information about effects at all rate dosages of PXD are presented in Appendix 5. For information about statistical analyses considering greenhouse studies the reader is referred to Appendix 6.

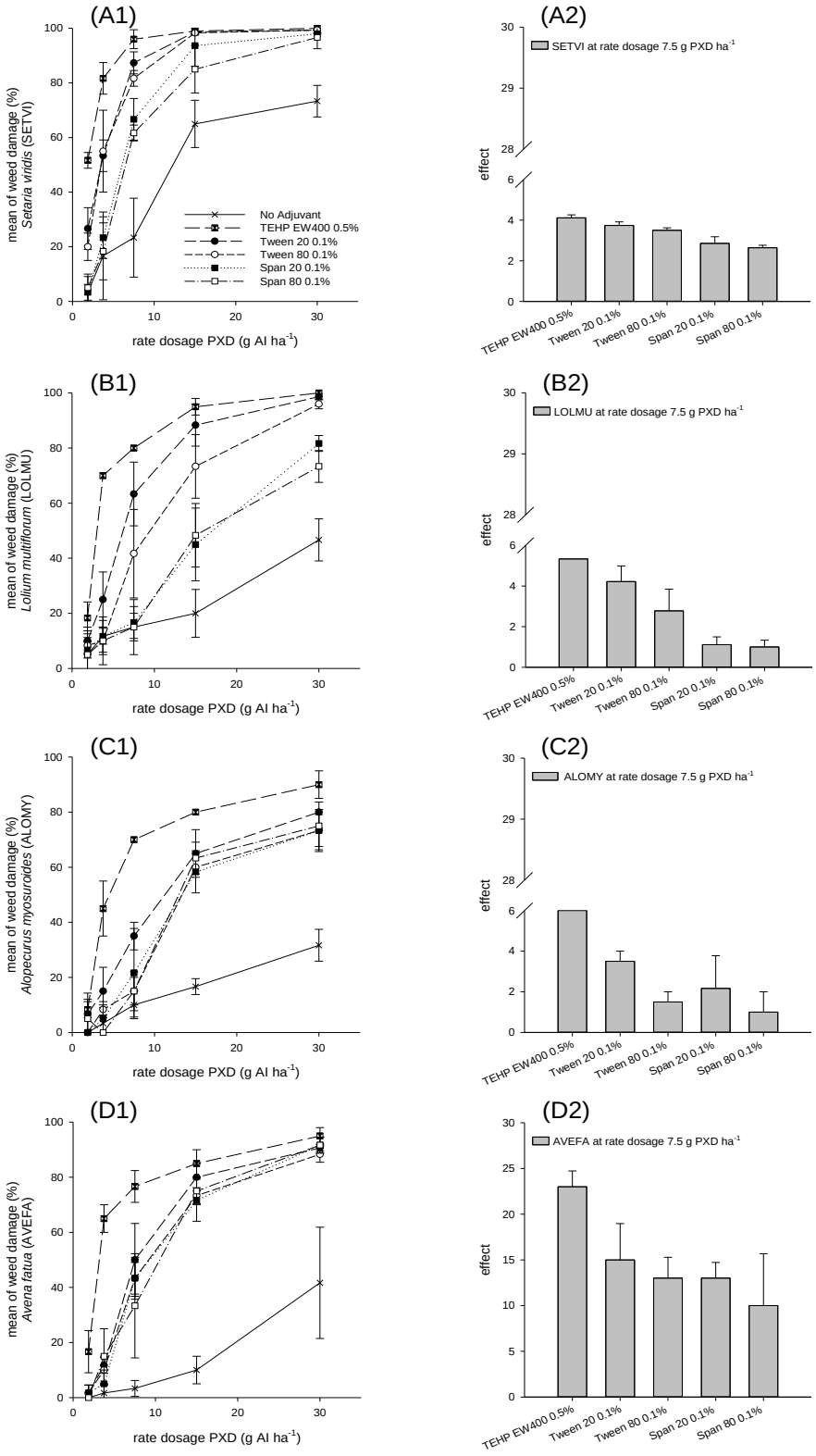

Figure 53: Dose response of mean grass-weed control for PXD with different adjuvant treatments on *Setaria viridis* (SETVI) (A), *Lolium multiflorum* (LOLMU) (B), *Alopecurus myosuroides* (ALOMY) (C) and *Avena fatua* (AVEFA) (D).

Effects of adjuvant treatments to the non-adjuvanted control are expressed as bar charts at medium rate dosages at 7.5 g PXD ha^{-1} (A2-D2). All effects are presented in Appendix 5. Bars and symbols represent mean values and error bars illustrate the standard deviation. Details about statistical analyses are illustrated in Appendix 6.

The effects of adjuvant treatments compared to the non-adjuvanted control are illustrated as bar charts at medium rate dosages at 7.5 g PXD ha^{-1} (Figure 53, A2- D2). A comparison of absolute effects due to plant species is most appropriate, in this case.

Maximum effects could be observed for AVEFA (D2) ranging between 10 for Span 80 and 23 for TEHP EW400. Tween 20 reached effects of about 15. Minimum effects were visible at LOLMU (B2) for Span 20 (1.1) and Span 80 (1.0). Also at ALOMY (C2) for Tween 80 (1.5) and Span 80 (1.0) effects were low. The 7.5 g PXD ha^{-1} treatment on SETVI (A2) showed nearly no differences between adjuvants, compared to the other treated plant species. Adjuvant effects were quite similar and ranged between 3-4 (SETVI, Figure 53, A2).

The particular ranking of dose responses due to the adjuvant treatment was visible with LOLMU results (B2): TEHP EW400 0.5% > Tween 20 0.1% > Tween 80 0.1% > Span 20 0.1% ≥ Span 80 0.1%. Comparable low effects for Tween 80 0.1% were analysed at ALOMY (C2).

To summarise, effects for selected adjuvants (Tween and Span) ranged from two to four for SETVI, LOLMU and ALOMY. The highest effects were obtained at AVEFA. There, effects ranged from 10 to 15.

4.4 Discussion

4.4.1 Cuticular penetration experiments

In cuticular penetration experiments, the lipophilic herbicide Pinoxaden (PXD, log $K_{O/W}$ = 3.2) and selected surfactants have been applied simultaneously to the outer, waxy surface of the cuticular membrane (CM) of the model cuticle of *Prunus laurocerasus*. The influence of adjuvants acting as humectants on the PXD penetration was investigated by conducting experiments at three different humidity levels (30% RH = low, 50% RH = medium, 80% RH = high). The *'simulation of foliar penetration'* (SOFP) approach, as it was applied in this study, is a solid and reproducible method to analyse penetration rates in order to determine adjuvant effects. It was shown for the first time that a highly lipophilic compound like PXD diffuses through a comparatively thick CM at very low humidity levels like 30% RH. In SOFP studies, variables like droplet spreading, droplet drying and possible re-hydration, concentration gradients and thus driving forces may change rapidly in the deposit. Therefore, solute diffusion proceeds under non-steady state conditions (Buchholz, 2006). SOFP is a valuable method for studying effects of evaporation, relative humidity and also surface active effects on cuticular penetration rates. Accordingly, the method has the advantage of simulating a spray droplet more realistic to the situation in the field, compared to other cuticular penetration set-ups, like *'unilateral desorption from the outer surface'* (UDOS) or *'simultaneous bilateral desorption'* (BIDE) (Schönherr & Baur, 1994). The consequential disadvantage of SOFP is the impossibility of determining the exact permeance (P) as it can be analysed in steady state systems in which the donor solution contains a stable solute concentration. Due to many complexities and unknown variables, SOFP results can often be discussed only qualitatively (Baur *et al.,* 1997a).

Preliminary studies indicate the enhancing effect of the formulated product Axial 100 EC in comparison to the pure and non-formulated AI PXD, which was dissolved in water/acetonitrile (50% v/v). Using the Axial 100 EC formulation resulted in increased flow rates by at least one order of magnitude. Although, the product Axial 100 EC includes no additional adjuvants, it is still further formulated with a variety of auxiliary substances, including e.g. different emulsifiers, solvents, surfactants, the safening substance cloquintocet-mexyl and other minor ingredients. Due to the fact that a formulation is generally designed to approve the

biodelivery of the AI (Holloway, 1998; Foy, 1993; Kirkwood, 1993), it was obvious that Axial 100 EC resulted in ten-times higher PXD flow rates than the pure PXD. The ratio between PXD as active substance and the respective adjuvant was one to two. It was suggested, that the double amount of adjuvants would result in a considerable effect on PXD in SOFP experiments with *Prunus laurocerasus* as a model CM. The surfactant concentration in the droplet was several times higher than the critical micelle concentration (cmc), ensuring the presence of stable micelles in solution. No preliminary experiments were conducted to test this ratio, as there was no reason, because the effects on PXD flow rates were clearly visible for certain adjuvants. Placing focus on these experiments, further studies investigating different adjuvant concentrations should be figured out.

First, a comprehensive and systematic discussion on the basis of the surfactant structure is considered with the help of the Genapol O class. The advantage of not only investigating Span and Tween surfactants, but also the Genapol O series, is the reduced complexity due to a stable major lipophilic tail ($C_{18:1}$) and a closer EO distribution (5, 8, 10 and 20 EO) among this class. The water sorption behaviour of Genapol O increases linear with increasing oxygen content/ EO content (Figure 54Figure 54, B). Therefore, a structural comparison regarding the humectant property and humidity effects are rather appropriate, compared than to highly complex Tweens.

The following section focussing the Genapol O surfactants is generally based on the symposium publication: Asmus, E., Arand, K., Popp, C., Friedmann, A.A., Riederer, M. (2016). Water sorption potential of non-ionic adjuvants and its impact on cuticular penetration. *Proceedings of the 11th International Symposium on Adjuvants and Agrochemicals*, pp. 177-182.

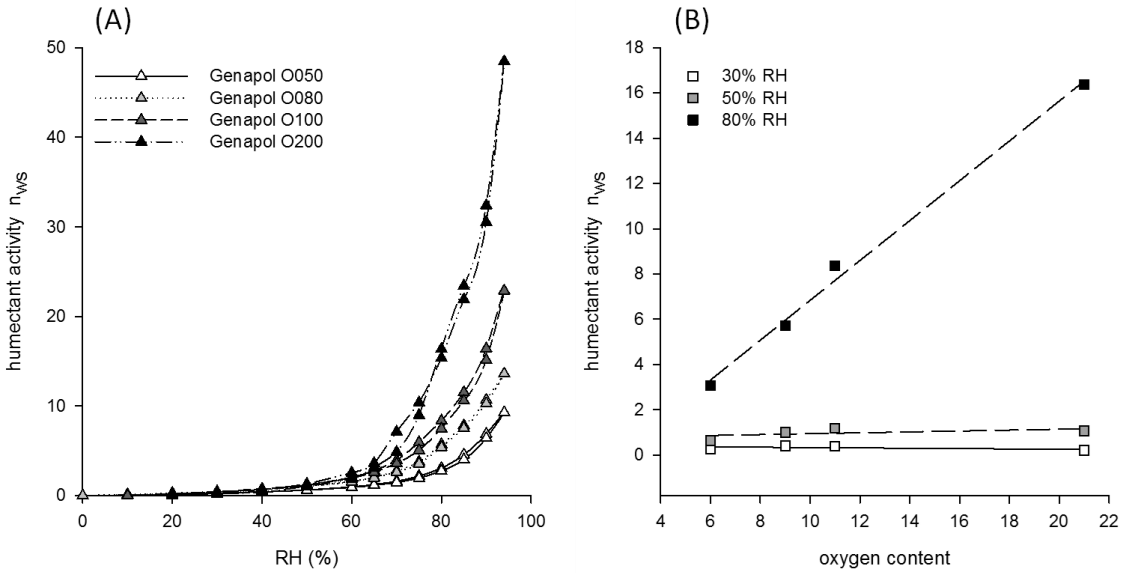

Figure 54: Water sorption isotherms measured between 0% and 95% RH showed an exponential shape and no hysteresis (A). Correlation of humectant activity n_{ws} (mol_{water} $mol_{surfactant}^{-1}$) and oxygen content of Genapol O surfactants at 30%, 50% and 80% RH (B).

During bulk water evaporation, the lipophilic PXD partitions between the formulation residue and the cuticle. Both, the PXD molecules and the surfactants are generally able to penetrate the cuticle to an unknown extent, leaving a surface deposit acting as donor. The process of water evaporation is very fast and when the droplet volume decreases, the absolute PXD concentration increases until precipitation occurs. The AI would precipitate as a crystalline deposit causing that the compound is no longer solved in an aqueous medium and thus being no more available for uptake into the plant. The driving force for AI permeation is the difference in concentration between donor and receiver medium and is determined by the AI amount sorbed in the CM during water evaporation (Schönherr & Baur, 1994; Baur & Schönherr, 1996). In SOFP measurements, all Genapol O adjuvants significantly accelerated the PXD flow rate at low humidities (30% RH), while the water content in the deposit was low (Figure 54). While the enhancing effect of Genapol O050 and Genapol O080 was not significantly different at varying humidity levels, Genapol O100 and Genapol O200 resulted in a decreased PXD flow at high humidities (80% RH) (Figure 49).

Findings from water sorption experiments (Figure 54) revealed a significant rehydration of the residue which results in a considerable increase of water volume

in the formulation residue. Accordingly, PXD concentration in the deposit solution decreases again with a higher water sorption. Subsequently, the driving force for the equilibrium partitioning is directed towards the surface residue where the total amount of PXD increases. A higher fraction of the total PXD amount is therefore withheld in the residue and is not available for diffusion across the CM. Hence, the cuticular penetration to the receiver compartment is reduced and no longer enhanced in comparison with the control of pure Axial 100 EC. While the acceleration effect on PXD permeation is independent of RH in Genapol O050 and Genapol O080, the penetration enhancement decreases with RH in the case of the high EO Genapol O100 and Genapol O200. This confirms reports that high EO surfactants do not enhance the cuticular penetration of lipophilic solutes (Ramsey *et al.,* 2005) at least at high RH. However, these results show that the high EO surfactant Genapol O200 improves the cuticular penetration of the lipophilic AI PXD at low humidities in the same way as low EO Genapol O surfactants do. Therefore, the assumption that low EO surfactants would favour the diffusion of lipophilic solutes, while high EO surfactants enhance permeation only of hydrophilic AIs needs to be further proved. Nevertheless, adjuvant effects observed from SOFP experiments could not be explained only from their humectant character, particularly, only a highly lipophilic compound was analysed. In non-steady state SOFP experiments many complexities and unknown variables interact with each other and effects cannot be considered separately (Buchholz, 2006).

Baur *et al.* (1997a) showed that low EO surfactants of the Genapol C series (also known as Triton X series) (EO ≤ 10) partition readily into the cuticle and may act there as plasticisers by increasing the fluidity of the waxes. It seems likely, that low EO species (Genapol O050, O080 and O100) are able to enhance the penetration of PXD by this mechanism. Genapol C surfactants are derived from coconut oil and represent a mixture of saturated straight-chain C_{12} and C_{18} fatty alcohol ethoxylates. In contrast, Genapol O products consist of mainly unsaturated branch-chained oleic alcohols representing the lipophilic part of the surfactant monomers. Since, among other considerations, it might be suggested that the plasticising effect of surfactants could be based on their chemical nature bearing multiple branches to interact with cuticular waxes (personal communication

Adrian A. Friedmann), it might be possible that Genapol O monomers would interact more effectively with cuticular waxes than straight-chain Genapol C surfactants. Therefore, it is most likely that Genapol O adjuvants have a plasticising effect regarding cuticular PXD flow rates observed in this study. With an increasing EO content of Genapol O surfactants, polarity also increases and molecules would sorb into the CM to lower degrees. According to this suggestion, the PXD penetration promoting effect of Genapol O200 should be reduced because of its high EO content (20 EO). However, the observation from SOFP studies showed a significant increase of PXD penetration at 30% and 50% RH by adding Genapol O200 (Figure 49). An explanation for this finding might be that these selected adjuvants are polydisperse mixtures with a broad distribution of EO numbers. Baur *et al.,* (1997a) additionally showed, by studying Genapol C200 (20 EO) and Genapol C050 (5 EO), that both surfactants share about 6% of their molecular composition. Consequently, even in high-EO surfactants, a substantial fraction of smaller lipophilic monomers exist which are able to improve the penetration of lipophilic PXD. This explanation may be due to the accelerating effect of Genapol O200 at 30% and 50% RH. After fast penetration of the smaller and more lipophilic homologues of Genapol O200 into the cuticular wax, the whole composition of the surfactant residue will change by leaving the larger and more polar homologues behind. Therefore, the PXD accelerating effect disappears at a high humidity level and humectant effects of high EO surfactants may be taken into account. Because of the very high water sorption, the droplet gets re-hydrated and micelles of the remaining large EO surfactants act as trap for the lipophilic PXD and slow down or stop the constant PXD supply across the CM.

The PXD penetration was not significantly increased by adding Span 20 and Span 80 surfactants to the Axial EC 100 formulation. This finding might be explained by the primary surface active MoA observed for Spans in previously shown experiments. Stock and Holloway (1993) postulated that large adjuvants, e.g. with a high EO content (15–20), would support the diffusion of water-soluble compounds. In contrast, these surfactants generally have only poor spreading properties. Therefore, spreading would be increased for smaller surfactants with a low HLB, as it accounts for Spans. It could be speculated that spreading effects

alone, as it might be true for Span 20 and Span 80, would not contribute to an enhanced PXD penetration. However, because of the limited surface area of cuticular membranes on SOFP chambers, super-spreading is not possible, *a priori* and spread areas on the cuticle in SOFP studies were not further monitored.
On the one hand, SOFP is a valuable method for studying effects of evaporation considering complex concentration changes in the droplet residue and of relative humidity on cuticular flow rates. But on the other hand, diffusion proceeds under non-steady state conditions in SOFP experiments, (Buchholz, 2006), which bears many complexities and unknown variables. It is likely, that Spans would rather improve PXD uptake *in planta* than in cuticular penetration experiments, because of distinct spreading properties on the leaf surface (e.g. *Triticum aestivum*) as discussed in chapter I. An accelerating effect on the PXD penetration in order to work as plasticisers, could not be affirmed. Differences because of changing humidities were not observed (Figure 47). The increased water sorption of non-ethoxylated Spans was almost non-existent (chapter II). Therefore, an action as humectant, by re-hydrating the droplet residue, can also be excluded.

A comprehensive discussion, regarding the cuticular action of the class of Tweens, needs to consider multiple effects and variables, since polydisperse Tweens bearing a more complex structure with different EO contents and also changing major alkyl chains (Borisov *et al.,* 2011), compared to non-ethoxylated Spans and the Genapol O series, whereas the alkyl chain represent a stable distribution. Observed effects like humectancy and plasticising properties, cannot be discussed separately. A significant increasing effect on the PXD penetration was observed for the Tween 80 series (Tween 80, Tween 81, Tween 85) (Appendix 4), all bearing an unsaturated oleic acid as major alkyl chain, resulting in a branching of the lipophilic tail. Since Tween 81 is a comparatively small and more lipophilic molecule (5 EO) and Tween 85 with 20 EOs a large one, but carrying three branch-chained fatty acid tails, it might be suggested that Tween 81 and Tween 85 would sorb more effective on cuticular waxes to act as plasticisers and result in a quite larger PXD penetrating effect than Tween 80. Contrastingly, the PXD penetration increasing effect for Tween 80 is slightly higher, especially at 30 % RH, than for Tween 81 and Tween 85 (Appendix 4). It is most likely, that promoting humidity

effects as observed for Genapol O200 account also for Tween 80. The interaction between the increasing plasticising effect of small Tween 80 monomers and the increasing water sorption potential of large EO monomers could provide an explanation for the slightly (not significantly) decreased effect concerning humidity levels, as it was observed for the high EO content Genapol O surfactants.

Tween 40 (C_{16}), Tween 60 and Tween 65 (both C_{18}) resulted in a not significant but slight increase of PXD flow rates (Figure 48). Thus, a strong acceleration effect due to plasticising may be excluded. The major alkyl chains represent saturated and therefore straight-chain lipophilic tails. The high EO content (20 EO) and strong water sorption of these Tweens may account for a strong humectant property (chapter II) which causes an attraction of lipophilic PXD in micelles in the re-hydrated droplet. Nevertheless, slightly increased PXD flow rates were independent of humidity.

The addition of Tween 20 showed the maximum effect observed for Tweens at 50% RH. In contrast, PXD flow rates medium increased at 30% RH and the penetration promoting effect disappeared completely at 80% RH (Figure 48, Appendix 4). There was no statistically significant difference due to humidity observed for all Tweens, with the exception of Tween 20. The surfactant is generally used in many areas of life sciences because of its various properties improving different fields of application. Surprisingly, there is less knowledge about the MoA of Tween 20, neither from the producers nor from the plant protection companies including Tween 20 in commercial agrochemical formulations. Therefore, it is still unclear why Tween 20 offers these various promoting properties. Results from SOFP studies in this work reveal this very interesting and potentially improving character of Tween 20, too. Since it has primary straight alkyl chains, the explanation of plasticising effects due to branching cannot be adopted here. The only difference to other Tweens (e.g. Tween 40, Tween 60) is the comparatively short alkyl chain length of only 12 carbon atoms, while carrying 20 EOs in mean (see also Figure 13). By arguing with its broad Poisson distribution of EO numbers, it may be true that polydisperse mixtures of Tween 20 also bear very large homologues of around 35 EOs, but also very small monomers of ca. 5 EOs. On the one hand, high EO homologues have to be considered as highly polar due to the additional small straight-chain lipophilic tail. These large polar

monomers might act as very strong humectants causing the low effect observed for 80% RH. Because of changing humidity levels, effects might become significantly different. A medium humidity of 50% RH might be the best circumstance for the promoting effect of Tween 20. On the other hand, very small and linear EO homologues, with only about 5 EOs are also considered to act as good accelerating molecules, comparable to branched-chain plasticisers (personal communication Christian Popp). This fraction of Tween 20 homologues seems to cause the high effects on PXD penetration in general (at 30% and 50% RH). However, these results cannot be discussed separately, since observed effects might be the result of a balance between AI deliquescence, dilution effects and rapidly changing driving forces of PXD.

Another explanation of the humidity dependent and the promoting cuticular penetration effects might be the enormous complex distribution of fatty acids in Tween 20. Although, Borisov *et al.* (2011) identified POE sorbitan monolaurate (C_{12}) as a major component of Tween 20, they evaluated their finding as '*only showing the tip of the iceberg, as these monoesters account for only about 30% of the total content'* of Tween 20 (Borisov *et al.,* 2011). Interestingly, the relative amounts of unsaturated oleic acid ($C_{18:1}$) in Tween 20 batches ranged statistically significant from 0% to 15% (Figure 14). Moreover, the degree of esterification by analytically specifying only the lauric acid component of Tween 20, contains significant amounts of other species, although POE sorbitan monolaurate was with 43% the major component (POE sorbitan dilaurate = 36.5% and POE sorbitan trilaurate = 20.5%) (Borisov *et al.,* 2011). To conclude, this extremely wide distribution of molecular structures of one product might be the basis for the results especially found in SOFP studies and more generally for its common broad usage in life science industries.

Therefore, further work is necessarily required to fundamentally elucidate the cuticular action of Tween 20, especially the plasticising MoA of cuticular waxes on the basis of the molecular structure. It would be an advantage to predict, whether a molecule may act as plasticiser because of its bulky and branched-chain or small and linear structure. In further studies a fractioning of Tween 20 could be carried out to gain knowledge of the detailed composition of complex ethoxylated mixtures. Adopting preparative LC or GC-MS approaches (Heini *et al.,* 2012a) would offer the possibility to study e.g. the cuticular penetration or plant uptake effects by using

specific fractions of homologues covering a smaller structural distribution than the basic product (Heini *et al.,* 2012b). To summarise, the enormous structural complexity of Tween 20 (Figure 14, Borisov *et al.,* 2011) which causes the wide range of physico-chemical properties needs to be significantly reduced. Therefore, effects on specific MoA could be analysed more systematically.

Another important investigation concerning the action of adjuvants on cuticular penetration would be to study the permeation of adjuvant molecules itself. In this study, some preliminary attempts have been made to analyse the Tween 20 permeation through the CM of cherry laurel (results not shown). Since there could have been analysed about 2,500 single and double charged ions in a Tween 20-water-solution, a detailed elucidation of all components is very demanding and requires a lot of experience in mass spectrometry and/or bioinformatics. Polydispersity became clearly evident because of the periodical mass structures. In a steady-state cuticular penetration study, where 0.1% of Tween 20 dissolved in water was filled in a donor compartment, the donor concentration of Tween 20 decreased significantly, although, the receiver solution contained only very few compounds which might be taken into consideration to have been originated from Tween 20. The identification of surfactant compounds which are able to penetrate through CMs would be a great advantage, since these homologues could be characterised in detail and be used as penetration aids in formulations to accelerate the agrochemical plant uptake.

To summarise, the SOFP set-up using the model compound PXD and the quantification by LC-MS was a solid, exact and reproducible approach to analyse penetration rates in order to determine adjuvant effects. The additional factor of applying different humidity levels was also demonstrated in order to influence the PXD penetration with certain adjuvants. In the preliminary comparison of PXD flow rates without adding any adjuvants, no significant humidity effect could be observed. Since PXD has a strong lipophilic character due to a relatively high log $K_{O/W}$ of 3.2, the hypothesis that lipophilic AIs would penetrate the CM via the lipophilic pathway without being affected by humidity, may be confirmed.

In the literature, two basic routes of solute penetration across the plant cuticle are extensively discussed: the lipophilic pathway (Coret & Chamel, 1994; Niederl *et*

al., 1998; Schönherr *et al.,* 2001), and the hydrophilic route (Schönherr, 2002; Schlegel *et al.,* 2005; Popp *et al.,* 2005). It was postulated, that surfactants promote the lipophilic diffusion route primary by having a plasticising effect on cuticular waxes, (Schreiber *et al.,*1996) resulting in an increased fluidity of amorphous regions (Riederer & Schreiber, 1995). Accelerator substances might decrease the crystallinity and therefore enhance the fluidity of the amorphous phase (Schreiber *et al.,*1996). In contrast, considering the hydrophilic pathway, surfactants are likely to act as humectants (Stock & Briggs, 2000) which are re-hydrating a droplet deposit by the attraction of water from the atmosphere (Ramsey *et al.,* 2005). A high amount of water sorbed in the CM would result in a swelling of the cuticle which leads to an increased transpiration (Schreiber, 2005) and so the water-filled pathways become prevalent. Therefore, a high humidity might result in a swelling effect, improving hydrophilic routes for water-soluble AIs. Further work would be required to elucidate humectant action of adjuvants by also analysing an extremely hydrophilic compound like glyphosate, glufosinate or paraquat as model compounds. Also the determination of a fix value of the potential adjuvant effect on a model AI could be analysed better with a steady-state model system than with an approach in which several unknown variables and complexities have to be considered. However, the integration of these variables is the major advantage of SOFP.

4.4.2 Adjuvant impact on *in vivo* action of Pinoxaden

Greenhouse trials were conducted to estimate the effects of selected adjuvants on the action of Pinoxaden (PXD) on different *Poaceae* species. It is important to distinguish between the analyses of PXD uptake and PXD effect *in planta*. In this study, the effective uptake of PXD into the plant tissue was not measured, however, it was rather important to evaluate the weed damage due to PXD spray application by adding different adjuvants.

For example, in an uptake experiment it was shown, that over 90% of radiolabelled PXD was already incorporated into the crops within 5 h after application (Wenger *et al.,* 2012). Treatment solutions were applied in droplets to the adaxial leaf surface of barley, winter wheat, or durum wheat (BBCH 12). After 24 h, about 20% of PXD had been translocated out of the treated leaf by a basipetal movement below the treated area (Wenger *et al.,* 2012). However, spray application experiments may be more related to field conditions and provide a different perspective on PXD action, compared to cuticular penetration or plant uptake experiments.

The big disadvantage of *in vivo* greenhouse studies is the experimental set-up, considering statistical analysability. In order to obtain more reliable results, the combination of different PXD concentration levels, plant species, negative and positive controls and overall replications had to be considered. For the purpose of keeping the greenhouse experiments within reasonable bounds, the selection of adjuvants had to be reduced to only four. Tween 20, Tween 80, Span 20 and Span 80 were chosen because of their related chemical structures allowing a comparison between ethoxylation and non-ethoxylation. Comparing Tweens and Spans also includes their different MoA, which could be evaluated for these adjuvants until now. To summarise, greenhouse experiments may be a compromise between collecting information (adjuvant selection) and statistical quality, e.g. repetitions.

Optical estimations of weed damage due to ACCase symptoms were conducted 14 DAA. Effects by an expected loss of biomass, compared to non-sprayed plants, e.g. a prevented tillering of damaged plants, were also taken into account. Therefore, the damage estimation may be as close as possible, compared to field herbicide application and must be assessed by an experienced senior assistant.

Differences could be observed either due to adjuvant treatment, PXD concentration level or between plant species. With an increasing rate dosage of PXD, an increasing weed damage could be observed. However, weed damage effects strongly depend on plant species. As *Setaria viridis* was most susceptible, already a low PXD concentration level caused strong chlorotic injuries. With this, it becomes very important to take possible differences between translocation effects of single plant species into consideration, as the assessment of herbicidal damages includes all species dependent physiological effects. For this reason, different plant species were selected to be analysed in this study.

The increase of weed damage (%) was not linear related, to PXD rates. All treatments revealed a linear increase in weed damage at lower concentration levels, up to about 7.5 or 15 g PXD ha^{-1}. At higher concentration rates, a saturation in weed damage was observed, depending on plant species and adjuvant treatment. Because of wide variations due to weed species (Stock, Holloway, Grayson, & Whitehouse, 1993), the experimental set-up, regarding different plants but also different PXD rates, was therefore well designed.

One central objective in this study was to evaluate, if results gained *in vitro* in the laboratory, can be transferred to spray application studies on living plants. These two fundamental investigations, firstly, cuticular penetration and secondly, the greenhouse trials were both performed in order to answer this question. As a direct comparison between both experiments, the results of weed damages were averaged on all analysed weed species (Figure 55, A). Relative humidity was set in the greenhouse bay at 65%. Regarding to cuticular penetration results, the 50% or 80% RH treatments could be possibly adopted for a comparison. In the greenhouse, a high humidity of 80% may be reached during watering or with respect to the canopy microclimate. On the other hand, a high humidity during foliar application may decrease very fast under field conditions because of rapidly evaporation and high temperatures on the plant surface. However, the maximum humidity value monitored in the greenhouse over two weeks was 72% RH and the mean value was around 60% RH (data not shown). Therefore, the medium humidity-treatment of 50% RH concerning the cuticular penetration was selected for this comparison (Figure 55, B).

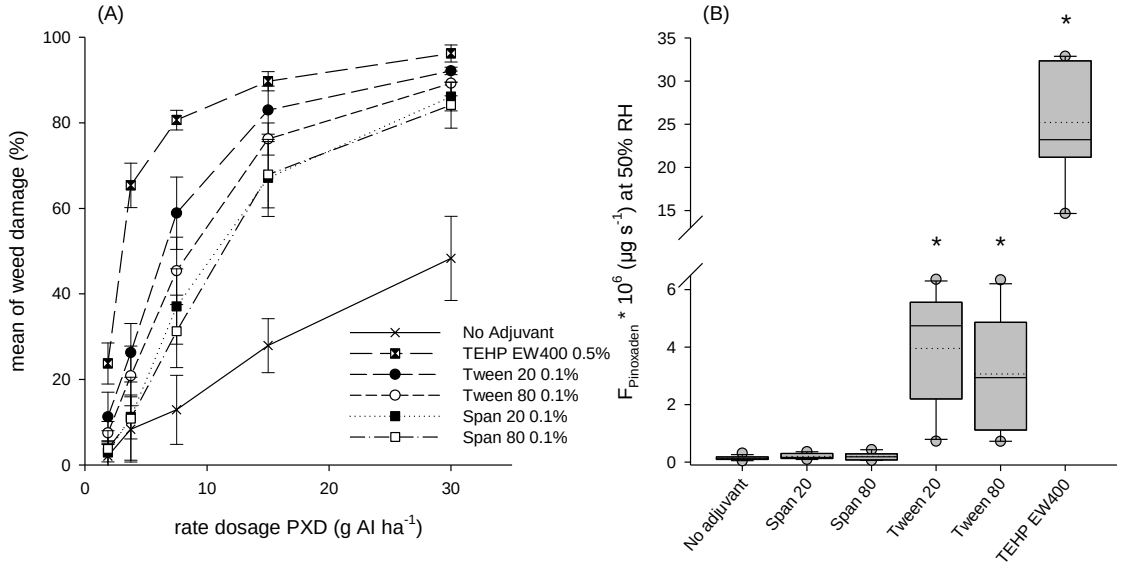

Figure 55: Results gained from *in vivo* greenhouse studies (A) or cuticular penetration (SOFP) measurements at 50% RH (B).
Dose response of mean grass-weed control for PXD with different adjuvant treatments averaged on all tested weeds (SETVI, LOLMU, ALOMY, AVEFA) (A). Symbols represent mean values and error bars illustrate the standard deviation.
Box-plots of cuticular flow rates (F) of PXD with different surfactants at 50% RH (B). Continuous lines represent the median and dotted lines the average. Whiskers illustrate 5th to 95th percentiles and dots minimum and maximum values. Box-plots indicated with * are significantly different from the non-adjuvanted control (Kruskal-Wallis Test with Dunn's Test, $p < 0.05$).

Even though the absolute weed damage was different, depending both on plant species and also on PXD rates, the ranking order of adjuvant effects was same for all observations: TEHP EW400 0.5% > Tween 20 0.1% > Tween 80 0.1% > Span 20 0.1% ≥ Span 80 0.1% (Figure 55, A). The effects the adjuvants showed in cuticular penetration experiments, displayed the same ranking, however, the concentration ratios between PXD and adjuvants were different. Already the non-adjuvanted control with Axial 100 EC resulted in moderate damage rates, whereas the PXD flow rates were comparably low. In greenhouse trials, weed damage rates caused by Span 20 and Span 80 were also higher than expected from SOFP tests. In fact, it seems likely, that SOFP experiments display more extreme effects in adjuvant action. A comparison of adjuvant effects with their corresponding non-adjuvanted control tests confirms this assumption (Table 6). Adjuvant effects from mean weed damages in % (averaged over all four weed species) at the medium PXD concentration (7.5.g PXD ha^{-1}) were compared with effects of the cuticular penetration flow rates (µg s^{-1}) at 50% RH (Table 6). It is obvious, that effects from *in vivo* assessments show a more narrow distribution than those resulted from

SOFP tests. As stated above, the non-adjuvanted control with Axial 100 EC already resulted in moderate damage rates. Therefore, adjuvant effects in greenhouse studies do not show such maximum effects like 192, which are possibly achieved in SOFP experiments (TEHP) (Table 6).

Table 6: Adjuvant effects: comparison between greenhouse studies and cuticular penetration (SOFP) measurements at 50% RH.
In vivo tests (left): values in brackets indicate standard deviation, n=3, see also Appendix 5. Cuticular penetration experiments (right): values in brackets indicate median F_{PXD} *10^6 (µg s^{-1}) and 25%-75% quantile, please also refer to Appendix 4.

Adjuvant	Effects to non-adjuvanted control		
	In vivo tests (mean of weed damage at 7.5.g PXD ha^{-1}) at ca. 65% RH	Cuticular penetration -SOFP (median F_{PXD} *10^6 (µg s^{-1}) at 50% RH)	
Span 20	4.8 (5.5)	1	(0.164 (0.1 – 0.3))
Span 80	3.7 (4.3)	2	(0.184 (0.1 – 0.3))
Tween 20	6.6 (5.6)	39	(4.740 (2.2 – 5.6))
Tween 80	5.2 (5.3)	24	(2.939 (1.2 – 4.9))
TEHP EW400	9.9 (8.8)	192	(23.216 (21.2 – 32.4))

The most possible reason for this may be the interaction of a variety of different MoA and species dependent physiological effects, displayed in the greenhouse results. Whereas SOFP results mainly revealed the accelerating effect of adjuvants (e.g. effect of TEHP on PXD), surface-effective MoA as retention and spreading would be underestimated. For this, greenhouse tests combine all MoA concerning foliar application as it would appear on the field. Therefore, Spans were primarily selected because of their surface active properties, acting mainly on the leaf surface, after droplet deposition. Especially Span 20 revealed a maximum spreading behaviour after one minute after application (covered leaf area; chapter I). It was stated, that a very low surface tension, well below 30 mN m^{-1}, would promote stomatal infiltration and thus leads to an increased uptake into the plant (Schönherr & Bukovac, 1972; Stevens *et al.,* 1993; Knoche, 1994; Schönherr *et al.,* 2005). This physical phenomenon might be also relevant for *in planta* effects, because of low equilibrium surface tension results, especially for Spans.

Results from SOFP measurements revealed nearly no increasing PXD penetration through the cuticle of *Prunus laurocerasus*. This outcome would confirm the assumption, that Spans only effect droplet spreading behaviour and do not contribute directly to an enhanced PXD penetration. Because of the limited area of cuticular membranes on SOFP chambers, super-spreading is not possible, *a priori*. The area on living plants is not restricted and spreading can occur at high levels (especially the effective surface area of wheat is extremely increased due to three-dimensional surface structures as epicuticular waxes, trichomes, etc.). Span effects are also slightly increased from *in vivo* studies, but are higher than in SOFP results. This could probably show the improving properties of Span in general, acting mainly as surface spreaders and not as accelerating adjuvants in the cuticle. The high effect of Tween 20 shown in SOFP experiments at 50% RH has to be interpreted carefully, because of the significant discrepancy between the humidity effects (Figure 48). As the PXD penetration was increased by the factor of about 40 at 50% RH, the effect at 80% RH was only three (Appendix 4). However, these humidity effects in SOFP experiments need to be further proved. Nevertheless, the effect of Tween 20 0.1% in greenhouse studies was maximum for selected adjuvants (6.6) and only slightly lower than the positive control TEHP EW400 0.5% (9.9), which was five-times higher concentrated (Table 6). In all previous experiments investigated in this work, Tween 20 continuously exhibited medium and well results. For example, in DST and retention track spraying studies, Tween 20 displayed the best results of all adjuvants chosen in this study. The good potential for droplet adherence during spraying may be one reason for the high greenhouse effects. Also the general potential for an improved cuticular penetration cannot be rejected, although there are differences in humidity effects. In summary, it seems likely, that Tween 20 functions as an ‘all-rounder’ adjuvant, whereas it has no outstanding properties improving one distinct process during foliar application, but works medium or well regarding all application aspects. Almost the same findings seem to be true for Tween 80. Both results, from SOFP and greenhouse studies, indicated slightly lower effects for Tween 80 than for Tween 20, but increased, compared to Spans. Tween 80 also exhibits broad functions concerning the whole application process. SOFP measurements showed

no significant differences for humidity effects as observed for Tween 20, therefore, the improved acceleration effect on PXD penetration was proved.

The main objective of this work was to uncouple different aspects of foliar application, beginning from the droplet formation via retention and spreading aspects on the leaf surface and the cuticular penetration of PXD. Performing a greenhouse spray test by also including *in vivo* effects would bring all these factors together. In this particular study, it was shown that a prediction from these laboratory measurements to *in vivo* studies can be possibly adopted. But it is very important to keep in mind that well defined laboratory conditions are not necessarily equivalent to the situation on the field. For certain procedures, spray application characterisation has to be carried out and evaluated also under field conditions.

5 SUMMARISING DISCUSSION AND OUTLOOK

For a finishing and concluding evaluation of functions of the selected Tween, Span and Genapol O adjuvants, a summarising presentation of the most important properties, concerning the mode of action (MoA) of foliar application was considered.

For this, a graphical method, comparing data, adjuvants attained in measurements during this study, was chosen as the best suitable illustration. So-called '*spider'* or *'radar'* charts display information in form of three or more quantitative variables on separate axes (Chambers *et al.,* 1983), starting from the same point in the middle (Friendly, 1991). Radar charts are generally suited for strikingly displaying outliers and common features of two or more candidates or to show if one chart of one adjuvant is greater in all variables than others (Friendly, 1991). On the other hand, radar charts are poorly suited for comparing lengths of different spokes (Friendly, 1991). Radar charts should be also not adopted for evaluating different adjuvants due to one single variable (function). For this, single results were explained statistically precise in previous chapters.

Five main functions were selected to represent the MoA of adjuvants: dynamic surface tension (DST), retention, spreading, humectancy and cuticular penetration (Appendix 8). Because greenhouse studies (chapter III) incorporate all of these five features, they are considered to be comprehensive and encompassing results which may exhibit similar conclusions like radar charts. Therefore, greenhouse results were not used as separate spokes in radar charts.

Normally, the graphical method of radar charts is used for ordinal measurements, where all variables are on the same scale. This was not the case for these five experimental fundamental different results so the adoption of this method required data remodelling, especially because the direction of values are opposing each other. For example, a high value concerning the contact angle (CA) displays a poor spreading property but in contrast, high PXD flow rates in SOFP measurements showed an improving penetration ability. So each property corresponds to the sense 'better' in a different respect. Therefore, data is needed to be processed in a manner which is appropriate for a grading. All selected adjuvants of Spans, Tweens and Genapol O were considered and results gained in different

measurements were referred relatively to one hundred. A table of these data applied in radar charts can be found in Appendix 8.

For the detailed elucidation of the MoA of adjuvants, the class of polysorbates (Tween) was generally considered in this study because of their common promoting potential and their easy integration in agrochemical formulations. Despite the fact, that Tweens are generally known to have only a relatively moderate function, they are an interesting and structural complex surfactant class which provides a systematic analysis because of the wide variety of products (Borisov *et al.,* 2011). Nevertheless, the usage of Tweens in agrochemical formulations is mainly based on empiric and heuristic studies with the central objective to maximise the effectiveness of active substances. The groups of Spans and Genapol O were additionally selected because of their structural properties which might be helpful to understand the effects of Tweens.

Since Tween 20 and Tween 80 are representatives of the Tween class which are most commonly used in formulations, they are the first considered in this comparative study to be displayed by using radar charts (Figure 56). For having a similar chemical structure (except polyethoxylation) corresponding Spans like Span 20 and Span 80, were also included in this comparison (Figure 56). These two Tweens (blue) and two Spans (red) were ranked on each of the five different parameters.

It has to be kept in mind, that most adjuvants used in this work are polydisperse substances which exhibit a complex distribution of single homologues carrying different alkyl chains with different EO groups. Therefore, the information about the major alkyl chain and the mean EO content is only of an average value.

While Tween 20 and Span 20 carry an almost linear and comparatively short alkyl chain (C_{12}), Tween 80 and Span 80 possess a larger and more bulky, unsaturated oleic acid ($C_{18:1}$). Considering the addition of EO groups, Tweens are by far larger and more hydrophilic, than corresponding Spans (HLB values of Tweens 20=16.7; Tween 80=15.7 and Span 20=8.4; Span 80=6.8 (Table 1)). Stock and Holloway (1993) stated that adjuvants with a high EO content (15–20) would support the diffusion across the cuticular membrane by acting as humectants. These large surfactants generally have only poor surface active properties (e.g. spreading).

Consequently, spreading is increased for smaller surfactants having a low HLB. These findings coincide with the results in this study.

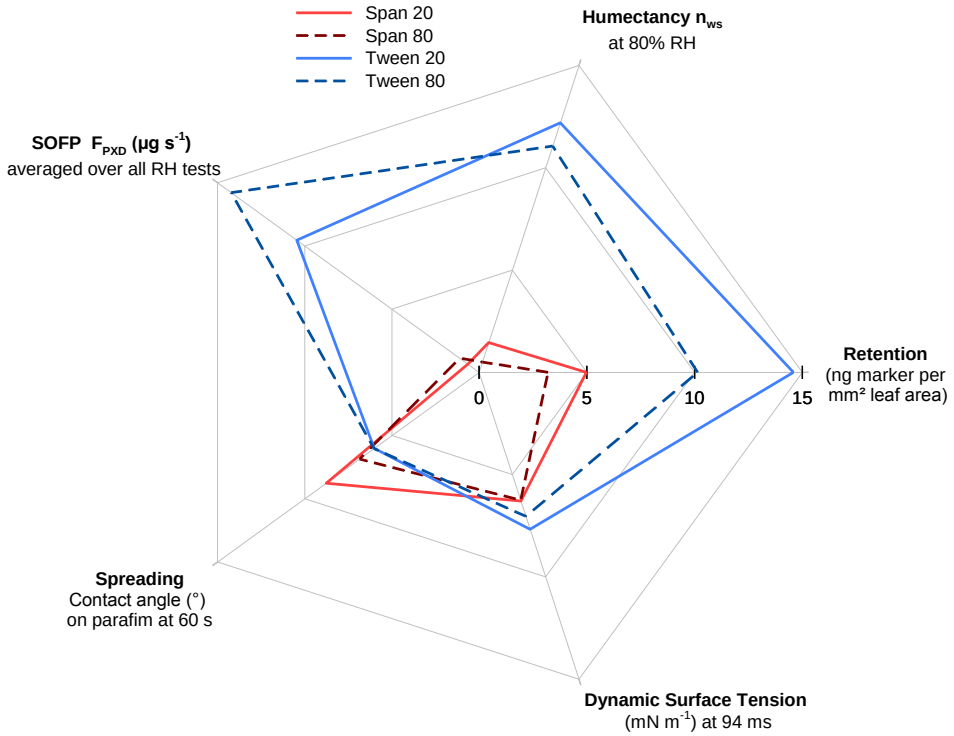

Figure 56: Radar chart displaying five different equivalent categories, representing the most important properties concerning MoA evaluated in this study. A comparison between Span 20, Span 80, Tween 20 and Tween 80 is illustrated.

While Tween 20 and Tween 80 are better humectants, Span 80 and especially Span 20 revealed a better spreading behaviour (Figure 56). The humectant activity was shown to be higher for Tween 20, representing the more hydrophilic molecular nature, compared to Tween 80 (chapter II).

Adjuvants having an overall large and balanced area in radar charts, where the dimensions on spokes are similar, can be evaluated to have improving and broader effects. Those adjuvants revealing a small area with a strong deformation towards a specific direction, have to be valued to have a very particular MoA. Tween 20 and Tween 80 are obviously covering a wide range of selected variables so they can be evaluated to have a broad spectrum of applications. Therefore, Tween 20 functions as an ‘all-rounder’ adjuvant. Whereas it has no outstanding MoA improving one distinct process during foliar application, it works well concerning the comprehensive aspects of foliar application. Almost the same

findings seem to be true for Tween 80. Whereas it has a lower droplet adhesion potential, it showed higher PXD flow rates than Tween 20. On the other hand, Span 20 covers only a small area in total and its radar chart is deformed to one side. Therefore, Span 20 must be considered to be a kind of 'specialist' adjuvant in terms of its surface spreading behaviour (chapter I).

One central objective in this study was to evaluate, if results gained *in vitro* in the laboratory (shown in radar charts), can be transferred to spray application studies for living plants (greenhouse studies, chapter III). Since Tween 20 and Tween 80 resulted in a much larger area than Spans (Figure 56), they are also to be considered to result in higher effects *in planta*. With this reflection, it could have been successfully demonstrated, that Tween 20, Tween 80, Span 20 and Span 80 showed an almost similar ranking in this comparative radar plot study as compared to greenhouse studies (Figure 55). This finding seems to confirm that the application of radar plots in this study can be adopted to estimate the adjuvant potential in greenhouse studies.

Considering the chemical structure of Tweens, especially the different major alkyl chain lengths, a comparison between Tween 20 (C_{12}), Tween 40 (C_{16}), Tween 60 (C_{18}) and Tween 80 ($C_{18:1}$) should be executed (Figure 57). These four selected Tweens share the same EO distribution of 20 EOs in mean. Since the information about the major alkyl chain bears a distribution, many other homologues carrying different alkyl chains must be kept in mind. Nevertheless, radar charts displayed large differences between these Tweens. For evaluating Tweens in order to compare their overall area in radar charts, the following ranking can be observed: Tween 20 = Tween 80 > Tween 40 > Tween 60. The increase of the length of the lipophilic alkyl chain (number of carbon atoms of the hydrophobic group: Tween 20 < Tween 40 < Tween 60 = Tween 80) decreases the solubility of the surfactant in water (Rosen, 1989, chapter 1). This effect should be visible concerning the humectant action, but because of the broad range of EO distribution, the influence of an increasing alkyl chain disappears comparing these selected Tweens (chapter II).

It is also known, that an increased alkyl chain length increases the tendency of the surfactant to absorb at an interface and to form micelles (Rosen, 1989, chapter 1).

These effects may be visible regarding to the cuticular penetration results as micelles must be considered to entrap lipophilic compounds (Baur *et al.,* 1997a) like PXD. Even though cuticular penetration of Tween 40 is much lower than of Tween 80, all other effects are similar (Figure 57).

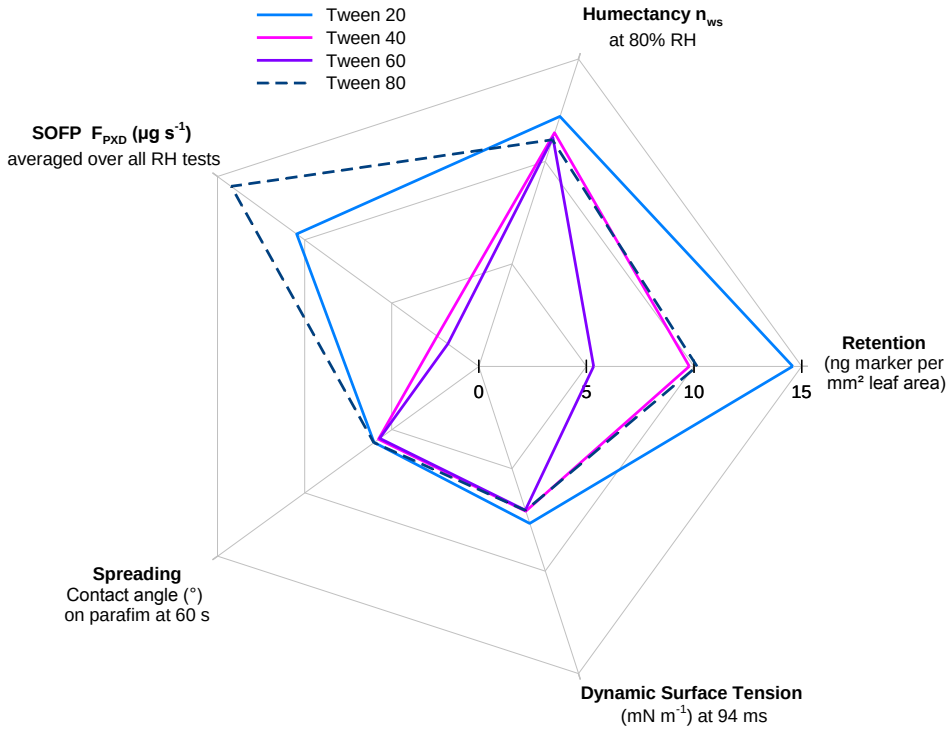

Figure 57: Radar chart displaying five different equivalent categories, representing the most important properties concerning MoA evaluated in this study for the Tween family. Tweens were selected according to their different major alkyl chain, but all carrying 20 EO groups in mean (Tween 20, Tween 40, Tween 60, Tween 80).

Further work is required in order to reveal the effects of surfactants during cuticular penetration. Determining diffusion coefficients (D) of surfactants with or without an AI, through extracted and reconstituted cuticular waxes (Schreiber, 1995; Schreiber *et al.,* 1996), would contribute to elucidate differences in cuticular penetration. Also the relationship between molecular size of solutes and diffusion coefficients in isolated cuticular membranes (Schönherr & Baur, 1994; Baur & Schönherr, 1997) and reconstituted cuticular waxes should be examined further to characterise adjuvant action regarding to cuticular penetration. Accordingly, it is very demanding to give evidence to the adjuvant MoA regarding to cuticular penetration referring only to non-steady state SOFP experiments carried which are out with only one highly lipophilic AI. The addition of the humidity factor also

complicates evaluation due to significant different effects, e.g. for Tween 20. The probably better approach assessing cuticular effects would be the method of *'unilateral desorption from the outer surface'* (UDOS) (Baur *et al.,* 1997a) or the determination of cuticular permeances (P) with the help of steady-state donor-receiver systems (Schreiber & Schönherr, 2009, chapter 2).
Whereas DST and spreading properties are almost similar for these Tweens (Figure 57), the droplet retention on wheat plants was quite different. This might be an evidence for the complexity of droplet adhesion prediction as there are also many other determining factors than DST, e.g. droplet volume, droplet velocity, angle of incidence or surface properties. (Taylor, 2011).

Since the Tween 80 series is characterised by its unsaturated oleic acid as major alkyl chain, the MoA of Tween 80, Tween 81 and Tween 85 are considered for a comparison (Figure 58). While Tween 80 and Tween 85 have a mean EO content of 20, Tween 81 only carries 5 EO groups in mean. Whereas Tween 85 represents a trioleate, Tween 80 and Tween 81 carry only one oleic acid.
For the evaluation of Tweens in order to compare their overall area in radar charts, the following ranking can be observed: Tween 80 > Tween 85 > Tween 81. Even though Tween 81 shows rather low effects in total, the cuticular penetration results were higher than expected. The reason for this might be the small molecular weight due to its low EO content which improves cuticular penetration (Stock & Holloway, 1993). Overall, radar charts of the Tween 80 series showed a slight deformation in the direction of the cuticular penetration results. It became already obvious from box-plots (Figure 48, chapter III), that branched-chain Tweens showed almost the highest flow rates of PXD. It could be possible that due to a branching, adjuvant molecules are able to break or disintegrate crystalline platelets in cuticular waxes and therefore enhance solute diffusion (Schreiber *et al.,* 1996).

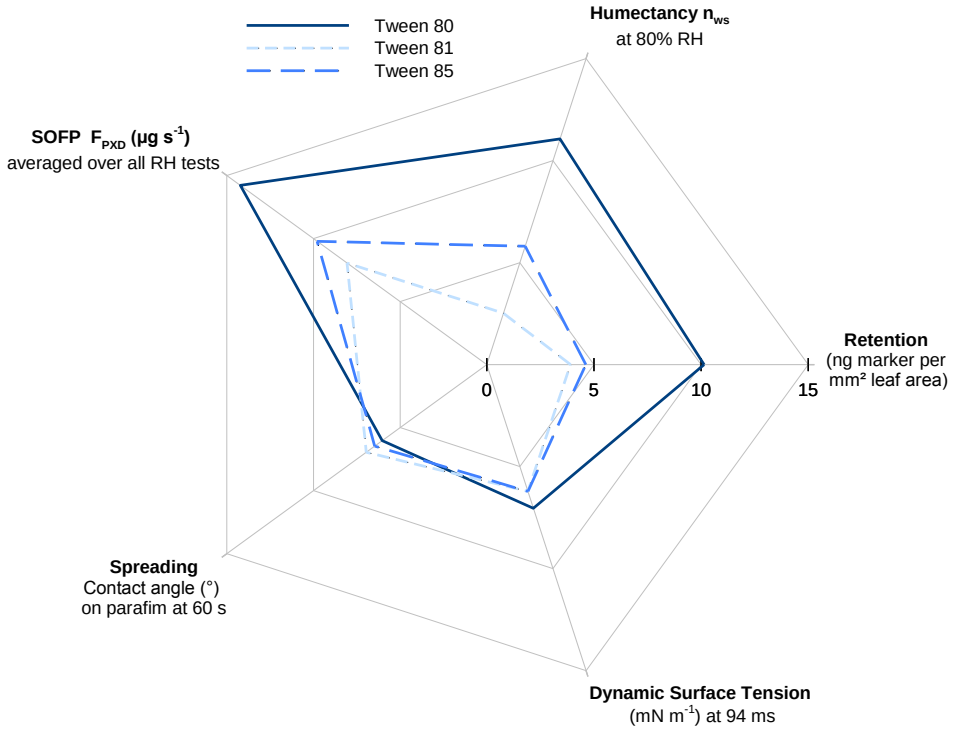

Figure 58: Radar chart displaying five different equivalent categories, representing the most important properties concerning MoA evaluated in this study for the Tween 80 family. Tweens were selected according to their identical major alkyl chain $C_{18:1}$ (Tween 80, Tween 81, Tween 85).

Rosen (1989) stated that branched-chain or/and ring-containing surfactants are generally more soluble in both water and hydrocarbons. Furthermore, they show a lower viscosity in aqueous media than straight-chain surfactants with the same number of carbon atoms (Rosen, 1989, chapter 1). It is likely, that the introduction of the cis-branching in Tweens would be an advantage considering measurements performed in this study, and it might also be a practical advantage to integrate them into complex formulations.

To summarise, the most improving characteristics evaluated in this work were revealed for Tween 20 and Tween 80, since both showed a broad potential considering the investigated properties. Also in greenhouse spray tests, including *in vivo* effects of adjuvants, which bring all these factors together, Tween 20 and Tween 80 resulted in high weed damage rates. Especially Tween 20 showed a high impact which was comparable to the Pinoxaden accelerating adjuvant TEHP EW400 which was applied as a positive control with a five-time higher concentration than Tween 20. Thus, the present work showed for the first time that findings obtained in laboratory experiments, like *in vitro* cuticular penetration

measurements, can be successfully transferred to spray application studies on living plants concerning the adjuvant MoA.

The benefit of also investigating the MoA of the Genapol O series is the reduced structural complexity due to a stable major unsaturated lipophilic tail ($C_{18:1}$) and a closer EO distribution (5, 8, 10 and 20 EO) among this surfactant class. On the basis of the chemical structure, comparative reflections regarding to EO effects are more appropriate than focussing on effects of the lipophilic group. Evaluating Genapol O in order to compare their total area in radar charts (Figure 59), the following ranking can be observed: Genapol O200 > Genapol O100 = Genapol O080 = Genapol O050.

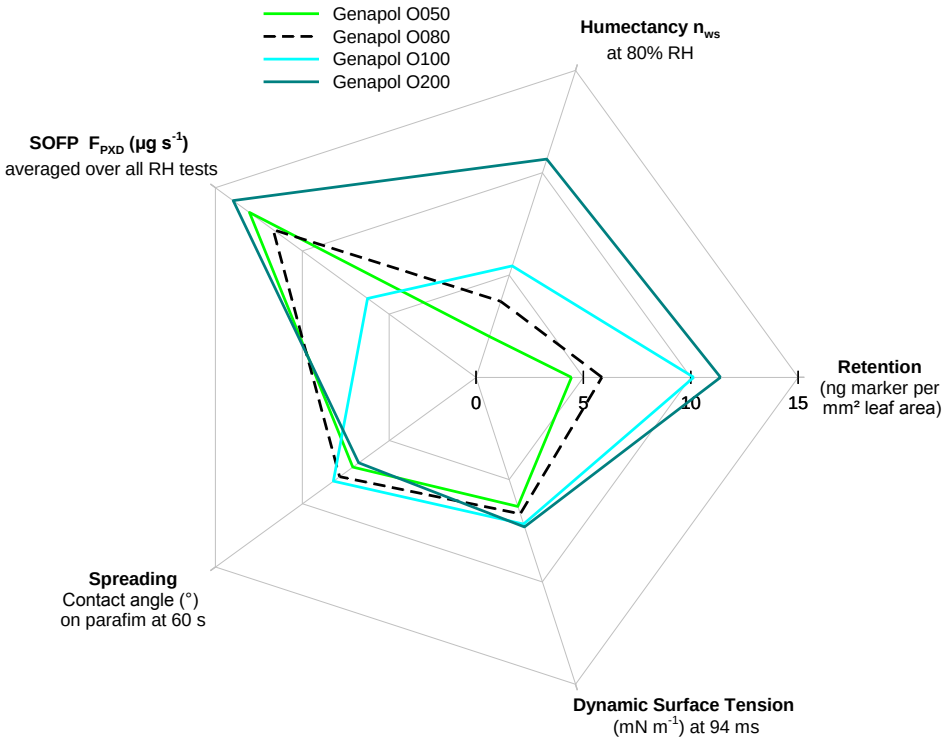

Figure 59: Radar chart displaying five different equivalent categories, representing the most important properties concerning MoA evaluated in this study for the Genapol O family (Genapol O050, Genapol O080, Genapol O100, Genapol O200).

Whereas Genapol O200 covers a broad spectrum of applications, Genapol O050 and Genapol O080 show a clear deformation towards the spoke of cuticular penetration which might be again due to the branched-chain character of molecules. Contrastingly, Genapol O100 showed comparatively low penetration

rates but well results regarding droplet adherence. Whereas DST and spreading properties were almost similar for all tested Genapol O adjuvants, retention was again quite different, as observed for Tweens.

The water sorption behaviour of Genapol O increases with an increasing EO content and accordingly with their increasing hydrophilic character (chapter II). This effect is clearly visible also in the radar chart (Figure 59).

Areas of radar charts of Genapol O200 and Tween 80 (not illustrated together in Figure 59) show almost the equal extension. The reason for this might be similarities in their chemical structure. Both have a high mean EO content of 20 and carry a branched alkyl chain with the same carbon content ($C_{18:1}$). Therefore, HLB values are also in the same range: Tween 80: 15.7 and Genapol O200: 15.1 (Table 1). Thereby, Tween 80 has to be evaluated as more bulky than Genapol O200, since its basic structure contains a sorbitan ring.

However, this finding seems to be a successful demonstration of systematic derivations from structural similarities of adjuvants to their MoA concerning foliar application. From this study, it seems alike that adjuvants having a wide EO distribution, offer a more broad potential than adjuvants with a small EO distribution. It might be a speculation that due to this broad distribution of single molecules, all bearing their individual specific physico-chemical nature, a wide range of properties concerning their MoA is covered. This would mean, for every requirement or problem that could occur during spray application, there might be an appropriate adjuvant homologue available which improves a specific MoA.

6 REFERENCES

Adamson, A. W., & Gast, A. P. (1997). Physical chemistry of surfaces. Wiley, New York, NY, US.

Ambwani, D. S., & Fort, T. (1979). In: Good, R. J., & Stromberg, R. R. (eds.) (1979). Surface and colloid science: volume 11: Experimental methods. Plenum, New York, NY, US, 93-119.

Andrade P, R. D., Lemus M, R., & Pérez C, C. E. (2011). Models of sorption isotherms for food: Uses and limitations. Vitae, 18, 325-334.

Arand, K., Stock, D., Burghardt, M., & Riederer, M. (2010). pH-dependent permeation of amino acids through isolated ivy cuticles is affected by cuticular water sorption and hydration shell size of the solute. Journal of Experimental Botany, 61(14), 3865-3873.

ASTM-American Society for Testing and Materials E 1519 (1999). Annual book of ASTM standards, Vol. 11.05. Designation E 1519-95, Standard terminology relating to agricultural tank mix adjuvants. ASTM International, West Conshohocken, PA, US, 905-906.

Avato, P., Bianchi, G., & Salaminik, F. (1987). Ontogenetic variations in the chemical composition of maize surface lipids. In: Stumpf, J., Mudd, B. & Nes, W. D. (eds.) (1987). The metabolism, structure, and function of plant lipids. Plenum, New York, NY, US, 549-551.

Barthlott, W., Neinhuis, C., Cutler, D., Ditsch, F., Meusel, I., Theisen, I., & Wilhelmi, H. (1998). Classification and terminology of plant epicuticular waxes. Botanical Journal of the Linnean Society, 126, 237-260.

Baur, P. (1998). Mechanistic aspects of foliar penetration of agrochemicals and the effect of adjuvants. Recent Research Developments in Agricultural and Food Chemistry, 2, 809-837.

Baur, P., & Schönherr, J. (1996). Foliar uptake of systemic compounds: Principles and optimization. Gartenbauwissenschaft, 61, 105-115.

Baur, P., & Schönherr, J. (1997). Penetration of an ethoxylated fatty alcohol surfactant across leaf cuticles as affected by concentration, additives, and humidity. Zeitschrift für Pflanzenkrankheiten und Pflanzenschutz, 104, 380-393.

Baur, P., Buchholz, A., & Schönherr, J. (1997). Diffusion in plant cuticles as affected by temperature and size of organic solutes: similarity and diversity among species. Plant, Cell & Environment, 20(8), 982-994.

Baur, P., Grayson, B. T., & Schönherr, J. (1997a). Polydisperse ethoxylated fatty alcohol surfactants as accelerators of cuticular penetration. 1. Effects of ethoxy chain length and the size of the penetrants. Pesticide Science, 51, 131-152.

Baur, P., Marzouk, H., Schönherr, J., & Grayson, B. T. (1997b). Partition coefficients of active ingredients between plant cuticle and adjuvants as related to rates of foliar uptake. Journal of Agricultural and Food Chemistry, 45, 3659-3665.

Bergeron, V., Bonn, D., Martin, J. Y., & Vovelle, L. (2000). Controlling droplet deposition with polymer additives. Nature, 405, 772-775.

Bergman, Å., Rydén, A., Law, R. J., de Boer, J., Covaci, A., Alaee, M., *et al.* (2012). A novel abbreviation standard for organobromine, organochlorine and organophosphorus flame retardants and some characteristics of the chemicals. Environment International, 49, 57-82.

Bianchi, G., Lupotto, E., Borghi, B., & Corbellini, M. (1980). Cuticular wax of wheat. Planta, 148, 328-331.

Bird, D. A. (2008). The role of ABC transporters in cuticular lipid secretion. Plant Science, 174, 563-569.

Björklund, S., Engblom, J., Thuresson, K., & Sparr, E. (2013). Glycerol and urea can be used to increase skin permeability in reduced hydration conditions. European Journal of Pharmaceutical Sciences, 50, 638-645.

Borisov, O. V., Ji, J. A., Wang, Y. J., Vega, F., & Ling, V. T. (2011). Toward understanding molecular heterogeneity of polysorbates by application of liquid chromatography–Mass spectrometry with computer-aided data analysis. Analytical Chemistry, 83, 3934-3942.

Börner, H. (ed.) (2009). Pflanzenkrankheiten und Pflanzenschutz. Springer, Berlin Heidelberg, Germany.

Brandner, J. D. (1998). The composition of NF-defined emulsifiers: Sorbitan monolaurate, monopalmitate, monostearate, monooleate, polysorbate 20, polysorbate 40, polysorbate 60, and polysorbate 80. Drug Development and Industrial Pharmacy, 24, 1049-1054.

Brewer, C., Smith, W., & Vogelmann, T. (1991). Functional interaction between leaf trichomes, leaf wettability and the optical properties of water droplets. Plant, Cell & Environment, 14, 955-962.

Brunauer, S. (1940). The Adsorption of gases and vapors, vol. 1. Oxford University Press, Oxford, UK.

Brutin, D. (ed.) (2015). Droplet wetting and evaporation: From pure to complex fluids. Academic Press, London, UK.

Buchholz, A. (2006). Characterisation of the diffusion of non-electrolytes across plant cuticles: properties of the lipophilic pathway. Journal of Experimental Botany, 57, 2501-2513.

Buchholz, A., & Trapp, S. (2016). How active ingredient localisation in plant tissues determines the targeted pest spectrum of different chemistries. Pest Management Science, 72, 929-939.

Burghardt, M., & Riederer, M. (1996). Sorption of monodisperse and polydisperse nonionic surfactants in isolated plant cuticles and reconstituted cuticular wax. Journal of Experimental Botany, 47, 51-51.

Burghardt, M., & Riederer, M. (2006). Cuticular transpiration. In: Riederer, M., & Müller, C. (eds.) Biology of the plant cuticle. Blackwell Publishing Ltd, Oxford, UK, 292-311.

Burghardt, M., Schreiber, L., & Riederer, M. (1998). Enhancement of the Diffusion of Active Ingredients in Barley Leaf Cuticular Wax by Monodisperse Alcohol Ethoxylates. Journal of Agricultural and Food Chemistry, 46, 1593-1602.

Butler Ellis, M. C., Webb, D. A., & Western, N. M. (2004). The effect of different spray liquids on the foliar retention of agricultural sprays by wheat plants in a canopy. Pest Management Science, 60, 786-794.

Butler Ellis, M., Tuck, C., & Miller, P. (1997). The effect of some adjuvants on sprays produced by agricultural flat fan nozzles. Crop Protection, 16, 41-50.

Carrier, O., & Bonn, D. (2015). Contact angles and the surface free energy of solids. In: Brutin, D. (ed.) (2015). Droplet wetting and evaporation: From pure to complex fluids. Academic Press, London, UK, 15-23.

Cassie, A., & Baxter, S. (1944). Wettability of porous surfaces. Transactions of the Faraday Society, 40, 546-551.

Castro, M. J., Ojeda, C., & Cirelli, A. F. (2014). Advances in surfactants for agrochemicals. Environmental Chemistry Letters, 12, 85-95.

Chambers, J. M., Cleveland, W. S., Kleiner, B., & Tukey, P. A. (1983). Graphical Methods for Data Analysis. Wadsworth, Belmont, CA, US.

Cohen, S., Marcus, Y., Migron, Y., Dikstein, S., & Shafran, A. (1993). Water sorption, binding and solubility of polyols. Journal of the Chemical Society, Faraday Transactions, 89, 3271-3275.

Cook, G. T., Babiker, A. G. T., & Duncan, H. J. (1977). Penetration of bean leaves by aminotriazole as influenced by adjuvants and humidity. Pesticide Science, 8, 137-146.

Coret, J. M., & Chamel, A. R. (1993). Influence of some nonionic surfactants on water sorption by isolated tomato fruit cuticles in relation to cuticular penetration of glyphosate. Pesticide Science, 38, 27-32.

Coret, J., & Chamel, A. (1994). Effect of some ethoxylated alkylphenols and ethoxylated alcohols on the transfer of [14C] chlorotoluron across isolated plant cuticles. Weed Research, 34, 445-451.

Cussler, E. L. (ed.) (2009). Diffusion: mass transfer in fluid systems. Cambridge University Press, Cambridge, UK.

Cutler, D. F., Alvin, K. L., & Price, C. E. (eds.) (1982). The plant cuticle. Academic Press, London, UK.

De Ruiter, H., Uffing, A. J., Meinen, E., & Prins, A. (1990). Influence of surfactants and plant species on leaf retention of spray solutions. Weed Science, 567-572.

Ensikat, H., Boese, M., Mader, W., Barthlott, W., & Koch, K. (2006). Crystallinity of plant epicuticular waxes: electron and X-ray diffraction studies. Chemistry and Physics of Lipids, 144, 45-59.

Fagerström, A., Kocherbitov, V., Ruzgas, T., Westbye, P., Bergström, K., & Engblom, J. (2013). Effects of surfactants and thermodynamic activity of model active ingredient on transport over plant leaf cuticle. Colloids and Surfaces B: Biointerfaces, 103, 572-579.

Fernández, V., & Khayet, M. (2015). Evaluation of the surface free energy of plant surfaces: toward standardizing the procedure. Frontiers in Plant Science, 6, 1-11.

Fernánez, V., Sotiropoulos, T., & Brown, P. H. (eds.) (2013). Foliar fertilization: scientific principles and field pratices. International Fertilizer Industry Association, Paris, France.

Forney, C. F., & Brandl, D. G. (1992). Control of humidity in small controlled-environment chambers using glycerol-water solutions. HortTechnology, 2, 52-54.

Forster, W. A., & Kimberley, M. O. (2015). The contribution of spray formulation component variables to foliar uptake of agrichemicals. Pest Management Science, 71,1324-1334.

Forster, W. A., Mercer, G., & Schou, W. (2012). Spray droplet impaction models and their use within AGDISP software to predict retention. New Zealand Plant Protection Society, 65, 85-92.

Foy, C. L. (1993). Progress and developments in adjuvant use since 1989 in the USA. Pesticide Science, 38, 65-76.

Friendly, M. (1991). Statistical graphics for multivariate data. SAS SUGI, 16, 1157-1162.

Gaskin, R. E., & Holloway, P. J. (1992). Some physicochemical factors influencing foliar uptake enhancement of glyphosatemono(isopropylammonium) by polyoxyethylene surfactants. Pesticide Science, 34, 195-206.

Gaskin, R. E., Steele, K. D., & Forster, W. A. (2005). Characterising plant surfaces for spray adhesion and retention. New Zealand Plant Protection Society, 58, 179-183.

Godfray, H. C. J., Beddington, J. R., Crute, I. R., Haddad, L., Lawrence, D., Muir, J. F., Toulmin, C., *et al.* (2010). Food Security: The Challenge of feeding 9 billion people. Science, 327, 812-818.

Good, R. J., & Stromberg, R. R. (eds.) (1979). Surface and colloid science: vol. 11: Experimental methods. Plenum, New York, NY, US.

Grayson, B. T., Webb, J. D., Pack, S. E., & Edwards, D. (1991). Development and assessment of a mathematical model to predict foliar spray deposition under laboratory track spraying conditions. Pesticide Science, 33, 281-304.

Green, J. (2000). Adjuvant outlook for pesticides. Pesticide Outlook, 11, 196-199.

Green, J., & Beestman, G. B. (2007). Recently patented and commercialized formulation and adjuvant technology. Crop Protection, 26, 320-327.

Green, J., & Hazen, J. (1998). Understanding and using adjuvants properties to enhance pesticide activity. In: McMullan, P. (ed.) (1998). Proceedings 5th International Symposium on Adjuvants and Agrochemicals. Memphis, TN, US.

Griffin, W. C. (1954). Calculation of HLB values of non-ionic surfactants. Journal of the Society of Cosmetic Chemists, 5, 249-256.

Guo, Z., & Liu, W. (2007). Biomimic from the superhydrophobic plant leaves in nature: Binary structure and unitary structure. Plant Science, 172, 1103-1112.

Gutenberger, A., Zeisler, V. V., Berghaus, R., Auweter, H., & Schreiber, L. (2013). Effects of poly- and monodisperse surfactants on14C-epoxiconazole diffusion in isolated cuticles of Prunus laurocerasus. Pest Management Science, 69, 512-519.

Haas, K., & Schönherr, J. (1979). Composition of soluble cuticular lipids and water permeability of cuticular membranes from Citrus leaves. Planta, 146, 399-403.

Harkins, W. D., & Jordan, H. F. (1930). Surface tension by the ring method. Science, 72, 73-75.

Hazen, J. L. (2000). Adjuvants-terminology, classification and chemistry. Weed Technology, 14(4), 773-784.

Heini, J., Mainx, H. G., & Gerhards, R. (2012b). Evaluation of the potency of different seed oil ethoxylates to increase herbicide efficacy in comparison to commercial adjuvants. Julius-Kühn-Archiv, 434, 549-556.

Heini, J., Walker, F., Schoene, J., Mainx, H.-G., & Gerhards, R. (2012a). Fractioning of an ethoxylated soybean oil adjuvant and studies on the potency of the fractions in combination with bromoxynil octanoate and sulfonylurea herbicides. Journal of Plant Diseases and Protection, 208-215.

Heredia, A. (2003). Biophysical and biochemical characteristics of cutin, a plant barrier biopolymer. Biochimica et Biophysica Acta (BBA)-General Subjects, 1620, 1-7.

Hess, F. D. (1999). Surfactants and additives. Proceedings of the California Weed Science Society, 51, 156-172.

Hess, F. D., & Falk, R. H. (1990). Herbicide deposition on leaf surfaces. Weed Science, 280-288.

Hofer, U., Muehlebach, M., Hole, S., & Zoschke, A. (2006). Pinoxaden - for broad spectrum grass weed management in cereal crops. Journal of Plant Diseases and Protection -Zeitschrift für Pflanzenkrankheiten und Pflanzenschutz, Sonderheft XX, 989-995

Hoffmann, M. M., Bennett, M. E., Fox, J. D., & Wyman, D. P. (2005). Water partitioning in 'dry' poly (ethylene oxide) alcohol (C m E n) nonionic surfactant—a proton NMR study. Journal of Colloid and Interface Science, 287, 712-716.

Holloway, P. J. (1969). Chemistry of leaf waxes in relation to wetting. Journal of the Science of Food and Agriculture, 20, 124-128.

Holloway, P. J. (1998). Improving agrochemical performance: possible mechanisms for adjuvancy. In Knowles, D. A. (ed.) Chemistry and Technology of Agrochemical Formulations, Springer Netherlands, Dordrecht, Netherlands, 232-263.

Holloway, P. J., & Edgerton, B. M. (1992). Effects of formulation with different adjuvants on foliar uptake of difenzoquat and 2,4-D: model experiments with wild oat and field bean. Weed Research, 32, 183-195.

Holloway, P. J., Butler Ellis, M. C., Webb, D. A., Western, N. M., Tuck, C. R., Hayes, A. L., & Miller, P. C. H. (2000). Effects of some agricultural tank-mix adjuvants on the deposition efficiency of aqueous sprays on foliage. Crop Protection, 19, 27-37.

Hu, H., & Larson, R. G. (2005). Analysis of the effects of Marangoni stresses on the microflow in an evaporating sessile droplet. Langmuir, 21, 3972-3980.

Ivanova, N. A., & Starov, V. M. (2011). Wetting of low free energy surfaces by aqueous surfactant solutions. Current Opinion in Colloid & Interface Science, 16, 285-291.

Janku, J., Bartovska, L., Soukup, J., Jursik, M., & Hamouzová, K. (2012). Density and surface tension of aqueous solutions of adjuvants used for tank-mixes with pesticides. Plant Soil Environment, 12, 568-572.

Jeffree, C. E. (1996). Structure and ontogeny of plant cuticles. Plant cuticles: an integrated functional approach. BIOS Scientific Publishers Ltd.: Oxford, UK, 33-82.

Jetter, R., & Riederer, M. (2016). Localization of the transpiration barrier in the epi-and intracuticular waxes of eight plant species: water transport resistances are associated with fatty acyl rather than alicyclic components. Plant Physiology, 170, 921-934.

Jetter, R., & Schäffer, S. (2001). Chemical composition of the Prunus laurocerasus leaf surface. Dynamic changes of the epicuticular wax film during leaf development. Plant Physiology, 126, 1725-1737.

Jetter, R., Kunst, L., & Samuels, A. L. (2006). Composition of plant cuticular waxes. In: Riederer, M., & Müller, C. (eds.) Biology of the plant cuticle. Blackwell Publishing Ltd, Oxford, UK, 145-181.

Jetter, R., Schäffer, S., & Riederer, M. (2000). Leaf cuticular waxes are arranged in chemically and mechanically distinct layers: evidence from Prunus laurocerasus L. Plant, Cell & Environment, 23, 619-628.

Kerstiens, G. (1996). Plant cuticles—an integrated functional approach. Journal of Experimental Botany, 47, 50-60.

Kirkwood, R. C. (1993). Use and mode of action of adjuvants for herbicides: A review of some current work. Pesticide Science, 38, 93-102.

Kirkwood, R. C. (1999). Recent developments in our understanding of the plant cuticle as a barrier to the foliar uptake of pesticides†. Pesticide Science, 55, 69-77.

Kirsch, T., Kaffarnik, F., Riederer, M., & Schreiber, L. (1997). Cuticular permeability of the three tree species Prunus laurocerasus L., Ginkgo biloba L. and Juglans regia L.: comparative investigation of the transport properties of intact leaves, isolated cuticles and reconstituted cuticular waxes. Journal of Experimental Botany, 48, 1035-1045.

Knoche, M. (1994). Organosilicone surfactant performance in agricultural spray application: a review. Weed Research, 34, 221-239.

Koch, K., & Barthlott, W. (2009). Superhydrophobic and superhydrophilic plant surfaces: an inspiration for biomimetic materials. Philosophical Transactions of the Royal Society A: Mathematical, Physical and Engineering Sciences, 367, 1487-1509.

Koch, K., Barthlott, W., Koch, S., Hommes, A., Wandelt, K., Mamdouh, W., Broekmann, P. (2006). Structural analysis of wheat wax (Triticum aestivum, cv 'Naturastar'L.): from the molecular level to three dimensional crystals. Planta, 223, 258-270.

Koch, K., Bhushan, B., & Barthlott, W. (2008). Diversity of structure, morphology and wetting of plant surfaces. Soft Matter, 4, 1943-1963.

Koch, K., Neinhuis, C., Ensikat, H. J., & Barthlott, W. (2004). Self assembly of epicuticular waxes on living plant surfaces imaged by atomic force microscopy (AFM). Journal of Experimental Botany, 55, 711-718.

Krämer, W., Schirmer, U., Jeschke, P., & Witschel, M. (eds.) (2012). Modern crop protection compounds (2nd ed). Wiley, Weinheim, Germany.

Krüss GmbH. Bubble pressure tensiometer. http://www.kruss.de/services/education-theory/glossary/bubble-pressure-tensiometer/. 05.03.2016.

Krüss GmbH. Drop shape analysis. http://www.kruss.de/services/education-theory/glossary/drop-shape-analysis/. 09.12.2015.

Krüss GmbH. Du Noüy ring method. http://www.kruss.de/services/education-theory/glossary/du-nouey-ring method/. 10.12.2015.

Krüss GmbH. Dynamic surface tension. http://www.kruss.de/services/education-theory/glossary/dynamic-surface-tension/. 04.01.2016.

Krüss GmbH. Pendant drop. http://www.kruss.de/services/education-theory/glossary/pendant-drop/. 10.12.2015.

Krüss GmbH. Young-Laplace fit. http://www.kruss.de/services/education-theory/glossary/young-laplace-fit/. 10.12.2015.

Kudsk, P., & Kristensen, J. (1992). Effect of environmental factors on herbicide performance. Proceedings of the first international weed control congress, Melbourne, 173-186.

Levin, Z., & Hobbs, P. V. (1971). Splashing of water drops on solid and wetted surfaces: hydrodynamics and charge separation. Philosophical Transactions of the Royal Society of London A: Mathematical, Physical and Engineering Sciences, 269, 555-585.

Macisaac, S. A., Paul, R. N., & Devine, M. D. (1991). A scanning electron microscope study of glyphosate deposits in relation to foliar uptake. Pesticide Science, 31, 53-64.

Martin, J. T., & Juniper, B. E. (1970). The cuticles of plants. Edward Arnold, London, UK.

McMullen, P. M. (2000). Utility Adjuvants. Weed Technology, 14, 792-797.

Mercer, G. N., & Sweatman, W. L. (2006). Process driven models for spray retention of plants. In: Wake G. (ed.) Proceedings of the 2006 Mathematics in Industry study group, 57–85.

Mercer, G. N., Sweatman, W. L., & Forster, W. A. (2010). A model for spray droplet adhesion, bounce or shatter at a crop leaf surface. Progress in Industrial Mathematics at ECMI 2008, 945-951.

Moroi, Y. (1992). Micelles - Theoretical and applied aspects. Plenum, New York, NY, US.

Muehlebach, M., Boeger, M., Cederbaum, F., Cornes, D., Friedmann, A. A., Glock, J., Wagner, T. (2009). Aryldiones incorporating a [1,4,5]oxadiazepane ring. Part I: Discovery of the novel cereal herbicide Pinoxaden. Bioorganic & Medicinal Chemistry, 17, 4241-4256.

Muehlebach, M., Cederbaum, F., Cornes, D., Friedmann, A. A., Glock, J., Hall, G., Widmer, H. (2011). Aryldiones incorporating a [1,4,5]oxadiazepane ring. Part 2: Chemistry and biology of the cereal herbicide Pinoxaden. Pest Management Science, 67, 1499-1521.

Nairn, J. J., Forster, W. A., & van Leeuwen, R. M. (2013). 'Universal' spray droplet adhesion model – accounting for hairy leaves. Weed Research, 53, 407-417.

Nairn, J. J., Forster, W. A., & van Leeuwen, R. M. (2016). Effect of Solution and Leaf Surface Polarity on Droplet Spread Area and Contact Angle. Pest Management Science, 72, 551-557.

Neinhuis, C., & Barthlott, W. (1997). Characterisation and distribution of water-repellent, self-cleaning plant surfaces. Annals of Botany, 79, 667-677.

Niederl, S., Kirsch, T., Riederer, M., & Schreiber, L. (1998). Co-Permeability of 3H-Labeled Water and14C-Labeled Organic Acids across Isolated Plant Cuticles Investigating Cuticular Paths of Diffusion and Predicting Cuticular Transpiration. Plant Physiology, 116, 117-123.

Nikolov, A. D., Wasan, D. T., Chengara, A., Koczo, K., Policello, G. A., & Kolossvary, I. (2002). Superspreading driven by Marangoni flow. Advances in Colloid and Interface Science, 96, 325-338.

Oerke, E. C., & Dehne, H. W. (2004). Safeguarding production—losses in major crops and the role of crop protection. Crop Protection, 23, 275-285.

Orgell, W. H. (1955). The isolation of plant cuticle with pectic enzymes. Plant Physiology, 30, 78.

Owens, D. K., & Wendt, R. C. (1969). Estimation of the surface free energy of polymers. Journal of Applied Polymer Science, 13, 1741-1747.

Pasquali, R. C., Taurozzi, M. P., & Bregni, C. (2008). Some considerations about the hydrophilic–lipophilic balance system. International Journal of Pharmaceutics, 356, 44-51.

Peltonen, L. J., & Yliruusi, J. (2000). Surface Pressure, Hysteresis, Interfacial Tension, and CMC of Four Sorbitan Monoesters at Water–Air, Water–Hexane, and Hexane–Air Interfaces. Journal of Colloid and Interface Science, 227, 1-6.

Penner, D. (2000). Activator Adjuvants. Weed Technology, 14, 785-791.

Popp, C., Burghardt, M., Friedmann, A., & Riederer, M. (2005). Characterisation of hydrophilic and lipophilic pathways of Hedera helix L. cuticular membranes: permeation of water and uncharged organic compounds. Journal of Experimental Botany, 56, 2797-2806.

Popp, J. (2011). Cost-benefit analysis of crop protection measures. Journal für Verbraucherschutz und Lebensmittelsicherheit, 6, 105-112.

Popp, J., Pető, K., & Nagy, J. (2012). Pesticide productivity and food security. A review. Agronomy for Sustainable Development, 33, 243-255.

Preston, W. C. (1948). Some Correlating Principles of Detergent Action. The Journal of Physical and Colloid Chemistry, 52, 84-97.

Price, C. E. A. (1982). A review of factors influencing the penetration of pesticides through plant leaves. In: Cutler, D. F., Alvin, K. L., & Price, C. E. (eds.) The Plant Cuticle. Academic Press, London, UK, 237-252.

Ramsey, R. J. L., Stephenson, G. R., & Hall, J. C. (2005). A review of the effects of humidity, humectants, and surfactant composition on the absorption and efficacy of highly water-soluble herbicides. Pesticide Biochemistry and Physiology, 82, 162-175.

Rein, M. (1993). Phenomena of liquid drop impact on solid and liquid surfaces. Fluid Dynamics Research, 12, 61-93.

Remus-Emsermann, M. N., de Oliveira, S., Schreiber, L., & Leveau, J. H. (2011). Quantification of lateral heterogeneity in carbohydrate permeability of isolated plant leaf cuticles. Frontiers in Microbiology, 2, 1-7.

Riederer, M. (1991). Die Kutikula als Barriere zwischen terrestrischen Pflanzen und der Atmosphäre. Naturwissenschaften, 78, 201-208.

Riederer, M., & Friedmann, A.A. (2006). Transport of lipophilic non-electrolytes across the cuticle. In: Riederer, M., & Müller, C. (eds.) Biology of the Plant Cuticle. Blackwell Publishing Ltd, Oxford, UK, 250-279.

Riederer, M., & Müller, C. (eds.) (2006). Biology of the plant cuticle. Blackwell Publishing Ltd, Oxford, UK.

Riederer, M., & Schneider, G. (1990). The effect of the environment on the permeability and composition of Citrus leaf cuticles. Planta, 180, 154-165.

Riederer, M., & Schreiber, L. (1995). Waxes: the transport barriers of plant cuticles. In: Hamilton, R. J. (ed.) Waxes: Chemistry, molecular biology and functions, vol. 6. The Oily Press, West Ferry, Dundee, Scotland, 131-156.

Riederer, M., & Schreiber, L. (2001). Protecting against water loss: analysis of the barrier properties of plant cuticles. Journal of Experimental Botany, 52, 2023-2032.

Riederer, M., Burghardt, M., Mayer, S., Obermeier, H., & Schönherr, J. (1995). Sorption of monodisperse alcohol ethoxylates and their effects on the mobility of 2, 4-D in isolated plant cuticles. Journal of Agricultural and Food Chemistry, 43, 1067-1075.

Rodham, D. K. (2000). Colloid and interface science in formulation research for crop protection products. Current Opinion in Colloid & Interface Science, 5, 280-287.

Rosen, M. J. (1989). Surfactants and interfacial phenomena, (2nd Ed.). Wiley, New York, NY, US.

Rothman, A. (1982). High-performance liquid chromatographic method for determining ethoxymer distribution of alkylphenoxy polyoxyethylene surfactants. Journal of Chromatography A, 253, 283-288.

Ruchs, C. A., O'Connell, P. J., & Boutsalis, P. (2006). AXIAL, a cereal selective graminicide for the control of annual ryegrass (Lolium rigidum Gaudin) an other major grass weeds. Fifteenth Australian Weeds Conference, 838-841.

Sagiv, A. E., & Marcus, Y. (2003). The connection between in vitro water uptake and in vivo skin moisturization. Skin Research and Technology, 9, 306-311.

Schlegel, T. K., Schönherr, J., & Schreiber, L. (2005). Size selectivity of aqueous pores in stomatous cuticles of Vicia faba leaves. Planta, 221, 648-655.

Schönherr, J. (1982). Resistance of plant surfaces to water loss: transport properties of cutin, suberin and associated lipids. In: Lange, O., Nobel, P. S., Osmond, C. B., & Ziegler, H. (eds.) Physiological plant ecology II, Springer, Berlin Heidelberg, Germany, 153-179.

Schönherr, J. (1993a). Effects of alcohols, glycols and monodisperse ethoxylated alcohols on mobility of 2, 4-D in isolated plant cuticles. Pesticide Science, 39, 213-223.

Schönherr, J. (1993b). Effects of monodisperse alcohol ethoxylates on mobility of 2, 4-D in isolated plant cuticles. Pesticide Science, 38, 155-164.

Schönherr, J. (2002). A mechanistic analysis of penetration of glyphosate salts across astomatous cuticular membranes. Pest Management Science, 58, 343-351.

Schönherr, J., & Baur, P. (1994). Modelling penetration of plant cuticles by crop protection agents and effects of adjuvants on their rates of penetration. Pesticide Science, 42, 185-208.

Schönherr, J., & Bukovac, M. J. (1972). Penetration of stomata by liquids: Dependence on surface tension, wettability, and stomatal morphology. Plant Physiology, 49, 813-819.

Schönherr, J., & Luber, M. (2001). Cuticular penetration of potassium salts: Effects of humidity, anions, and temperature. Plant and Soil, 236, 117-122.

Schönherr, J., & Riederer, M. (1986). Plant cuticles sorb lipophilic compounds during enzymatic isolation. Plant, Cell & Environment, 9, 459-466.

Schönherr, J., Baur, P., & Buchholz, A. (1999). Modelling foliar penetration: its role in optimising pesticide delivery. Royal Society of Chemistry, 233, 134-154.

Schönherr, J., Fernández, V., & Schreiber, L. (2005). Rates of cuticular penetration of chelated FeIII: role of humidity, concentration, adjuvants, temperature, and type of chelate. Journal of Agricultural and Food Chemistry, 53, 4484-4492.

Schönherr, J., Schreiber, L., & Buchholz, A. (2001). Effects of temperature and concentration of the accelerators ethoxylated alcohols, diethyl suberate and tributyl phosphate on the mobility of [14C] 2, 4-dichlorophenoxy butyric acid in plant cuticles. Pest Management Science, 57, 17-24.

Schou, W. C., Forster, W. A., Mercer, G. N., Teske, M. E., & Thistle, H. W. (2011). Building canopy retention into AGDISP: Preliminary models and results. Meeting of the American Society of Agricultural and Biological Engineers, Louisville, Kentucky, US.

Schreiber, L., & Schönherr, J. (2009). Water and solute permeability of plant cuticles. Measurement and data analysis. Springer, Berlin, Germany.

Schreiber, L. (1995). A mechanistic approach towards surfactant/wax interactions: effects of octaethyleneglycolmonododecylether on sorption and diffusion of organic chemicals in reconstituted cuticular wax of barley leaves. Pesticide Science, 45, 1-11.

Schreiber, L. (2001). Effect of temperature on cuticular transpiration of isolated cuticular membranes and leaf discs. Journal of Experimental Botany, 52, 1893-1900.

Schreiber, L. (2002). Co-permeability of 3H-labelled water and 14C-labelled organic acids across isolated Prunus laurocerasus cuticles: effect of temperature on cuticular paths of diffusion. Plant, Cell & Environment, 25, 1087-1094.

Schreiber, L. (2005). Polar paths of diffusion across plant cuticles: New evidence for an old hypothesis. Annals of Botany, 95, 1069-1073.

Schreiber, L. (2006). Review of sorption and diffusion of lipophilic molecules in cuticular waxes and the effects of accelerators on solute mobilities. Journal of Experimental Botany, 57, 2515-2523.

Schreiber, L., & Schönherr, J. (2009). Water and solute permeability of plant cuticles: Springer.

Schreiber, L., Bach, S., Kirsch, T., Knoll, D., Schalz, K., & Riederer, M. (1995). A simple photometric device analysing cuticular transport physiology: surfactant effect on permeability of isolated cuticular membranes of Prunus laurocerasus L. Journal of Experimental Botany, 46, 1915-1921.

Schreiber, L., Riederer, M., & Schorn, K. (1996). Mobilities of organic compounds in reconstituted cuticular wax of barley leaves: effects of monodisperse alcohol ethoxylates on diffusion of pentachlorophenol and tetracosanoic acid. Pesticide Science, 48, 117-124.

Semenov, S., Starov, V., & Rubio, R. G. (2015). Droplets with surfactants. In: Brutin, D. (ed.) (2015). Droplet wetting and evaporation: From pure to complex fluids. Academic Press, London, UK, 315-337.

Serrano, M., Coluccia, F., Martha, T., L`Hardion, F., & Métraux, J.-P. (2015). The cuticle and plant defense to pathogens. Plant cell wall in pathogenesis, parasitism and symbiosis, 5, 6-13.

Singh, M., Orsenigo, J., & Shah, D. (1984). Surface tension and contact angle of herbicide solutions affected by surfactants. Journal of the American Oil Chemists' Society, 61, 596-600.

Soaps and Detergent Association, Glycerine: an overview. (1990). Glycerine & Oleochemical Division, New York, NY, US.

Stammitti, L., Garrec, J.-P., & Derridj, S. (1995). Permeability of isolated cuticles of Prunus laurocerasus to soluble carbohydrate. Plant physiology and biochemistry, 33, 319-326.

Starov, V., & Sefiane, K. (2009). On evaporation rate and interfacial temperature of volatile sessile drops. Colloids and Surfaces A: Physicochemical and Engineering Aspects, 333, 170-174.

Steudle, E., & Frensch, J. (1996). Water transport in plants: role of the apoplast. Plant and Soil, 187, 67-79.

Stevens, P. J. G., & Bukovac, M. J. (1987a). Studies on octylphenoxy surfactants. Part 1: Effects of oxyethylene content on properties of potential relevance to foliar absorption. Pesticide Science, 20, 19-35.

Stevens, P. J. G., & Bukovac, M. J. (1987b). Studies on octylphenoxy surfactants. Part 2: Effects on foliar uptake and translocation. Pesticide Science, 20, 37-52.

Stevens, P. J. G., Kimberley, M. O., Murphy, D. S., & Policello, G. A. (1993). Adhesion of spray droplets to foliage: The role of dynamic surface tension and advantages of organosilicone surfactants. Pesticide Science, 38, 237-245.

Stock, D., & Briggs, G. (2000). Physicochemical properties of adjuvants: Values and applications. Weed Technology, 14, 798-806.

Stock, D., & Holloway, P. J. (1993). Possible mechanisms for surfactant-induced foliar uptake of agrochemicals. Pesticide Science, 38, 165-177.

Stock, D., Edgerton, B. M., Gaskin, R. E., & Holloway, P. J. (1992). Surfactant-enhanced foliar uptake of some organic compounds: Interactions with two model polyoxyethylene aliphatic alcohols. Pesticide Science, 34, 233-242.

Stock, D., Holloway, P. J., Grayson, B. T., & Whitehouse, P. (1993). Development of a predictive uptake model to rationalise selection of polyoxyethylene surfactant adjuvants for foliage-applied agrochemicals. Pesticide Science, 37, 233-245.

Taylor, P. (2011). The wetting of leaf surfaces. Current Opinion in Colloid & Interface Science, 16, 326-334.

Tu, M., & Randall, J. (2003). Adjuvants. Weed Control Methods Handbook, The nature Conservancy, 1-24.

Tukey, H. B. (1970). The leaching of substances from plants. Annual Review of Plant Physiology, 21, 305-324.

van der Wal, A., & Leveau, J. H. J. (2011). Modelling sugar diffusion across plant leaf cuticles: the effect of free water on substrate availability to phyllosphere bacteria. Environmental Microbiology, 13, 792-797.

Vargaftik, N., Volkov, B., & Voljak, L. (1983). International tables of the surface tension of water. Journal of Physical and Chemical Reference Data, 12, 817-820.

Venzmer, J. (2015). Superspreading. In: Brutin, D. (ed.) (2015). Droplet wetting and evaporation: From pure to complex fluids. Academic Press, London, UK, 71-84.

Volpe, C. D., & Siboni, S. (1997). Some reflections on acid–base solid surface free energy theories. Journal of Colloid and Interface Science, 195, 121-136.

Watanabe, T., & Yamaguchi, I. (1992). Studies on wetting phenomena on plant leaf surfaces. 3: A retention model for droplets on solid surfaces. Pesticide Science, 34, 273-279.

Wenger, J., Niderman, T., & Mathews, C. (2012). Acetyl-CoA Carboxylase inhibitors. In: Krämer, W., Schirmer, U., Jeschke, P., & Witschel, M. (eds.) (2012). Modern crop protection compounds: vol.1 Herbicides. (2nd ed). Wiley, Weinheim, Germany, 447-477.

Wenzel, R. N. (1936). Resistance of solid surfaces to wetting by water. Industrial & Engineering Chemistry, 28, 988-994.

Wirth, W., Storp, S., & Jacobsen, W. (1991). Mechanisms controlling leaf retention of agricultural spray solutions. Pesticide Science, 33, 411-420.

Xu, L., Zhu, H., Ozkan, H. E., Bagley, W. E., & Krause, C. R. (2011). Droplet evaporation and spread on waxy and hairy leaves associated with type and concentration of adjuvants. Pest Management Science, 67, 842-851.

Yeats, T. H., & Rose, J. K. (2013). The formation and function of plant cuticles. Plant Physiology, 163, 5-20.

Young, T. (1805). An Essay on the Cohesion of Fluids. Philosophical Transactions of the Royal Society of London, 95, 65-87.

Zabka, V., Stangl, M., Bringmann, G., Vogg, G., Riederer, M., & Hildebrandt, U. (2008). Host surface properties affect prepenetration processes in the barley powdery mildew fungus. New Phytologist, 177, 251-263.

Zabkiewicz. (2000). Adjuvants and herbicidal efficacy – present status and future prospects. Weed Research, 40, 139-149.

Zeisler, V., & Schreiber, L. (2016). Epicuticular wax on cherry laurel (Prunus laurocerasus) leaves does not constitute the cuticular transpiration barrier. Planta, 243, 65-81.

APPENDIX

Appendix 1: Parameters describing the linear regression between moisture content (% mass) or humectant activity n_{ws} and EO content (A) or HLB value (B) shown in Figure 39. Standard Errors are given in brackets.

Regression line	RH	y-intercept	slope	R^2	P
a	90%	22.76 (7.70)	1.86 (0.63)	0.81	0.099
b	90%	-1.93 (1.25)	1.72 (0.10)	0.99	0.004
c	90%	-12.40 (9.01)	4.75 (0.76)	0.95	0.025
d	90%	-29.15 (8.84)	3.94 (0.75)	0.93	0.034

Appendix 2: Parameters describing the linear regression between moisture content (% mass) or humectant activity n_{ws} and EO content shown in Figure 41, A and B. Standard Errors are given in brackets.

Regression line	RH	y-intercept	slope	R^2	P
moisture cont. vs EO					
a	30%	0.17 (0.21)	0.03 (0.01)	0.30	0.020
b	80%	10.34 (2.73)	0.36 (0.16)	0.25	0.036
c	90%	20.51 (5.17)	0.73 (0.30)	0.28	0.024
n_{ws} vs EO					
d	30%	-0.04 (0.09)	0.04 (0.01)	0.74	<0.001
e	80%	2.18 (1.06)	0.54 (0.06)	0.83	<0.001
f	90%	3.77 (1.87)	1.15 (0.10)	0.89	<0.001

Appendix 3: Parameters describing the linear regression between moisture content (% mass) or humectant activity n_{ws} and HLB value shown in Figure 41, C and D. Standard Errors are given in brackets.

Regression line	RH	y-intercept	slope	R^2	P
moisture cont. vs HLB					
g	30%	-0.56 (0.36)	0.11 (0.03)	0.41	0.004
h	80%	-5.77 (2.41)	1.95 (0.21)	0.84	<0.001
i	90%	-10.39 (4.52)	3.79 (0.40)	0.85	<0.001
n_{ws} vs HLB					
j	30%	-0.33 (0.28)	0.07 (0.02)	0.33	0.012
k	80%	-6.56 (2.76)	1.46 (0.24)	0.69	<0.001
l	90%	-12.46 (6.16)	2.87 (0.55)	0.63	<0.001

Appendix 4: P-values of statistical analysis of significant differences between humidity levels of each adjuvant treatment of cuticular penetration experiments (Kruskal-Wallis One Way Analysis of Variance of Ranks). Statistical tests were performed with SigmaPlot 12.5.

Treatment	RH level (%)	n	P value	Post-hoc-Test for sig. different treatments	Median F_{PXD}* 10^6 (µg s^{-1})	25% - 75% quantile F_{PXD}*10^6 (µg s^{-1})	Effect
No Adjuvant (control)	30	19	0.322	no stat. sign. difference	0.120	0.078 - 0.172	
	50	17			0.121	0.100 - 0.192	
	80	16			0.103	0.072 - 0.129	
Span 20	30	7	0.373	no stat. sign. difference	0.083	0.070 - 0.182	1
	50	9			0.164	0.123 - 0.301	1
	80	7			0.189	0.045 - 0.420	2
Span 80	30	7	0.252	no stat. sign. difference	0.204	0.106 - 0.408	2
	50	8			0.184	0.074 - 0.288	2
	80	8			0.363	0.117 - 0.762	4
Tween 20	30	9	<0.001	Dunn`s Test: P<0.05 80% RH sign. different to 30% RH and 50 % RH	1.999	1.020 - 2.986	17
	50	10			4.740	2.197 - 5.560	39
	80	10			0.320	0.176 - 0.674	3
Tween 40	30	8	0.096	no stat. sign. difference	0.961	0.547 - 1.091	8
	50	9			0.390	0.203 - 1.105	3
	80	7			0.260	0.071 - 0.466	3
Tween 60	30	7	0.191	no stat. sign. difference	0.719	0.179 - 1.771	6
	50	9			0.203	0.064 - 0.689	2
	80	8			0.274	0.166 - 0.807	3
Tween 65	30	7	0.534	no stat. sign. difference	1.292	0.115 - 1.523	11
	50	8			0.647	0.277 - 0.865	5
	80	8			0.677	0.080 - 1.276	7
Tween 80	30	7	0.197	no stat. sign. difference	4.263	3.725 - 4.621	36
	50	10			2.939	1.115 - 4.863	24
	80	10			2.397	1.629 - 4.099	23
Tween 81	30	10	0.772	no stat. sign. difference	2.176	0.854 - 2.969	18
	50	7			1.674	0.551 - 3.549	14
	80	8			1.598	0.526 - 2.961	16
Tween 85	30	9	0.081	no stat. sign. difference	2.952	2.216 - 3.676	25
	50	10			1.732	0.576 - 2.535	14
	80	8			1.927	1.109 - 2.819	19
Genapol O050	30	9	0.071	no stat. sign. difference	1.673	1.369 - 2.569	14
	50	9			2.772	1.668 - 3.329	23
	80	10			4.361	1.894 - 5.900	42
Genapol O080	30	9	0.248	no stat. sign. difference	2.609	1.350 - 3.829	22
	50	9			1.856	0.849 - 2.183	15
	80	10			3.423	0.882 - 5.307	33
Genapol O100	30	10	<0.001	Tukey Test: P<0.05 80% RH sign. different to 30% RH and 50% RH	1.904	1.332 - 2.763	16
	50	10			1.605	1.398 - 1.933	13
	80	10			0.706	0.440 - 1.242	7
Genapol O200	30	10	0.003	Dunn`s Test: P<0.05 80% RH sign. different to 30% RH and 50% RH	4.327	1.064 - 5.457	36
	50	9			4.275	3.014 - 4.718	35
	80	10			0.833	0.337 - 0.930	8
Glycerol	30	9	0.651	no stat. sign. difference	0.901	0.392 - 1.105	8
	50	10			0.918	0.454 - 1.639	8
	80	9			0.994	0.434 - 1.295	10
Atlas G1096	30	10	0.251	no stat. sign. difference	0.614	0.316 - 0.923	5
	50	9			0.493	0.108 - 0.519	4
	80	7			0.396	0.199 - 0.590	4
TEHP EW400	30	9	0.917	no stat. sign. difference	24.511	18.497 - 29.274	204
	50	8			23.216	21.176 - 32.355	192
	80	10			24.918	22.329 - 28.555	242

Appendix 5: Mean effect values of greenhouse studies. Bold values indicate the highest effect of the adjuvant treatment to the corresponding control (all visible in AVEFA assessments). No effects could be calculated (blank rows) when the non-adjuvanted control value was zero. Values in brackets indicate the standard deviation, n=3.

Weed	Rate g PXD ha^{-1}	0.5% TEHP	0.1% Tween 20	0.1% Tween 80	0.1% Span 20	0.1% Span 80
LOLMU	1.875	3.7 (1.2)	2.0 (1.0)	1.7 (0.6)	1.3 (0.6)	1.0 (1.0)
	3.75	6.0 (0.0)	2.1 (0.9)	0.9 (0.4)	1.0 (0.2)	0.9 (0.7)
	7.5	5.3 (0.0)	4.2 (0.8)	2.8 (1.1)	1.1 (0.4)	1.0 (0.3)
	15	4.8 (0.2)	4.4 (0.4)	3.7 (0.6)	2.3 (0.7)	2.4 (0.6)
	30	2.1 (0.0)	2.1 (0.0)	2.1 (0.0)	1.8 (0.1)	1.6 (0.1)
ALOMY	1.875					
	3.75	13.5 (3.0)	4.5 (2.6)	2.5 (0.9)	1.5 (1.5)	0.0 (0.0)
	7.5	7.0 (0.0)	3.5 (0.5)	1.5 (0.5)	2.2 (1.6)	1.0 (1.0)
	15	4.8 (0.0)	3.9 (0.5)	3.6 (0.0)	3.5 (0.5)	3.8 (0.3)
	30	2.8 (0.2)	2.5 (0.0)	2.3 (0.2)	2.3 (0.2)	2.4 (0.3)
AVEFA	1.875					
	3.75	**39.0 (3.0)**	7.0 (1.7)	6.0 (3.0)	3.0 (3.0)	9.0 (6.0)
	7.5	23.0 (1.7)	**15.0 (4.0)**	**13.0 (2.3)**	**13.0 (1.7)**	**10.0 (5.7)**
	15	8.5 (0.5)	8.0 (0.5)	7.3 (0.3)	7.2 (0.8)	7.5 (0.5)
	30	2.3 (0.1)	2.2 (0.0)	2.1 (0.1)	2.2 (0.1)	2.2 (0.1)
SETVI	1.875	15.5 (0.9)	8.0 (2.3)	6.0 (1.5)	1.0 (0.9)	1.5 (1.5)
	3.75	4.9 (0.3)	3.2 (0.3)	3.3 (0.9)	1.4 (0.5)	1.1 (0.6)
	7.5	4.1 (0.1)	3.7 (0.2)	3.5 (0.1)	2.9 (0.3)	2.6 (0.1)
	15	1.5 (0.0)	1.5 (0.0)	1.5 (0.0)	1.4 (0.1)	1.3 (0.1)
	30	1.4 (0.0)	1.4 (0.0)	1.4 (0.0)	1.3 (0.0)	1.3 (0.1)
Mean of weeds	1.875	9.6 (8.4)	5.0 (4.2)	3.8 (3.1)	1.2 (0.2)	1.3 (0.4)
	3.75	15.9 (15.9)	4.2 (2.1)	3.2 (2.1)	1.7 (0.9)	2.7 (4.2)
	7.5	9.9 (8.8)	6.6 (5.6)	5.2 (5.3)	4.8 (5.5)	3.7 (4.3)
	15	4.9 (2.9)	4.5 (2.7)	4.0 (2.4)	3.6 (2.5)	3.8 (2.7)
	30	2.2 (0.6)	2.0 (0.5)	2.0 (0.4)	1.9 (0.4)	1.9 (0.5)
TRZAW	1.875					
	3.75					
	7.5					
	15	12.0 (3.0)	3.0 (0.0)	5.6 (3.1)	4.0 (1.7)	7.0 (1.7)
	30	6.0 (2.0)	1.8 (0.4)	2.3 (0.8)	2.0 (0.4)	2.0 (0.9)

Appendix 6: Statistical analysis of greenhouse studies. Normality test: Shapiro-Wilk test; ANOVA: Kruskal-Wallis One Way Analysis of Variance on Ranks. Statistical tests were performed with SigmaPlot 12.5.

Weed	Rate g PXD ha^{-1}	Normality Test passed	Equal Variance Test passed	ANOVA on Ranks and Post-Hoc Test	P value		Number of sign. differences
LOLMU	1.875	yes	no	no	0.162	There is not a stat. sign. difference	/
	3.75	yes	no	Tukey	0.046	There is a stat. sign. difference	/
	7.5	yes	yes	One-Way ANOVA: Tukey	<0.001	There is a stat. sign. difference	9
	15	yes	yes	One-Way ANOVA: Tukey	<0.001	There is a stat. sign. difference	11
	30	yes	yes	One-Way ANOVA: Tukey	<0.001	There is a stat. sign. difference	/
ALOMY	1.875	no	no	no	0.068	There is not a stat. sign. difference	/
	3.75	no	no	Dunns Test (treatment group size unequal)	0.046	There is a stat. sign. difference	6
	7.5	yes	yes	One-Way ANOVA: Tukey	<0.001	There is a stat. sign. difference	9
	15	yes	yes	One-Way ANOVA: Tukey	<0.001	There is a stat. sign. difference	5
	30	yes	yes	One-Way ANOVA: Tukey	<0.001	There is a stat. sign. difference	/
AVEFA	1.875	no	no	Tukey	0.046	There is a stat. sign. difference	1
	3.75	yes	no	Tukey	0.029	There is a stat. sign. difference	8
	7.5	yes	yes	One-Way ANOVA: Tukey	<0.001	There is a stat. sign. difference	5
	15	yes	yes	One-Way ANOVA: Tukey	<0.001	There is a stat. sign. difference	1
	30	no	no	Tukey	0.029	There is a stat. sign. difference	11
SETVI	1.875	yes	yes	One-Way ANOVA: Tukey	<0.001	There is a stat. sign. difference	9
	3.75	yes	yes	One-Way ANOVA: Tukey	<0.001	There is a stat. sign. difference	10
	7.5	yes	yes	One-Way ANOVA: Tukey	<0.001	There is a stat. sign. difference	5
	15	yes	yes	One-Way ANOVA: Tukey	<0.001	There is a stat. sign. difference	1
	30	no	no	Tukey	0.034	There is a stat. sign. difference	8
Mean of weeds	1.875	yes	yes	One-Way ANOVA: Tukey	<0.001	There is a stat. sign. difference	9
	3.75	yes	yes	One-Way ANOVA: Tukey	<0.001	There is a stat. sign. difference	13
	7.5	yes	yes	One-Way ANOVA: Tukey	<0.001	There is a stat. sign. difference	10
	15	yes	yes	One-Way ANOVA: Tukey	<0.001	There is a stat. sign. difference	1
	30	yes	no	Tukey	0.006	There is a stat. sign. difference	/
TRZAW	1.875	no	no	no	0.562	There is not a stat. sign. difference	2
	3.75	yes	yes	One-Way ANOVA: Tukey	0.047	There is a stat. sign. difference	/
	7.5	yes	yes	One-Way ANOVA ?	0.087	There is not a stat. sign. difference	5
	15	yes	yes	One-Way ANOVA: Tukey	<0.001	There is a stat. sign. difference	5
	30	yes	yes	One-Way ANOVA: Tukey	0.002	There is a stat. sign. difference	/

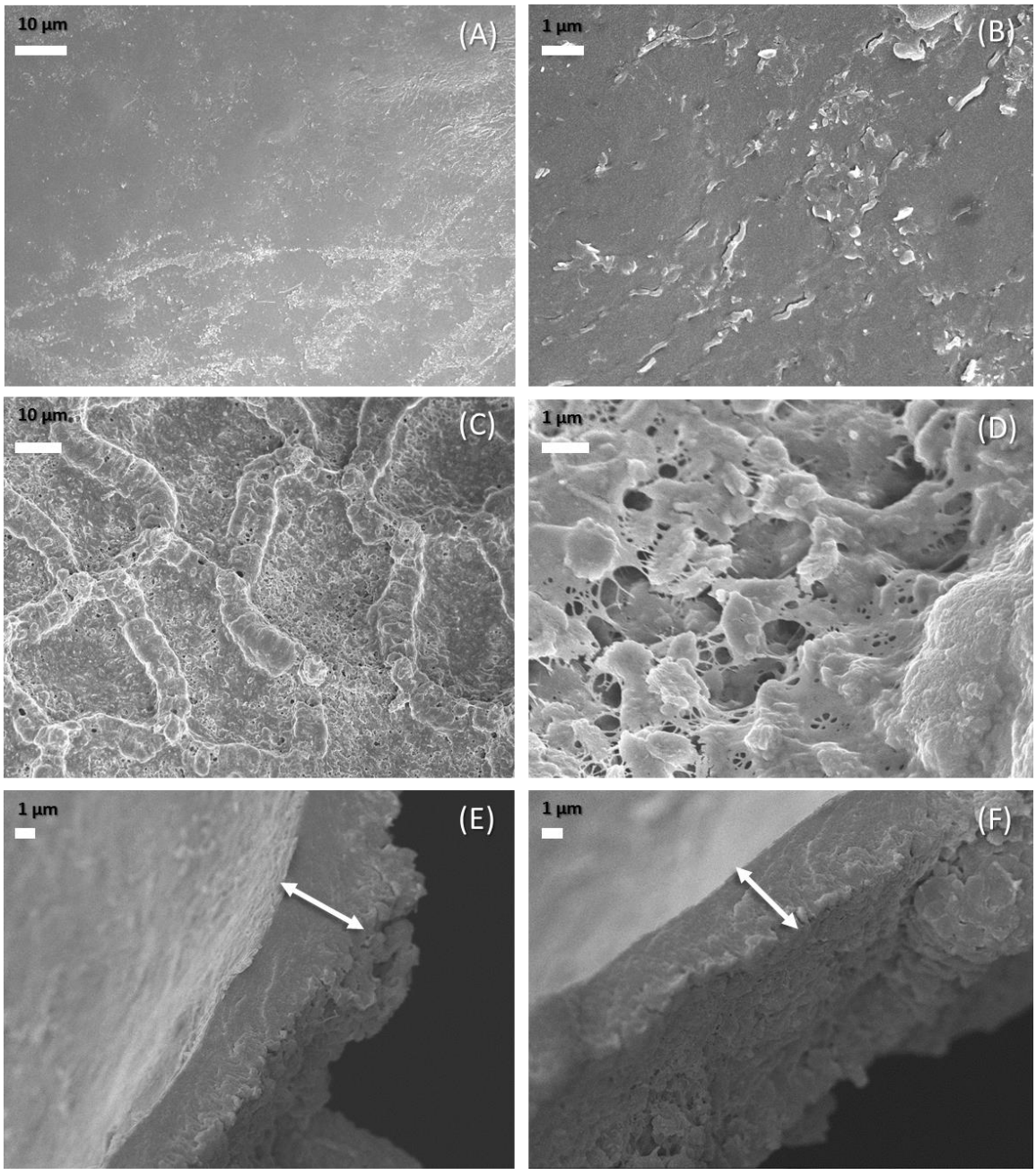

Appendix 7: Scanning Electron Microscopy (SEM) pictures illustrating isolated cuticular membranes (CM) of *Prunus laurocerasus* cv. Herbergii. Surface microstructures of the adaxial side of the leaf revealing no three-dimensional epicuticular wax structures (A and B). The inner side of CM displaying imprints of the epidermal cells (C and D). Netlike structures eventually might show cutin filaments (D).
Cross-section view of CM indicating the cuticle thickness of about 4 µm (E and F).

Appendix 8: Data remodelled for evaluating comparisons applied in radar charts. All selected adjuvants displayed in the table were considered for recalculations. Results gained in different measurements were referred relatively to one hundred (sum).
Retention: mean values of track sprayer experiments in ng Tinopal OB per mm^2 leaf area; Humectancy: humectant activity n_{ws} (number of mols of water sorbed per mol surfactant) at 80% RH; Cuticular Penetration: median values of flow rates of PXD from SOFP experiments averaged over all humidity levels; Spreading: mean contact angle after 60 s on parafilm; DST: dynamic surface tension at 94 ms surface age. All experiments, except humectancy, were conducted using an adjuvant concentration of 0.1%.

Adjuvant (conc. 0.1%)	Retention	Humectancy	Cuticular penetration	Spreading	DST
Water (control)	3.6	/	0.5	4.7	6.2
Span 20	5.0	1.5	0.6	8.8	6.3
Span 80	3.2	0.5	1.1	6.9	6.3
Tween 20	14.6	12.2	10.5	6.0	7.7
Tween 40	9.8	11.4	2.4	5.8	7.1
Tween 60	5.3	11.2	1.8	5.7	7.0
Tween 65	3.6	6.7	3.9	6.2	6.3
Tween 80	10.1	11.1	14.2	6.0	7.0
Tween 81	3.9	2.5	8.1	7.0	6.2
Tween 85	4.6	5.8	9.8	6.5	6.2
Genapol O050	4.4	2.0	13.0	7.1	6.3
Genapol O080	5.9	3.7	11.7	7.9	6.7
Genapol O100	10.1	5.4	6.2	8.2	7.2
Genapol O200	11.4	10.7	14.0	6.8	7.3
Atlas G1096	4.4	15.4	2.2	6.6	6.2
Sum	**100.0**	**100.0**	**100.0**	**100.0**	**100.0**

ACKNOWLEDGEMENTS

PUBLICATIONS AND PRESENTATIONS

Publications

Asmus, E., Popp, C., Friedmann, A.A., Arand, K., Riederer, M. (2016). Water Sorption Isotherms of Surfactants: A Tool to Evaluate Humectancy. *Journal of Agricultural and Food Chemistry* (doi: 10.1021/acs.jafc.6b01378).

Asmus, E., Arand, K., Popp, C., Friedmann, A.A., Riederer, M. (2016). Water sorption potential of non-ionic adjuvants and its impact on cuticular penetration. *Proceedings of the 11th International Symposium on Adjuvants and Agrochemicals*, pp. 177-182.

Presentations

06/2016	ISAA 11th International Symposium on Adjuvants for Agrochemicals, Monterey (CA, US) Platform presentation: Water sorption potential of non-ionic adjuvants and its impact on cuticular penetration
02/2016	Syngenta Crop Protection, Bracknell (UK) Oral presentation: Mode of action of adjuvants for foliar application
11/2015	Syngenta Crop Protection, Münchwilen (CH) Oral presentation: Mode of action of adjuvants for foliar application
06/2015	Conference: Plant Wax 2015, Ascona (CH) Poster presentation: Calculation of surface free energy of wax-covered leaf surfaces
09/2014	Conference: 59. Deutsche Pflanzenschutztagung, Freiburg (GER) Poster presentation: Dynamic droplet behaviour on plant surfaces is affected by surface active adjuvants

CURRICULUM VITAE

AFFIDAVIT

I hereby confirm that my thesis entitled ‘Modes of Action of Adjuvants for Foliar Application’ is the result of my own work. I did not receive any help or support from commercial consultants. All sources and / or materials applied are listed and specified in the thesis.
Furthermore, I confirm that this thesis has not yet been submitted as part of another examination process neither in identical nor in similar form.

Würzburg, 29.06.2016
Place, Date Signature

EIDESSTATTLICHE ERKLÄRUNG

Hiermit erkläre ich an Eides statt, die Dissertation „Wirkmechanismen von Adjuvantien für die Blattflächenapplikation’ eigenständig, d.h. insbesondere selbständig und ohne Hilfe eines kommerziellen Promotionsberaters, angefertigt und keine anderen als die von mir angegebenen Quellen und Hilfsmittel verwendet zu haben.

Ich erkläre außerdem, dass die Dissertation weder in gleicher noch in ähnlicher Form bereits in einem anderen Prüfungsverfahren vorgelegen hat.

Würzburg, 29.06.2016
Ort, Datum Unterschrift